ADVANCEMENT OF ADSORPTION PROCESS ON ACTIVATED CARBON USING MICROWAVE AND HIGH GRAVIMETRIC TECHNOLOGIES

ANIRBAN KUNDU

THESIS SUBMITTED IN FULFILMENT OF THE REQUIREMENTS FOR THE DEGREE OF DOCTOR OF PHILOSOPHY

FACULTY OF SCIENCE
UNIVERSITY OF MALAYA
KUALA LUMPUR

2016

UNIVERSITI MALAYA

ORIGINAL LITERARY WORK DECLARATION

Name of Candidate: **ANIRBAN KUNDU**

Matric No: SCH 110090

Name of Degree: SHC-DOCTOR OF PHILOSOPHY

Title of Thesis (“this work”):
ADVANCEMENT OF ADSORPTION PROCESS ON ACTIVATED CARBON USING MICROWAVE AND HIGH GRAVIMETRIC TECHNOLOGIES

Field of Study: ENVIRONMENTAL SCIENCE AND MANAGEMENT

I do solemnly and sincerely declare that:

(1) I am the sole author/writer of this Work;
(2) This Work is original;
(3) Any use of any work in which copyright exists was done by way of fair dealing and for permitted purposes and any excerpt or extract from, or reference to or reproduction of any copyright work has been disclosed expressly and sufficiently and the title of the Work and its authorship have been acknowledged in this Work;
(4) I do not have any actual knowledge nor do ought I reasonably to know that the making of this work constitutes an infringement of any copyright work;
(5) I hereby assign all and every rights in the copyright to this Work to the University of Malaya (“UM”), who henceforth shall be owner of the copyright in this Work and that any reproduction or use in any form or by any means whatsoever is prohibited without the written consent of UM having been first had and obtained;
(6) I am fully aware that if in the course of making this Work I have infringed any copyright whether intentionally or otherwise, I may be subject to legal action or any other action as may be determined by UM.

Candidate’s Signature: Date

Subscribed and solemnly declared before,

Witness’s Signature: Date

Name:

Designation:

ABSTRACT

This thesis describes the efficacy of microwave technology for the preparation of a novel activated carbon from an agricultural waste and the utilisation of the activated carbon in an innovative rotating packed bed (RPB) contactor. In RPB, centrifugal force provides the driving force for the adsorption of heavy metals and dye such as chromium and Direct Red 23 (DR23) on activated carbon.

Activated carbon became a material of choice as an adsorbent for industrial and environmental applications more recently. Typical process of producing activated carbon requires heating a carbonaceous material for one to seven hours. Although activated carbon with surface area ranging between 800 to 1600 m^2/g can be produced, the process is slow and inefficient due to heat as well as material losses. Moreover, the contactor volume is often large to meet the process requirement. Consequently, this research is primarily focused on the following objectives: i) optimisation of process variables in microwave assisted activated carbon production from waste material, ii) evaluation of the prepared activated carbon for heavy metal and dye removal, iii) application of high gravimetric (HIGEE) technology in RPB contactor to minimise the contact time for adsorption, and iv) optimisation of the process parameters of RPB contactor for heavy metal and dye removal, estimation of the adsorption kinetics and adsorption isotherm.

Activated carbon was prepared using waste palm kernel shells (PKS) as the raw material by two different impregnating materials, namely phosphoric (H_3PO_4) and sulphuric acid (H_2SO_4). The activated carbon prepared by microwave activation and based on three different impregnation ratios of H_3PO_4 had specific surface areas of 872, 1256 and 952 m^2 /g. The chromium removal capacity of the activated carbon was 19.1 mg/g. The process parameters for activated carbon preparation were optimised with the aid of Taguchi method and response surface methodology (RSM). The specific surface area of the activated carbon, prepared from H_3PO_4 impregnation and optimised by Taguchi method (denoted as $MWAC_T$) was 1473.5 m^2/g during initial optimisation, and increased to 1535 m^2/g when the operating conditions were fine-tuned. For activated carbon (denoted as MWAC) prepared by H_2SO_4 impregnation and optimised by RSM, the specific surface area was 1011 m^2/g and zinc removal capacity of 14.6 mg/g. The $MWAC_T$ was applied to remove DR23 and almost total removal was achieved with the removal capacity of 24.75 mg/g. The adsorption in the RPB contactor was much faster than that in a shake flask for the same adsorbent to adsorbate ratio. The removal of DR23 using commercially activated carbon was almost 90% within 5h in RPB contactor in comparison to 55% in a shake flask. In RPB contactor almost 75% of chromium was adsorbed by $MWAC_T$ within 20 min and 90% within 3 h. Optimum conditions for the adsorption were found to be rotating speed of 1200 rpm, feed rate of 50 L/min, packing density of 179 kg/m^3 and initial solution pH of 2. These optimum conditions were robust to the external noise factor, which was initial chromium concentration in solution.

ABSTRAK

Tesis ini menghuraikan penggunaan kerberkesanan ketuhar gelombang mikro dalam menyediakan karbon novel diaktifkan daripada bahan terbuang pertanian dan penggunaan karbon diaktifkan dalam penyentuh berputar katil dibungkus (RPB) berinovatif, di mana daya emparan digunakan sebagai kuasa memandu, untuk penjerapan metal berat dan pewarna, khususnya Kromium, Zink , Methylene blue (MB) dan Direct Red 23 (DR23),

Karbon diaktifkan menjadi bahan pilihan sebagai adsorben untuk aplikasi industri dan alam sekitar sejak akhir-akhir ini. Proses biasa dalam menghasilkan karbon diaktifkan memerlukan pemanasan bahan berkarbon untuk satu hingga tujuh jam untuk menukar ia menjadi karbon berliang diaktifkan. Walaupun dapat menghasilkan karbon teraktif yang berkualiti baik, prosesnya adalah lambat dan kurang efisen kerana kehilangan haba dan bahan. Tambahan daripada itu, kontaktor isipadu selalunya besar dalam mencukupi syarat proses. Oleh itu, fokus penyelidikan ini lebih memberi tumpuan kepada objektif-objektif berikut: i) pengoptimuman pembolehubah proses dalam ketuhar gelombang mikro bantuan karbon teraktif daripada bahan buangan tempatan yang sedia ada, ii) Penilaian penyediakan karbon teraktif untuk metal berat dan penyingir pewarna, iii) Aplikasi penggunaan teknologi HIGEE dalam reaktor berputar lapisan terpadat untuk mengurangkan masa sentuhan untuk penjerapan, iv) pengoptimuman penjerapan proses dalam reaktor lapisan terpadat yang berputar untuk metal berat dan penyingkir pewarna serta mengira kinetik penjerapan dan, penjerapan isoterma

Karbon diaktifkan disediakan dengan menggunakan tempurung isirong sawit sebagai bahan mentah dengan menggunakan dua bahan impregnasi berbeza iaitu asid fosforik dan sulfurik. Karbon diaktifkan tersedia daripada pengaktifan gelombang mikro dan berdasarkan tiga nisbah impregnasi berbeza asid fosforik yang mempunyai permukaan tertentu adalah 872, 1256 dan 952 m^2/g. Kapasiti penyingkiran kromium karbon yang diaktifkan adalah 19.1 mg/g. Parameter-parameter proses bagi penyediaan telah dioptimumkan dengan bantuan kaedah Taguchi pengoptimuman dan tindak balas permukaan (RSM). Kawasan permukaan tertentu 1473.5 m^2/g dan 1.535 m^2/g telah diperolehi bagi karbon diaktifkan (dinamakan sebagai $MWAC_T$) disediakan daripada asid fosforik impregnasi dan dioptimumkan dengan kaedah Taguchi. Untuk karbon diaktifkan (dinamakan sebagai MWAC) yang disediakan oleh asid sulfurik impregnasi dan dioptimumkan oleh RSM, kawasan permukaan tertentu adalah 1.011 m^2/g yang mempunyai kapasiti penyingkiran Zink sebanyak 14.6 mg/g. The MWACT telah digunakan untuk membuang DR23 dan hampir semua jumlah penyingkiran ini dicapai dengan kapasiti penyingkiran 24.75 mg/g. Penjerapan dalam penyentuh RPB adalah sangat cepat berbanding kelalang koncang untuk adsorben yang sama bagi nisbah bahan terjerap. Penyingkiran DR23 pada karbon diaktifkan komersial adalah hampir 90% dalam 5 jam di RPB penyentuh berbanding dengan 55% dalam kelalang goncang. Peratus penyingkiran Chromium pada MWACT di RPB penyentuh adalah hampir 75% adalah dengan 20 min dan 90% dalam masa 3 jam. Keadaan optimum penjerapan, telah didapati berputar (RPM) kelajuan 1200, kadar suapan (L min-1) 50 , ketumpatan pembungkusan (kg/m^3) 179, dan pH penyelesaian awal sebanyak 2. Keadaan optimum telah mengambil kira kesan daripada faktor hingar luaran, kepekatan kromium awal dalam penyelesaian.

ACKNOWLEDGEMENTS

First and foremost I offer my sincere gratitude and appreciation to my supervisors Dr Ghufran Redzwan, Prof Mohd. Ali Hashim and Prof Bhaskar SenGupta who have supported and guided me throughout my work with their patience and knowledge whilst allowing me the room to work in my own way. I also want to thank Prof S C Santra for his contribution to my academic endeavours.

I would like to thank High Impact Research University of Malaya for providing me with sufficient research grants and excellent analytical facility. I also acknowledge the support provided by the laboratory technicians and office staff especially Ms Fazizah, En Jalaluddin, En Kamaruddin, En Azaruddin and En Kamalrul, during the entire period of my study. I am also thankful to IPS thesis unit, UM for their support and help during thesis writing.

Words cannot express how thankful I am to my mother, my father, my mother-in law, father-in-law, my elder sister Nabanita, my brother-in-law Sunit, my nephews all my family members for all their supports and sacrifices that they have made for me. I am indebted to my wife Gargi for her diligent support and encouragement in all situations with special care and love, which compelled me to thrive for betterment. I am grateful to you Gargi. Moreover, I thank all my friends who always supported me to complete this work.

TABLE OF CONTENTS

LIST OF FIGURES

LIST OF TABLES

LIST OF SYMBOLS AND ABBREVIATIONS

Symbols	Meaning
μm	Micron
ANOVA	Analysis of variance
As	Arsenic
BB	Box–Behnken
BET	Brunauer-Emmet Teller
C_0	Initial concentration
C_e	Equilibrium concentration
C_f	Final concentration
$CaCl_2$	Calcium chloride
$CaCO_3$	Calcium carbonate
CCD	Central composite design
Cd	Cadmium
Cr	Chromium
Cu	Copper
CO_2	Carbon-di-oxide
DF	Degree of freedom
DFT	Density functional theory
DR23	Direct Red 23
EDTA	Ethylenediaminetetraacetic acid
FCC	Federal communications commission
FT-IR	Fourier Transform Infra Red
Fe	Iron
GAC	Granular activated carbon
H_2S	Hydrogen sulphide
g	gravitational acceleration
h	Hour
HIGEE	High gravimetric
i	Linier coefficient
ICP-OES	Integrated Coupled Plasma-Optical Emission Spectrophotometer
IR	Impregnation ratio
j	Quadratic coefficient
K_{GA}	Gas-phase mass transfer coefficient
k_1	Lagergren rate constant
K_2	Pseudo-second-order rate constant
LBL	Layer-by-layer
K_2CO_3	Potassium bi carbonate
KOH	Potassium hydroxide
L	Littre
M^{2+}	Bivalent metal
MB	Methylene blue
MEUF	Micellar-enhanced ultrafiltration
Mn	Manganese
MWAC	Microwave activated carbon
$MWAC_T$	Microwave activated carbon by Taguchi method
nf	Nano filtration

Symbols	Meaning
NF	Noise factor
Ni	Nickle
NOx	Oxides of nitrogen
PAC	Powdered activated carbon
Pb	Lead
pH	Negative logarithm of the hydrogen ion concentration
PDMED	Poly (dimethylamine-co-epichlorohydrin-co-ethylenediamine)
PEI	Poly (ethyleneimine)
PKS	Palm kernel shell
q	Quantity adsorbed
q_e	Quantity adsorbed at equilibrium
q_{max}	Maximum adsorption capacity
r	radius
RPB	Rotating packed bed
RR198	Reactive Red 198
RR120	Reactive Red 120
rpm	Rotation per minute
RSM	Response surface methodology
R^2	Coefficient of determination
SBR	Sequence batch reactor
SEM	Scanning electron micrograph
Sox	Oxides of sulphur
T	Temperature
t	Time
TiO_2	Titanium di oxide
UF	Ultrafiltration
UV	Ultraviolet
UV-Vis	Ultraviolet-Visible
W	Watt
WHO	World Health Organization
y	Dependent variable
Zn	Zinc
$k_L\alpha$	Liquid-phase volumetric mass transfer coefficient
β	Regression coefficient
ε	Random error
ε'	dielectric constant or real permittivity
ε''	the dielectric loss function
δ	dielectric loss
ω	Rotational speed in rpm
ΔG^0	Free energy change
ΔH^0	Enthalpy change
ΔS^0	Entropy change

CHAPTER 1: INTRODUCTION

1.1 Research Background

Manufacturing activities not only generate useful goods for the society but also produce waste. When these wastes are not treated and disposed of properly, they negatively affect the environment. Environment can be defined as the sum total of all conditions and influences that affect the development and life of all organisms on earth, from the lowest form of life such as micro-organisms, bacteria, fungi to the highest form of life including human beings. One of the most integrated parts of the environment is hydrosphere or water.

It is almost redundant to mention the importance of water for all life forms especially to human beings to meet their basic needs in day-to-day life such as cooking, drinking, bathing, disposal of sewage, irrigation, generating electricity in power plants, cooling and manufacturing different products in industries, as well as the disposal of industrial wastes. A great extent of the undesirable substances are added to water resources during all these activities. This alters the basic chemistry of water in rivers and streams. With increasing industrialisation, huge volume of wastewater is being discharged into hydrosphere causing water pollution. This industrial wastewater contains heavy metals, dyes, phenols, cyanides, acids, sulphates, and organic substances. Out of these pollutants, heavy metal and dye possess lethal risk to flora and fauna alike.

Heavy metals have atomic weights ranging from 63.5 to 200.6 and specific gravity more than 5.0. Since the last century, heavy metals have become one of the most hazardous group of pollutants because of their significant potential toxicity and bio-magnification capability. Efforts to reduce the concentration of heavy metals in effluent wastewaters have increased many folds for compliance with permissible discharge levels as well as for fulfilling ethical obligations (Machida et al., 2004; Sittig, 1991). Various manufacturing activities such as metal plating facilities, mining operations, fertiliser, tanneries, batteries, paper and pesticides contribute to heavy metal pollution especially in developing countries. Heavy metals of particular concern, in relation to the treatment of industrial wastewaters, include zinc, copper, nickel, mercury, cadmium, lead and chromium. Similar to heavy metals, dyes are also toxic in nature. Dyes are material, which is used to colour products in many industries such as textile, paper and plastics. High volume of water is consumed by these industries and a considerable amount of coloured wastewater is generated (Crini, 2006). According to O'Neill et al. (1999) many of these dyes are also toxic and even carcinogenic and this poses a serious hazard to aquatic life. However, wastewater containing dyes such as methylene blue, direct red 23 are very difficult to treat since they are recalcitrant organic molecules (Sun and Yang, 2003).

1.1.1 Progress in wastewater treatment

Since ancient time, the system of wastewater management and treatment have evolved many folds. Evidence of one of the oldest wastewater management systems was identified in the Mohenjo-Daro region near the river Indus which dates back to 1500 BC (Wiesmann et al., 2007). However, in 1913, engineers in the UK invented the activated sludge treatment process that gradually became the industry standard in combination with other treatment units. In the present time, the overall treatment system may comprise of units such as activated / extended aeration plant, primary only treatment plants, solids removal and disinfection plant, sequencing batch reactor (SBR) and facultative/aerated lagoons with moderate variations and advancement. Typically, a wastewater treatment system consists of separate processing units that can treat polluted water to a level that is safe for discharge on land or to receiving water bodies. Wastewater treatment in its primary, secondary and tertiary phases facilitates removal of suspended solids, biodegradable organics, pathogenic bacteria, nutrients and pesticides. However, industrial wastewater containing toxic substances, dye and heavy metals require special techniques to treat the pollutants. This purification or treatment of wastewater is achieved with the aid of various technologies such as reverse osmosis, ion exchange, electrodialysis, electrolysis, chemical oxidation and reduction, acid/base neutralisation, chemical precipitation of metals, flocculation, membrane filtration, micro filtration, ultra-filtration and nano-filtration (Fu and Wang, 2011). Stringent regulations, constraint of budget and the ever-increasing costs associated with these treatments create a demand for an alternative approach to wastewater treatment. Adsorption, in contrast to the other conventional techniques, is a versatile, economical and easily adaptable technology (Hashemian and Foroghimoqhadam, 2014). The process known as adsorption, involves the preferential partitioning of substances from the gaseous or liquid phase onto the surface of a solid substrate.

1.1.2 Contaminant removal by adsorption process

Adsorption is an efficient technique, which can be applied for the removal of soluble and insoluble contaminants and biological pollutants with removal efficiency of 90–99%. As a result, much work has been carried out on wastewater treatment by adsorption.

Adsorption is used in different technical products and processes of various scale including smaller applications such as odour control in car cabins to massive water treatment plant or air separation. In petrochemical industry, adsorption is used for a number of operations such as drying of cracked gas and liquids in ethylene plants, purification of ethylene, propylene, butene, and hexene prior to polymerization. In a chemical plant, the use of adsorption can be observed for CO_2 removal from ammonia synthesis gas, CO_2 removal from H_2/CO mixtures, NO_x removal from gases, CO_2 and water removal from air in air separation plants. In refineries, iso-normal separation, HF alkylation feed drying, polar component removal from isomerization feeds, chloride removal from hydrogen and hydrogen drying are carried out by adsorption method

(Dąbrowski, 2001). These processes depend upon the separation capacity of microporous and/or mesoporous solids such as activated carbon or silica gel.

Adsorption on activated carbon, being a very convenient and cost effective method, is widely used in the industrial wastewater treatment. Heavy metal, inorganics, dyes and other pollutants from the wastewater stream are adsorbed efficiently to maintain the discharge standard set by different countries or respective authorities (Ahmad et al., 2009a; Ahmad et al., 2009b; Anees Ahmad et al., 2007; Dąbrowski, 2001; Marsh and Reinoso, 2006; Rafatullah et al., 2010a). At industrial level, pollutants are removed from water by using columns and contactors filled with suitable adsorbents. According to a calculation by Ali and Gupta (2007), the average cost to treat a million litres of wastewater by adsorption varies from 10 to 200 US$ in comparison to 10–450 US$ per million litres wastewater with the technologies other than adsorption. Although adsorption is less costly than other processes, the cost and complexity of traditional wastewater treatment using activated carbon are making it increasingly difficult for communities and industries to implement and afford. Hence, much attention has been given to the production of low cost activated carbon and other adsorbents. Along with the advances in production methods, application of the adsorption process in industry also requires further development.

1.1.3 Role of microwave technology to eradicate the problems in preparation of activated carbon

Microwave oven which was first designed in 1952 became one of the most famous household cooking appliances during 1980s and 1990s due to its short cooking time and energy saving. Surprisingly, the domestic application of microwave oven actually initiated the industrial application of microwave technology. However, use of microwave technology in material processing became popular not before 1990s (Menéndez et al., 2010). According to Jones et al. (2002), microwave heating has a few advantages over conventional heating, such as higher heating rates, indirect heating, selective heating, greater control of the heating or drying process, smaller equipment size and waste reduction. Microwave heating, also known as dielectric heating, transfers electromagnetic energy to thermal energy. It is a kind of energy conversion rather than heating. The microwaves can penetrate deep into materials and transfer energy, thus volumetric heating of materials is possible unlike heating via an external source (Motasemi and Afzal, 2013).

It is generally accepted that reduction of the production cost remains the main challenge for widespread use of activated carbon. In recent years, researchers (Rafatullah et al., 2010b) have used low cost materials to reduce the cost of production. However, the high consumption of energy in a conventional muffle furnace during the preparation remains a constraint to cost reduction. Heating in a muffle furnace typically takes one to seven hours (Baccar et al., 2009; Dural et al., 2011; Nabais et al., 2011; San Miguel et al., 2003; Tay et al., 2009) to convert the raw material into porous activated carbon, consuming considerably high amount of energy. The reason for requiring this long heating time may be due to the fact that heating occurs from the surface of the material towards the core. This makes the process time consuming and there is no guarantee that the heating would be uniform. Thus, a requirement for developing a more effective heating method for the production of activated carbon with optimal operating conditions is very important. This can be achieved by reduction of the heating time, optimisation of the energy as well as chemical use. Microwave technology can reduce the production time considerably as microwaves can penetrate into the raw material and consequently the heat is produced due to molecular interaction with the microwave energy. In this way, heat is generated throughout the bulk of the material, thus reducing the processing time and improving the overall quality of the activated carbon (Thostenson and Chou, 1999).

1.1.4 High gravimetric technology: an approach towards process intensification

Enhancement of mass transfer with the aid of a centrifugal force field was achieved through the innovation of high gravimetric technology (HIGEE) in the late 1970s by scientist at the Imperial Chemical Industries (London). The mass transfer process is carried out in a doughnut shaped bed called rotating packed bed (RPB) (Stankiewicz and Moulijn, 2000). As mentioned by Lin and Liu (1999), RPB contactor was first designed by Collin Ramshaw and Roger H. Mallinson in the year 1981 for effective mass transfer process between two fluid phases. This doughnut shaped bed is spun at high speed to achieve high centrifugal force in a RPB. Due to the elevated force, very thin liquid films and/or tiny droplets are created in the packing area. Thus, gas-liquid or liquid-liquid or solid-liquid interfaces are renewed constantly, which aid in considerable intensification of mass transfer between the phases through mixing (Wang et al., 2008). Initially, these RPB-HIGEE systems were used in separation processes such as distillation and absorption. However, it can also be applied in mass transfer limited reacting systems. Advantages of using high gravimetric systems are higher throughput and formation of thinner liquid film over the packing. This in turn results in decreased external mass transfer resistance, higher surface packing per unit volume of packed bed, better distribution of liquid over the packing and lower static holdup. This aid in reducing the size of the processing equipment significantly in comparison to a conventional packed bed. Moreover, it is likely to reduce the overall cost of wastewater treatment (Lin and Liu, 1999; Ramshaw and Mallinson, 1981).

1.2 Problem statement

Heavy metal and dye pollution is a severe threat to the environment as well as to human being. Available technologies for treatment of wastewater containing such pollutants are inefficient and costly. Therefore, a robust optimisation of the process parameters is required for environmental friendly production of activated carbon and for the reduction of production cost. Similarly, a detailed study and optimisation of the process parameters for rotating packed bed contactor are required for the evaluation of its applicability in adsorption of heavy metal and dye.

1.3 Aim and objectives

Aim

Enhancement of the efficiency and cost-effectiveness of adsorption process on activated carbon using advanced technologies.

Objectives

The following objectives were set to realise the aim of the study, thereby aid the advancement of the research on heavy metal and dye removal by adsorption on activated carbon.

I. Optimisation of process variables in microwave assisted activated carbon production from locally available waste material, palm kernel shell.
II. Evaluation of the efficacy of the prepared activated carbon for removal of heavy metal and dye.
III. Application of HIGEE technology in rotating packed bed contactor to minimise the contact time for adsorption.
IV. Optimisation of the process parameters of rotating packed bed contactor for heavy metal and dye removal, estimation of the adsorption kinetics, adsorption isotherm.

1.4 Outline of the Thesis

This thesis is comprised of five chapters namely introduction, literature review, methodology, results and discussion while conclusion is the last chapter.

In the introductory chapter, a brief background of the problem related to water pollution, its treatment and the possible solutions to solve these problems have been discussed. Different concepts related to the thesis have been introduced. The problem statement has been identified, the aim of the work has been established and the objectives of the research have been clearly stated. The following chapter titled as the literature review discusses the previous works and publications pertaining to this research for different treatment techniques for water pollution, application of microwave technology in different fields including activated carbon preparation for water treatment. The current research with RPB has also been discussed in the literature review, with its application in adsorption process. The chapter on methodology describes the detailed research methodologies for activated carbon production with the aid of microwave heating, building and commissioning of RPB, application of the activated carbon for adsorption in RPB, measurement of kinetics and optimisation studies. The fourth chapter comprises the results and the discussion. The last chapter includes conclusions and recommendations for future work.

CHAPTER 2: LITERATURE REVIEW

Presence of high levels of persistent and recalcitrant chemicals including heavy metals and dye in industrial effluents has caused major environmental concern all over the world. Since the inception of the end-of-pipe treatment concept, treating such effluents from industries became an essential part of industrial processes. Many methods have been used in this treatment process. Hence, the discussion on the currently available wastewater treatment process, including their advantages and disadvantages is indispensable. This chapter presents an in-depth discussion of the current and available literature on the different treatment methods for removal of heavy metals and dyes from industrial wastewater and related issues. This chapter also examines the use of activated carbon as an adsorbent and the related issues for its use in industry. The application of a rotating packed bed (RPB) as an instrument for adsorption has also been critically analysed here.

2.1 Past research trends for heavy metal removal from wastewater

Pollution by heavy metals, available as soluble ions in industrial wastewater, has become one of the most serious environmental problems today. These are required to be removed before discharging the wastewater in any water body or stream owing to their toxicity. Arsenic, mercury, barium, nickel, cadmium, selenium, chromium, silver, copper, zinc and lead constitute the common types of metallic substances found in industrial wastewater (Armenante, 1997; BrbootI et al., 2011). The heavy metals are very stable and persistent in nature and make the treatment process difficult. In recent years, various methods for heavy metal removal from wastewater have been extensively studied. These technologies include chemical precipitation, ion-exchange, electrochemical methods, membrane filtration, coagulation–flocculation and adsorption (Fu and Wang, 2011). An overview of such technologies is presented in the following sub sections.

2.1.1 Chemical Precipitation

Chemical precipitation is an established and commonly used technology for the removal of metals and other inorganics (Ku and Jung, 2001). This technique is also used extensively for the removal of suspended solids, fats, oil and grease as well as other organic substances like organophosphates from wastewater. In a chemical precipitation process, dissolved or suspended heavy metal contaminants are made to settle out of the solution as solid precipitates of metal hydroxide, metal sulphide or heavy metal chelate, by the application of chemicals. The solid precipitate is then separated from the liquid portion by filtration, centrifugation or other techniques (EPA, 2000). A voluminous precipitate can capture ions and particles during its formation and settling, in effect, "sweeping" ions and particles from the wastewater (Tchobanoglous and Burton, 1991). There are mainly two types of chemical precipitation techniques, which are used in industry, namely, hydroxide precipitation and sulphide precipitation.

Due to the amphoteric nature of heavy metals, their solubility reaches a minimum at a specific pH value. When the pH of the wastewater is adjusted with alkali to a specific value, the solubility of a heavy metal may reach its critical value that leads to precipitation of excess ions in the form of a metal hydroxide. The chemical reaction involved in heavy metal removal by hydroxide precipitation is presented in equation 2.1:

$$M^{2+} + 2(OH)^{-} = M(OH)_2\downarrow \tag{2.1}$$

Precipitation of metals in the form of sulphides is another process to remove heavy metals through chemical precipitation. Metal sulphides are very much insoluble. In fact, the metal sulphides are less soluble than their hydroxide counterparts. Sulphide precipitation occurs in highly alkaline medium and it requires addition of coagulants to settle the colloidal metal sulphide particles (Asterion, 2013). A summary of the removal of heavy metals by chemical precipitation is provided in Table 2.1.

Table 2.1 Removal of heavy metal by chemical precipitation

Chemical precipitant	Heavy metal removed	Initial concentration	Removal efficiency	pH	Reference
Lime ($Ca(OH)_2$)	Zn, Cd, Mn and Mg	450, 150, 1,085 and 3,154 mg/L	99%	>9.5	(Charerntanyarak, 1999)
Synthetic iron sulphide (H_2S)	Cu^{2+}, Cd^{2+} and Pb^{2+}	100 mg/L	>90%	<3	(Özverdi and Erdem, 2006)
Mixture of CaO and MgO (4:1, by weight)	Cr^{3+}	5363 mg/L	99%	8	(Guo et al., 2006)
Sulphate-reducing bacteria (H_2S)	Cu^{2+}, Zn^{2+}, Pb^{2+}	0.018, 1.34, 2.3 mM	>90%	3	(Alvarez et al., 2007)
Lime (CaO)	Cu^{2+}, Zn^{2+}, Cr^{3+}, Pb^{2+}	100 mg/L	>99	8-10	(Chen et al., 2009)
Calcium oxide (CaO)	Zn^{2+}	32 mg/L	>99	10	(Ghosh et al., 2011)
Sulphate-reducing bacteria (HS^{-} and/or S^{2-})	Cr_{total}, Cu(II), Fe(II), Ni(II) and Zn(II)	125, 33, 130, 218 and 250 mg/L	85-98%	6.67	(Kosińska and Miśkiewicz, 2012)

Chemical precipitation of metal ions in the forms of hydroxide, sulphide and chelate can be easily adopted by industry. They also have economic advantages over other physico-chemical methods. However, there are a few disadvantages for chemical precipitation techniques such as the necessity to maintain specific pH conditions, temperature and ion concentration. Hydroxide precipitation generates large volumes of relatively low density sludge, which can present dewatering and disposal problems

(Kongsricharoern and Polprasert, 1995). If the solution contains different metal ions then the selected pH for generation of precipitate of one metal may not be suitable for precipitation of another present in the same solution. Sulphide precipitants in acidic conditions can produce toxic H_2S fumes. These sulphide precipitates are sometimes colloidal in nature, creating separation problems. Chelating precipitates also pose a threat to environment as these can also be toxic. However, it is reported that scientists (Chang et al., 2002; Matlock et al., 2002; Ying and Fang, 2006) have designed and synthesized a new thiol-based compound, 1,3-benzenediamidoethanethiol ($BDET^{2-}$) dianion, ethyl xanthate and dipropyl dithiophosphate, an organic heavy metal chelator , which were successfully used for heavy metal treatment.

2.1.2 Ion exchange

Toxic ions present in wastewater are exchanged with the non-toxic ions from a solid material known as an ion exchanger (Gupta et al., 2012a). There are two types of ion exchangers namely cation exchangers and anion exchangers. Ion exchangers are natural or synthetic resins with active sites on their surfaces. The most commonly used ion exchangers are sodium silicates, zeolites, polystyrene sulfonic acid, and acrylic and metha-acrylic resins.

Ion exchange process has few distinctive advantages such as high treatment capacity, high removal efficiency and fast kinetics (Kang et al., 2004). Synthetic resins, natural zeolites, naturally occurring silicate minerals are some of the materials used to remove heavy metals from aqueous solutions due to their low cost and high abundance. Natural zeolite is a good material for ion exchange (Fu and Wang, 2011; Rosales et al., 2012). According to Gode and Pehlivan (2006), the removal of heavy metals depends upon factors such as pH, temperature, initial metal concentration and contact time. However, industrial use of these zeolites is still limited. Much work is required in this field.

Dąbrowski et al. (2004) discussed selective removal of different heavy metals such as Pb(II), Hg(II), Cd(II), Ni(II), V(IV,V), Cr(III,VI), Cu(II) and Zn(II) from water and industrial effluents by ion exchange methods. They have reviewed the studies on removal of various metals using different ion exchangers. Xu (2005) has discussed the state of development of different types of ion exchange membrane for application in different fields. Lewatit MP 64 and Lewatit MP 500, which are macroporous resins containing quarternary amine groups were studied for Cr(VI) removal. In a batch process, 82–88% removal from aqueous solution was achieved in 60 min (Pehlivan and Cetin, 2009). Dowex HCR S/S cation exchange resin was also evaluated for removal of nickel and zinc from aqueous media (Alyüz and Veli, 2009). About 98% removal efficiency was obtained at optimal condition. Vinodh et al. (2011) used quaternised poly (styrene ethylene butylene poly styrene) [QAPSEBS] for the removal of Cr(VI), Cu(II) and Ni(II) ions from water. A removal capacity of 50 to 80 % were obtained for the heavy metals concerned.

2.1.3 Membrane filtration

Essentially membrane filtration is the separation or removal of bacteria, microorganisms, particulates and natural organic materials, which are responsible for rendering colour, taste and odour to water, by a thin semi permeable material known as membrane. Membrane filtration possess a great potential for the heavy metal treatment. The technology is highly efficient, easy to operate and space saving. Commonly used membrane filtration techniques comprise ultrafiltration, reverse osmosis, nanofiltration and electrodialysis.

Fu and Wang (2011) in their review article elaborated the main characteristics of different membrane filtration techniques. They critically discussed the history and development of ultrafiltration, reverse osmosis, nanofiltration and electrodialysis. A discussion on the effort made by different researchers to remove heavy metals by these techniques in terms of the initial concentration, reaction conditions and removal efficiencies.

A laboratory scale experiment has been reported by Camarillo et al. (2012) for the removal of Cu(II) ions by using polymer enhanced ultrafiltration (PEUF). It has also reported a new kinetic model to predict the temporal evolution of metal concentration in both permeate and rejected streams in a batch process. Another published (Qiu and Mao, 2013) work reported a combination of copolymer of maleic acid and acrylic acid (PMA-100 and polyvinyl butyral (PVB) hollow fibre ultrafiltration membrane for the removal of different heavy metals such as Cu^{2+}, Zn^{2+}, Ni^{2+} and Mn^{2+} .

Micellar-enhanced ultrafiltration (MEUF) was employed by Landaburu-Aguirre et al. (2012) to remove heavy metals such as Cu and Cd from phosphorous rich drainage water of a fertiliser company. The optimum rejection coefficients at the pH value of 3.2 and SDS feed concentration of 75.6 mM were 84.3% and 75.0% for copper and for cadmium, respectively. They reported negligible irreversible fouling and secondary pollution due to SDS leakage.

In another study, Zn(II), Pb(II), Cr(III), and Cr(VI) were removed from aqueous solutions by polymer-enhanced ultrafiltration (PEUF) using unmodified starch as binding biopolymer (Baharuddin et al., 2015). The authors reported about 90% rejection of heavy metals for metal concentration of 10 mg/L at pH7.

Kanagaraj et al. (2015) modified polyether-imide (PEI) ultrafiltration membrane by blending 2% N-phthaloyl chitosan (NPHCs) with it. They used it to remove heavy metals such as Cr(III), Zn(II), Cd(II) and Pb(II). In case of heavy metal ions, the separation efficiency increased and flux decreased as the charge density of the ion increased due to the enhanced ion–polymer ligand formation. It was observed that the ionic rejections are in the descending order of Cr(III) > Zn(II) > Cd(II) > Pb(II). Hence, a conclusion was made that the ions of higher charge density tend to be bound more strongly to the polymer-chelating agent, resulting in higher rejection.

Nanofiltration has also been used in recent years for heavy metal removal. Commercial nanofiltration membrane (NF270) was used to remove heavy metals such as Cu^{2+}, Cd^{2+}, Mn^{2+}, Pb^{2+} and As^{3+} from wastewater (Al-Rashdi et al., 2013). The reaction condition used was 1000 mg/L concentration, pH = 1.5 ± 0.2 and 4 bar pressure. The rejection ratios under these conditions were 99%, 89% and 74% for cadmium, manganese and lead, respectively. However, the membrane could not retain As(III).

A high performance nanofiltration membrane was developed using chelating polymers containing negatively charged functional groups such as poly (acrylic acid-co-maleic acid) (PAM), poly (acrylic acid) (PAA) and poly (dimethylamine-co-epichlorohydrin-co-ethylenediamine) (PDMED) and the positively charged polyethyleneimine (PEI) cross-linked P84 hollow fibre substrates (Gao et al., 2014). The membrane showed very impressive performance for removal of heavy metals such as lead, copper, nickel, cadmium and zinc. The rejection was 98% for single metal and 99% for mixed ions

Static layer-by-layer (LBL) self-assembly of poly (ethyleneimine) (PEI) and poly (sodium 4-styrenesulfonate) (PSS) on the modified poly-arcylonitrile ultra-filtration membrane was employed by Chen et al. (2014) to synthesise a nanofiltration membrane. More than 90% rejection was obtained for Ni(II) and Cd(II) at operating pressure 0.4MPa.

Thong et al. (2014) reported a first attempt to develop a composite nanofiltration membrane made of a molecularly designed pentablock copolymer selective layer. They reported more than 98% rejection rate for Pb^{2+}, Cd^{2+}, Zn^{2+}, and Ni^{2+} by the novel membrane.

Polyamide nanofiltration membrane with a net negative surface charge was used to remove heavy metals for drinking water production. The operating conditions namely pH value, feed flow and applied pressure on heavy metal removal were optimised using response surface methodology. At the optimum operating condition, 93% nickel and 86% of lead were removed (Maher et al., 2014).

A novel forward osmosis process was demonstrated for the first time by Cui et al. (2014) for heavy metal removal. The system contains a thin-film composite forward osmosis membrane. The composite was prepared from interfacial polymerization on a macrovoid-free polyimide support and a novel bulky hydroacid complex $Na_4[Co(C_6H_4O_7)_2]\cdot 2H_2O$ (Na–Co–CA). A very high rejection rate of 99.5% was reported by them with water fluxes around 11 L/m^2h and initial concentration of metals (lead, copper, cadmium and mercury) of 2000 ppm. Mahmoud and Hoadley (2012) applied electrodeionisation (IXED) which is a hybrid technique of conventional ion exchange and electrodialysis to intensify mass transfer and increase limiting current density.

Though highly efficient but high cost, process complexity, membrane fouling and low permeate flux have limited their use in heavy metal removal.

2.1.4 Coagulation and flocculation

Coagulation and flocculation followed by sedimentation and filtration are also employed to remove heavy metals from wastewater. Coagulation is the destabilisation of colloids by neutralising the forces that keep them apart. Hankins et al. (2006) used cationic polyelectrolyte polydiallyldimethylammonium chloride (PolyDADMAC) for coagulation and flocculation after binding Pb^{2+} and Zn^{2+} ions to humic acid; but this method involves chemical consumption and increased sludge volume generation. This process alone is not sufficient for removal of heavy metals to a satisfactory level (Chang and Wang, 2007). According to Rubio et al. (2002), flotation has advantages in terms of metal selectivity, removal efficiency, overflow rates, detention periods, operating cost and production of more concentrated sludge. In recent years, some researches have used coagulation-flocculation for heavy metals. Pang et al. (2011) used aluminium sulfate (alum), polyaluminium chloride (PACl) and magnesium chloride ($MgCl_2$) as coagulants for removal of lead, zinc and iron. They reported above 99% removal with PAIC for the heavy metals. In a different study Ravikumar and Sheeja (2013) utilised a natural bio-polymer *Moringa oleifera* seed as a coagulant. They obtained a removal of 95% for copper, 93% for lead, 76% for cadmium and 70% for chromium. Commercially available coagulants such as ferric chloride solution (CLARFER) and a polyaluminium chloride (WAC HB) were used to treat combined sewer overflow (CSO) for coagulation (El Samrani et al., 2008). The WAC HB had lower optimum dosages and higher re-stabilization concentrations. The heavy metal removal was dependent upon the turbidity removal and coagulant dosage of Cu, Zn, Pb, Cr, soluble and suspended solids contents followed various patterns. Vedrenne et al. (2012) treated landfill leachate, containing Hg, Pb, and As, from Tetlama, Morelos (Mexico) with optimal dose of $FeCl_3 \cdot 6H_2O$ of 300 mg/L. The removal efficiency for Pb was very good (85%) whereas removal of As was moderate (46%). However, removal efficiency for Hg was only 9%.

Although, this method has been used by different researchers for wastewater treatment, however, the disadvantages associated with coagulation and flocculation are high initial capital outlay, maintenance and operational costs. This method alone is not sufficient to treat wastewater. Filtration is required for the flocs when they are precipitated.

2.1.5 Electrochemical treatment

Electrochemical treatment of wastewater containing heavy metals are regarded as effective to remove heavy metal. It requires fewer chemicals and achieves good reduction yields while producing less sludge. Electrocoagulation process using iron electrode with monopolar configuration was employed to remove Cu, Ni, Zn and Mn from synthetic wastewater. For the heavy metals Cu, Ni and Zn a removal of 96% was obtained while a removal of 72% was obtained for Mn. About 49 kWh/m^3 energy was consumed at 25 mA/cm^2 of current density during the removal process (Al Aji et al., 2012). Stainless steel mesh coated with single walled carbon nanotubes were used both as anode and as cathode for removal of lead. About 99% removal efficiency was obtained after 90 min treatment at optimal condition. Reduction and deposition of lead ions onto cathode was suggested as the plausible mechanism (Liu et al., 2013). Electrochemical treatment with iron anodes for treatment of wastewater containing binary mixture of heavy metal and dye were tested by Körbahti et al. (2011). They used [AB29|Cu(II)], [RR2|Cu(II)], [AR97|Ni(II)], and [RB4|Ni(II)] binary mixtures. Optimisation of the process parameters were done using RSM and at the optimised condition, a removal of 95% of both dye and metal removal was obtained.

Electrocoagulation is a technique, which has found more use in case of heavy metal removal in recent years. Al-Shannag et al. (2015) used electro-coagulation technique with the aid of six carbon steel electrodes in monopolar configuration to remove Cu^{2+}, Cr^{3+}, Ni^{2+} and Zn^{2+}, from metal plating wastewater. Metal removal was dependent upon electrocoagulation (EC) residence time and direct current density. At current density of 4 mA/cm^2, pH of 9.56 and EC time of 45 min they obtained 97% removal of heavy metals. Low energy consumption made their process economically feasible and suitable for scale up. Bhagawan et al. (2014) also used electrocoagulation technique with the aid of Fe-Fe electrode pair for the removal of Cr, Cu, Pb, Ni, and Zn. They obtained removal of more than 96% for all heavy metals at optimum condition of 1cm inter-electrode distance and electrode surface area of 40 cm^2 and applied voltage of 8 V. However, electrochemical technologies require high capital investment and running cost that restricts its development.

2.2 Past research trends for dye removal from wastewater

The history of dyestuff dates back to as long as 5000 years, when people used to derive colour from natural sources such as roots, bark and leaves of tree. In the year 1856, Sir William Perkin discovered the first synthetic dye for the colour mauve and thereafter numerous synthetic dyes have been produced. Now there are over 100,000 dyestuffs available commercially and the production amounts to 700,000 tons per year (Atalay and Ersöz, 2015; Robinson et al., 2001). As mentioned by Singh and Arora (2011), approximately 2% of the dyes produced annually are discharged directly to water bodies, and 10% is subsequently lost during the coloration process. According to another report by Atalay and Ersöz (2015), current available technologies can only remove about 50% of the total amount of dyes found in wastewater. Some dyes are reportedly allergic, carcinogenic, and mutagenic. Not only most of the dyestuffs are harmful to living creatures, they have the capacity to absorb and reflect sunlight entering the water, which affects the growth of bacteria, limiting it to levels insufficient to degrade impurities in the water biologically.

Treatment of wastewater containing dyes are done by using different physical, chemical and biological methods. There are few in-depth review articles available that discuss the technologies used for removal of dyestuffs and highlight the advantages and disadvantages of those technologies (Atalay and Ersöz, 2015; Robinson, et al., 2001; Singh and Arora, 2011). In the following sub-sections, recent work by the researchers for dye effluent treatment by different methods is discussed.

2.2.1 Advanced oxidation processes

Advanced Oxidation Processes (AOPs) have emerged as a favourable technology to treat wastewater that contain dyestuffs. In AOPs, highly reactive radicals, especially hydroxyl radicals, are produced which are responsible for the destruction and mineralisation of target compounds. There are two main types of advanced oxidation processes, namely photochemical and non-photochemical methods. Processes such as ozonation, ozonation with hydrogen peroxide, fenton method, and wet air oxidation are examples of non-photochemical oxidation, while photocatalytic oxidation, oxidation with H_2O_2, O_3 in presence of UV radiation and photo-Fenton methods are known as photochemical oxidation.

Ozonation is a very effective and powerful technology for degradation of dyestuffs. Ozone can indirectly or directly breakdown the conjugated double bonds in dyes. In recent years, some researches are conducted for decolourisation by ozonation. Decolourisation of synthetic wastewater containing methylene blue dye was performed by Turhan et al. (2012) in a batch bubble column reactor. They found that pH 12 and high ozone concentration provide good condition for decolourisation. The kinetics of decolourisation was pseudo-first-order. It was explained that self-decomposition of ozone at higher pH and increasing ozone concentration at high ozone dose to be responsible for quick decolourisation.

An investigation of Reactive Red 198 (RR198) and Reactive Red 120 (RR120) dye removal with photocatalytic ozonation with copper ferrite ($CuFe_2O_4$) nanoparticle (CF nanoparticle) prepared by co-precipitation method showed that relatively safe compounds (NO_3^- and SO_4^{2-}) are obtained as a mineralisation product using this method. Added advantage was the potential to treat high volumes of effluent using low pressure oxygen and no requirement of heating (Mahmoodi, 2011). Mahmoodi (2013) further studied the photocatalytic ozonation (UV/O_3) using multiwalled carbon nanotube (MWCNT) for decolourisation of Reactive Red 198 (RR198) and Direct Green 6 (DG6). He also studied the effect of operating parameters such as carbon nanotube dosage, dye concentration, salt (inorganic anions) and pH on dye degradation. The decolourisation process was very fast. Within 8 to 12 min, almost total removal was obtained. It was concluded that UV/O_3/MWCNT may be a viable one for treatment of large volume of aqueous coloured dye solution.

Combined biodegradation and ozonation was applied for the treatment of wastewater containing tannins and dyes. The combined method was able to remove 92–95%, 94–95%, and 85–87% of the wattle extract (tannin), dyes and chromium compounds, respectively. About 78% of dye could be removed by ozonation in 240 min (Kanagaraj and Mandal, 2012). Mezzanotte et al. (2013) investigated the colour removal efficiency and by-product generation of high dose ozonation such as 10–60 mg O_3/L of textile dyeing wastewater.

Photocatalytic degradation by titanium dioxide (TiO_2), offers an effective treatment option for wastewater because of its low cost, non-toxicity, stability and highly reactive behaviour. This method is particularly valuable in treating wastewater that contain dyestuffs, which are difficult to degrade by conventional methods. Extensive work was carried out for degradation of Tropaeolin 000, tartrazine and quinoline yellow (Gupta et al., 2012b; Gupta et al., 2011b; Gupta et al., 2011c). Various parameters such as dye concentration, photocatalyst concentration, pH of the solution, substrate concentration and electron acceptor such as hydrogen peroxide on the degradation rate was studied. The removal rate followed first order kinetics. The main advantage of the process was complete mineralisation of the dyestuff.

Degradation of Direct Green 6 and Reactive Orange72 dye were investigated by Karimi et al. (2014) using nano-strontium titanate as photo catalyst. Different operating parameters such as photo-catalyst concentration, dye concentration, temperature, pH and the concentration of hydrogen peroxide on the removal rate under UV irradiation was studied. Nano-strontium titanate was found to be a better catalyst than nano-titanium dioxide.

2.2.2 Membrane filtration

Membrane filtration was found equally applicable to dye removal as heavy metal removal. Recently several works have been reported on the application of ultrafiltration and nanofiltration units for treatment of dye effluents. Aouni et al. (2012) used Polyethersulfone membranes (10 kDa and 1 kDa) and nanofiltration membranes (NF200 and NF270) for treatment of Everzol Black, Everzol Blue, Everzol Red dyes. The nanofiltration membranes had about 90% colour retention rates whereas total decolourisation was observed for 1 kDa membrane.

Decolourisation of Reactive Black 5 (RB5) solutions with the aid of a multichannel tubular ultrafiltration (UF) ceramic membrane was investigated using different dye concentrations. About 80% rejection regardless of the experimental condition for dye concentration of 50 mg/L with permeate flux of 266.81 L/m^{2}h was obtained at 3 bar (Alventosa-deLara et al., 2012).

The efficiency of orange G dye removal was enhanced by deposition of powdered activated carbon (PAC) on an ultrafiltration membrane forming a compact filter cake. It was observed that the carbon pack removed the dye satisfactorily at optimum operating condition without reducing the permeate flux considerably. The dye rejection ratio increased from 43.6% for single UF without adsorption to nearly 100% for the combined PAC-UF process, achieving long time continuous treatment with water permeation flux of 47 L/m^2 h (Dong et al., 2011).

A fabricated nanofiltration membrane comprising aromatic poly (m-phenylene isophthalamide) (PMIA) nanofiltration (NF) membrane with polyvinyl pyrrolidone

(PVP) and LiCl as an additive was used for removal of dyes, Eriochrome black T, Eriochrome blue black B and Alizarine red. The recorded rejection rate was over 98%, with a flux about 80 L/m^{2}h. Acrylic grafted nanomembrane was used to remove several textile dyes from wastewater. As reported in the study, the dye rejection was 86–99.9% while the hydraulic permeability was 7.6 L/m^2 h bar. Presence of salt in the dye solution reduced the rejection rate considerably. In general, acrylic grafted nanomembrane was found to be very efficient for treatment of wastewater containing dye (Amini et al., 2011).

Another study on thin film composite of sodium carboxymethyl cellulose (CMCNa)/polypropylene (PP) hollow fibre nanomembrane to decolourise solutions of Congo Red, Sunset Yellow and Methyl blue reported that 80 to 99% rejection rate was obtained for all the dyes at permeability rate of 7 L/m^2 h bar (Yu et al., 2012b) .

Maurya et al. (2012) developed a hollow fibre based nanofiltration membrane by in-situ polymerisation of *m*-phenylene diamine with trimesoyl chloride. The performance of this nanomembrane was studied in the separation of dyes from water. A rejections rate of 60–97% for reactive black-5 and rhodamine-B with water flux of 10–35 mL/m^2 h at 25 psi for feed solutions containing 400–2000 ppm dye was obtained in the study.

2.2.3 Electrochemical treatment

Electrochemical treatment has also been developed as a technology for wastewater treatment over the past few decades. Electrocoagulation and electrochemical oxidation are two techniques used for treatment of dye (Ahmad et al., 2015). In the recent years, several researchers have used electrochemical treatment method for treating dye effluent

Amani-Ghadim et al. (2013) used electrocoagulation with iron (EC-Fe) and aluminium (EC-Al) anodes to remove C.I. Reactive Red 43. At the optimum condition, about 99% dye removal was obtained. Several researchers have tried different anodes for removal of different dyestuff such as titanium anode for removal of Procion Scarlet (Senthilkumar et al., 2012), PTFE for Eosin B removal (Prakash et al., 2011), iron for decolourisation of different textile dye (Körbahti, et al., 2011), graphite for leather dyes (Direct black 168, Acid red 119, Direct blue 78, Acid brown 98, Acid blue 312 and Acid yellow 166) removal (Rosales et al., 2011) and boron-doped diamond for C.I. Acid Blue 92 removal (Vahid and Khataee, 2013). All these studies showed promising results for dye removal.

The methods discussed above have their own advantage and disadvantages. Fenton reagent and membrane filtration would be good removal methods for all dye types. However, this method is associated with the problem of sludge generation. On the other hand, a photochemical process can be advantageous where no sludge is produced but the decolourisation process itself will create formation of toxic by-products. Decolourisation by the ion exchange method has no adsorbent loss on regeneration but it is only effective on certain type of dyes. In addition, the high maintenance and operational costs make many of these methods unacceptable to the industry (Ghoreishi and Haghighi, 2003).

2.3 Past research trends on adsorption on activated carbon for heavy metal and dye removal

Adsorption has been defined by IUPAC as "*Increase in the concentration of a substance at the interface of a condensed and a liquid or gaseous layer owing to the operation of surface forces*." It means that adsorption is the adhesion of atoms, ions, or molecules from a gas, liquid, or dissolved solid to a surface. When this is done by biological material, it is known as biosorption. Activated carbons have high internal surface area, ranging from 500 to 1500 m^2/g, which makes it an ideal adsorbent (Norit-AC) for variety of substances. In recent years, adsorption process has attracted much attention from the research fraternity for the versatility of its application in wastewater treatment. Low cost adsorbents are used by many researchers for removal of dyestuff and heavy metals (Dias et al., 2007; Fu and Wang, 2011; Gupta and Rastogi, 2008). Different materials have been used to prepare low cost adsorbent or activated carbon for removal of heavy metals and dyes from wastewater. Neem bark powder (Arshad et al., 2008; Kumar and Phanikumar, 2012; Srivastava and Rupainwar, 2011), almond shells (Doulati Ardejani et al., 2008; Mehrasbi et al., 2009), saw dust (Dakiky et al., 2002; Naiya et al., 2009), *Hevea Brasilinesis* (rubber wood), coconut tree saw dust (Selvi et al., 2001), hazelnut shell (Cimino et al., 2000), rice straw (Gao et al., 2008), eucalyptus bark (Sarin and Pant, 2006), palm shell (Owlad et al., 2010), modified holly sawdust (Siboni et al., 2011), rice bran, wheat bran (Wang, et al., 2008), activated *Terminalia arjuna* nuts (Mohanty et al., 2005), tamarind wood activated carbon (Acharya et al., 2009)**,** Bael fruit shell activated carbon (Anandkumar and Mandal, 2009; Gottipati and Mishra, 2010a), have been used by different research groups for removal of hexavalent chromium, zinc, lead, cadmium and dye.

Adsorption is usually coupled with desorption process to regenerate the adsorbent for reuse (Rozada et al., 2005; Walker and Weatherley, 1997; Xing et al., 2008; Yao et al., 2009). Desorption is a phenomenon where a substance is released from or through a surface. The process is the opposite of adsorption. The desorption mechanism may involve ion exchange or complexation, where metals are eluted from the biosorbent by an appropriate solution to produce a small, concentrated volume of metal-containing solution, from which metals may be recovered (Gupta and Rastogi, 2008; Mata et al., 2010; Njikam and Schiewer, 2012; Tan et al., 2002). A problem that arises from the handling of exhausted biomass from the biosorption process can be solved by desorption and reutilisation of the biosorbents in adsorption–desorption cycles. This will reduce the cost of the treatment process as well as the amount of the spent biosorbent (Khan et al., 2012; Mata, et al., 2010).

2.3.1 Optimisation studies on adsorption of heavy metal and dye

In the recent past, extensive research was conducted to optimise the adsorption process on activated carbon as well as other adsorbents. The commonly used optimisation method was observed to be central composite design (CCD) and Box-Behenken (BB) design in response surface methodology (RSM) and Taguchi method. An optimization of a problem is to solve quantitatively the best solution from all feasible solutions and to obtain the values of controllable variables determining the behaviour of a system as maximizing or minimizing functions.

Gottipati and Mishra (2010b) tested two-level full factorial design (FFD) in a shake-flask system for Cr(VI) removal with commercial activated carbon and activated carbon prepared from bael fruit (*Aegle marmelos*) shell (BFS AC). Optimisation of the process was carried out by using desirability (*D*) function by targeting the factors to desired levels for maximum removal of Cr(VI). According to the researcher, the factorial design reduces the number of experiments and also determines the effect of each factor on response as well as considers the interactive effects. They reported that a maximum removal of 96.34% was obtained at pH of 6.39, initial concentration of Cr(VI) of 7.51 mg/l, adsorbent dose of 2.18 g/l and temperature of 36.38 °C with 0.989 desirability with BFS AC.

Cronje et al. (2011) designed a 2^4 full factorial central composite design (CCD) experiment to obtain optimum condition for removal of Cr(VI). They used activated carbon derived from chemical activation of sugarcane bagasse by zinc chloride. From the response surface generated according to the second order equation it was observed that the optimum conditions for Cr(VI) removal were adsorbent dose of 6.85 g/L, temperature of 40 °C, initial concentration of Cr(VI) of 77.5 mg/L while initial pH of the Cr(VI) solution was found to be 8.58. However, the study does not elucidate the reasons behind such 3D surfaces. A similar 2^4 full factorial CCD experimental design was used to optimise and model lead removal from synthetic wastewater. Activated carbon derived from tamarind wood with chemical activation by zinc chloride was used for this purpose. Under the optimised operating condition such as adsorbent dose 1.44 g L^{-1}, temperature 50°C, initial concentration of lead (II) 49.23 mg L^{-1} and initial pH of the lead (II) solution 4.07, the removal of lead was more than 99% (Sahu et al., 2016). CCD was used for determining the optimum condition of Orange G dye removal from aqueous system by activated carbon prepared from the pods of *Thespesia populnea*. Parameters such as agitation time, initial dye concentration and adsorbent dosage were studied and their interactive effects were demonstrated by the contour plots. The optimum levels of time, carbon and Orange G dye for adsorption were found to be 4.03 h, 0.54 g and 17.6 mg L^{-1}, respectively (Arulkumar et al., 2011).

Box–Behnken design was used by de Luna et al. (2013) for removal of Eriochrome Black T (EBT) from aqueous solution using rice hull-based activated carbon. Process parameters such as initial dye concentration, adsorbent dose and pH were studied to optimise the removal efficiency of the activated carbon. The interactions were shown in three-dimensional curves. The ANOVA data showed that initial concentration (coded as A), adsorbent dose (coded as B), pH (coded as C) and C^2 had high F-value and low probability value (p-value) which imply that these quadratic model coefficients are significant. With very low p value of the model quadratic equation also suggested that the model equation was successfully validate the obtained data.

Barman et al. (2011) described Taguchi method as a simple and systematic approach to optimize design for performance, quality, and cost. They studied adsorption of Congo Red (CR) onto powdered and granular activated carbon and indigenously prepared low-cost adsorbents such as bagasse fly ash (BFA), rice husk ash (RHA), coconut shell carbon (CSC), fruit juice extract (FJE), BAEL (*Aegle marmelos*), and spent tea granules (STG).

It was observed that the STG is the best adsorbent and the optimum condition obtained for CR removal by STG was pH of 2, contact time of 500 min, temperature of 60 ^{o}C, and initial concentration of 500 mg/L. A systematic optimisation approach for removal of Pb and Hg by a nanostructure, zinc oxide-modified mesoporous carbon was described by Zolfaghari et al. (2011). An L_{16} (4^5) orthogonal array was chosen for the purpose of optimisation of agitation time, initial concentration, temperature, dose and pH of solution. The analysis of mean (ANOM) statistical approach is adopted herein to develop the optimal conditions. They reported that the optimum conditions for removal of Pb(II) and Hg(II) were the agitation time of 120 min, the initial concentration of 10 mg/l, the temperature of 35 °C, the dose of 0.7 g/l, and the pH of 6.

Taguchi method was used by Kavand et al. (2014) to obtain a robust optimum condition of the adsorption parameters such as, initial metal concentration of each metal ion ($C_{0,i}$), initial pH (pH_0), adsorbent dosage (m) and contact time (t) in a batch process. The interaction between the metal ions lead, nickel and cadmium were considered in different combination for the simultaneous uptake of metals. It was reported in the study that the optimum condition for metal ion adsorption was $C_{0,i}$ =100 mg L^{-1}, pH_0=7, m=2 g L^{-1} and t=80 min.

Yin et al. (2013) used RSM with the CCD to determine how Au(III) biosorption on organophosphonic acid functionalized spent buckwheat hulls (OPA-BH) to understand the influence of pH, biosorbent dosage and initial ion concentration on the removal of the metal. Almost similar work was done by Xu et al. (2013) for Au(II) removal. They tested the same parameters with rice husk based adsorbent. Zolgharnein et al. (2013) compared CCD, BB and Doehlert matrix for multivariate optimisation of Pb(II) removal. In these full-factorial designs, parameters such as pH, sorbent dosage and initial ion concentration were found to be significant for the adsorption process. The desirability function with maximum ion uptake was used to optimise the parameters. According to the article, CCD was the most accurate optimisation method. Witek-Krowiak et al. (2013) used three-variable-three-level BB design to determine the optimal conditions for biosorption of Cr(III) on soybean meal. They used MATLAB software to predict the optimum condition. Three independent factors namely, adsorbent dosage, the initial Cr(III) concentration and temperature was studied for the maximum uptake of Cr(III) by soybean meal, which was 61.07 mg/g.

In very interesting study Ghaedi et al. (2015) applied bee algorithm (BA) superimposed with response surface methodology to predict the optimum condition for copper (II) removal using activated carbon prepared from Pomegranate wood modified with 1-(2-fluorobenzoyl)-3-thiourea (FTPT). The BA technique solves a problem by imitating the behaviour of honeybees to find the optimum experimental condition among the solutions (Pham and Castellani, 2009). The optimum conditions obtained by the BA algorithm when superimposed with RSM are 1.6 g of adsorbent dosage, 28.6 mg L^{-1} of initial ion concentration, pH 5.6, 36.1 °C of temperature and 70 min of contact time.

2.4 Applications of microwave technology in industrial processes

The region between infrared and radiowave of the electromagnetic spectrum is termed as microwave region having wavelength 0.001 to 1 m. The microwave frequency is used extensively by communication systems such as radar and telecommunication. However, Federal Communications Commission (FCC) has reserved two frequencies at 915 and 2450 MHz, having a wavelength of 12.2 cm and energy of 1.02×10^{-5} eV, for the purpose of industrial, scientific, and medical (ISM) uses (Jones, et al., 2002; Kappe et al., 2012; Van Loock, 2006). Since last three decades, application of microwave technology has gained major attention due to its rapid, energy-efficient heating of materials. However, only few materials are there that can be heated rapidly by microwaves. Materials may be classified into three groups, i.e. conductors, insulators and absorbers, with respect to interaction with microwaves. The conductors reflect the microwave, the insulators allows the microwave to pass through them without any change and the absorbers absorb the microwave (Motasemi and Afzal, 2013). The materials, which absorb microwaves, are called dielectric materials and the microwave heating is called dielectric heating. Dielectrics contain dipoles, which may be present naturally or may be induced in the material. The dielectric loss tangent $\tan\delta = \varepsilon'' / \varepsilon'$ determines the ability of the microwave to heat a material where ε' is the dielectric constant or real permittivity and ε'' is the dielectric loss function or imaginary permittivity. The dielectric constant measures the reflected and absorbed amount of incident energy whereas the dielectric loss function measures the dissipation of electric energy in the form of heat within the material (Menéndez, et al., 2010; Zlotorzynski, 1995). Therefore, a large value of $\tan\delta$ signifies better conversion of microwave energy to thermal energy. In their review paper, Menéndez, et al. (2010) have opined that carbon materials are good absorber of microwave.

In conventional heating, the external surface of a material is heated first and the heat is transferred to the core of the material through conduction, convection and radiation. This creates a thermal gradient from the surface to the core (Hoseinzadeh Hesas et al., 2013c). Hence, it takes time to heat the whole material properly in a conventional heating process. However, in microwave or dielectric heating, depending upon the $\tan\delta$ value, the microwaves are absorbed in the material and electromagnetic energy is converted to thermal energy. Thus heat is generated throughout the volume of the material unlike the conventional heating process (Motasemi and Afzal, 2013). The mechanism is illustrated in Figure 2.1.

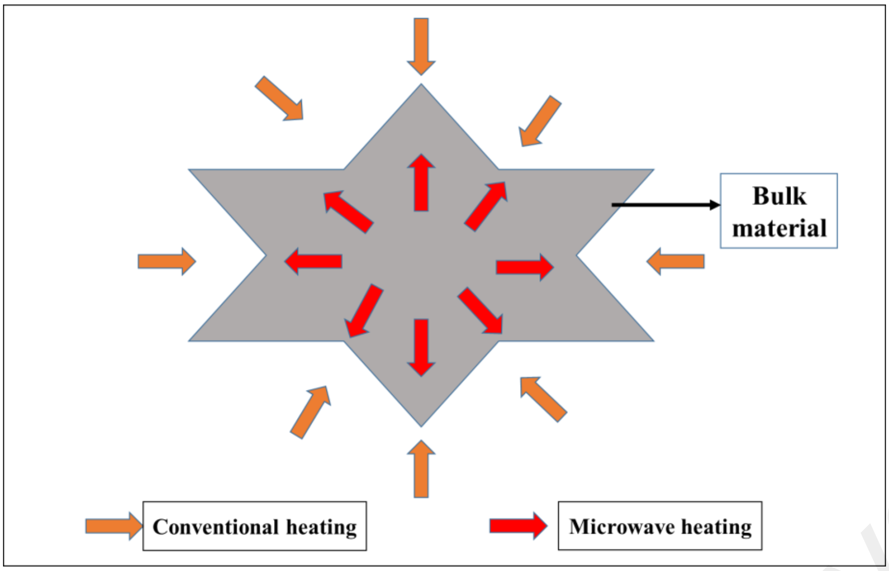

Figure 2.1 Conventional and microwave heating mechanism

Microwave heating processes are currently undergoing investigation for application in a number of fields where the advantages of microwave energy may lead to significant savings in energy consumption, processing time and overall performance (Jones, et al., 2002).

2.4.1 Phase separation, extraction and metallurgical processes

Phase separation and extraction processes have been increasingly using microwave technology since the last decade (Haswell and Howarth, 1999; Li et al., 2012; Li et al., 2013; Pasquet et al., 2011; Sun and Liu, 2008; Teo et al., 2013). An extensive review of the extraction of flavonoids, which is a bioactive compound effective against diseases such as cancer, cardiovascular disorders and inflammation is presented by Routray and Orsat (2012). They opined that microwave extraction demonstrates advantages such lower processing time and solvent requirement, integrity of the flavonoids, usability of both polar as well as nonpolar solvents, small sample size and use of less concentrated acid. Microwave technology has found its application in metallurgical processes such as pyrometallurgy, hydrometallurgy and mineral processing (D. Panias and Krestou, 2004).

2.4.2 Soil treatment

In recent years, microwave technology has been applied to soil treatment process successfully. Mun et al. (2009) treated soil, which was contaminated with parasite eggs from pet or wild animals. It was observed that microwave radiation at 700 W with 14% water content (w/w) achieved much better inactivation of parasite eggs (approximately 2.5 log inactivation of eggs in soil within 60 s). Whereas, in the UV irradiation at 3 mW/cm^2 for 3600 s approximately 0.32 and 0.01 log inactivation of eggs took place and in ozone treatment 0.13 log inactivation of eggs was achieved with 5.8 ± 0.7 mg/L of dissolved ozone dose for 30 min in a continuous reactor. In another study, Lin et al. (2010b) treated soil contaminated with potentially risky antibiotic chloramphenicol. Granular activated carbon (GAC) was used as microwave absorber. Larger microwave power and GAC dose was found to be effective for the degradation of chloramphenicol. A carbon-carbon bond rupture was confirmed and there were no extra toxic group in the degraded product. Thus, microwave irradiation was proved to be an effective technology for the treatment of soils contaminated with antibiotics. Soils contaminated with heavy and light-hydrocarbon were treated with microwave irradiation by Robinson et al. (2009). They observed greater than 95% removal of PHAs from both heavy and light-hydrocarbon contaminated soils, under moderate reaction condition. The possibility of scaling up the process to treat hydrocarbon-contaminated soil was also evaluated in the study. Two different batch processes such as stirred bed system and fixed bed system in kilogram scale were used for that purpose. Over 95% removal of the organic contaminants were possible using a stirred bed system, whereas organic removal in fixed bed systems is limited to 30–50%. Researchers (Wu, 2008) also successfully tested decontamination of soil laden with heavy metals. Toxic heavy metals such as Cd^{2+}, Mn^{2+}, Cr^{3+}, and Cr^{6+} could be successfully removed from contaminated soil.

2.4.3 Carbon-catalysed reactions and organic synthesis

Reactions which require high temperature and/or contain organic compounds having a low dielectric loss require microwave-carbon coupling for enhancement of reaction rate (Menéndez, et al., 2010). According to Lidström et al. (2001), microwave heating could be a valuable, non-conventional energy source for organic synthesis such as Diels-Alder reactions, thermolysis of esters, the decomplexation of metal complexes, pyrolysis of urea and esterification, which can accelerate many organic reaction to a great extent. A considerable advancement in the yield of the reaction can be obtained for removal of oxides of nitrogen and sulphur (Chang et al., 2012; Kong and Cha, 1995; Manivannan et al., 2015; Wei et al., 2011), decomposition of methane for hydrogen production (Deng et al., 2014; Fidalgo et al., 2008; Pinilla et al., 2012) and CO_2 reforming of CH_4 (Fidalgo and Menéndez, 2012) when microwave technology coupled with carbon catalyst was applied.

2.4.4 Preparation of activated carbon

Activated carbons are prepared from carbonaceous material by either physical or chemical activation. In both the activation processes, it is required to heat the raw material to an elevated temperature of 400 ^{o}C to 900 ^{o}C. Two properties of activated carbon, which make them suitable for adsorption are specific surface area and pore structure. The specific surface area is mainly measured by Brunauer-Emmet Teller (BET) equation and known as BET surface area. There are three types of pores present in materials namely micropores (<2 nm), mesopores (2–50 nm) and macropores (>50 nm). There are factors that also have effect on the adsorption capacity of activated carbon such as thermal stability, low acid/base reactivity and chemical structure of the surface (Njoku et al., 2014). In recent years, researchers (Hoseinzadeh Hesas, et al., 2013c) have tried different materials such as pineapple peel, rice husk, cotton stalk, orange peel, sunflower seed oil residue, tobacco stems, pistachio nut shell, oil palm EFB, oil palm fibre, bamboo, lotus stalk, waste tea, pine wood powder and pomelo skin for preparation of activated carbon with the help of microwave heating. A summary of the research on activated carbon preparation is given in Table 2.2. Recent studies shows that microwave power ranging from 360 to 1200W and irradiation time of 5 to 30 min produced activated carbon of good quality in terms of BET surface area which ranges from 621 to 2557 m^2/g. The impregnating material were mainly basic compounds such as KOH, K_2CO_3 and $ZnCl_2$ however, H_3PO_4 has also been applied as impregnating material when microwave heating is applied to produce activated carbon.

Table 2.2 Summary of recent studies of preparation of activated carbon using microwave technology

Raw material used	**Chemical used**	**Microwave power (W)**	**Irradiation time (min)**	**Electricity unit required (1kWh= 1 unit)**	**BET surface area (m^2/g)**	**Average pore size (Å)**	**Adsorbent (mg/g)**	**Adsorption capacity (mg/g)**	**References**
Pineapple peels	KOH	600	6	0.06	1006	23.44	MB	462.1	(Foo and Hameed, 2012b)
	K_2CO_3				680	25.97	MB	411.74	
Rice husks	KOH	600	7	0.07	752	34.14	MB	441.52	(Foo and Hameed, 2011f)
	K_2CO_3				1165	26.84	MB	362.6	
Cotton stalks	KOH	660	10	0.11	729		MB	294.12	(Deng et al., 2010a)
	K_2CO_3				621		MB	285.71	
Orange peels	K_2CO_3	600	6	0.06	1104	22.27	MB	382.75	(Foo and Hameed, 2012c)
Sunflower seed oil residues	K_2CO_3	600	8	0.08	1411	23.6	MB	473.44	(Foo and Hameed, 2011d)
							Acid blue	430.37	
Tobacco stems	K_2CO_3	700	30	0.35	2557		MB	517.5	(Li et al., 2008)
							Iodine	1834	

Raw material used	Chemical used	Microwave power (W)	Irradiation time (min)	Electricity unit required (1kWh= 1 unit)	BET surface area (m^2/g)	Average pore size (Å)	Adsorbent (mg/g)	Adsorption capacity (mg/g)	References
Pistachio nut shells	KOH	700	7	0.08	700		MB	296.57	(Foo and Hameed, 2011c)
Oil palm (Elaeis) residues	KOH	360	15	0.09	807		MB	344.83	(Foo and Hameed, 2011e)
Fruit residues	KOH	600	7	0.07	1372		MB	395.3	(Foo and Hameed, 2012a)
Oil palm fibers	KOH	360	5	0.03	708		MB	312.5	(Foo and Hameed, 2011a)
Cotton stalks	H_3PO_4	400	8	0.05	653		MB	245.7	(Deng et al., 2010b)
Lotus stalks	H_3PO_4	700	15	0.18	1434		Oxytetracycline	564.97	(Huang et al., 2011)
Pomelo skins	NaOH	500	5	0.042	1355		MB Acid Blue	501.1 444.45	(Foo and Hameed, 2011b)

Raw material used	Chemical used	Microwave power (W)	Irradiation time (min)	Electricity unit required (1kWh= 1 unit)	BET surface area (m^2/g)	Average pore size (Å)	Adsorbent (mg/g)	Adsorption capacity (mg/g)	References
Cotton stalks	$ZnCl_2$	560	9	0.084	795		MB Iodine	193.5 972.92	(Deng et al., 2009)
Pine wood powder	$ZnCl_2$	700	10	0.12	1459		MB Benzene Iodine	200 1100 1100	(Wang et al., 2009)
Oil palm shell	$ZnCl_2$	1200	15	0.3	1253		MB	287.85	(Hoseinzadeh Hesas et al., 2013b)
Rambutan *(Nephelium lappaceum)* peel	KOH	600	12	0.12	972		acid yellow 17	197.16	(Njoku, et al., 2014)
Date sphate	H_3PO_4	700	2	0.02	795		Methyl violet	224	(Emami and Azizian, 2014)

Raw material used	**Chemical used**	**Microwave power (W)**	**Irradiation time (min)**	**Electricity unit required (1kWh= 1 unit)**	**BET surface area (m^2/g)**	**Average pore size (Å)**	**Adsorbent (mg/g)**	**Adsorption capacity (mg/g)**	**References**
Coal in Xinjiang China	KOH	700	12	0.14	1770		Naphthalene	89.29	(Xiao et al., 2015)
							Phenanthrene	116.28	
							Pyrene	117.65	

However, few drawbacks such as high initial cost for experimentation and problem in scaling up the process due to insufficient knowledge on dielectric properties and equipment designing has hindered the use of microwave technology. More interdisciplinary study to explore the vast unknown potential of the microwave technology has been suggested by Yuen and Hameed (2009).

2.5 Application of HIGEE technology in rotating packed bed contactor

Research on production systems, which are quick, efficient, safe, eco-friendly as well as smaller in size has been devoted to new as well as existing facilities. The past few decades of research to develop such compact and sustainable systems led to process intensification. Process intensification was defined by Professor Colin Ramshaw of Newcastle University (UK), one of the pioneers of the modern process intensification in chemical industry, as a strategy for making dramatic reductions in the size of a chemical plant so as to reach a given production objective (Stankiewicz and Moulijn, 2000). Professor Ramshaw while working for Imperial Chemical Industries, U.K, developed the concept of rotating packed bed (RPB) as a tool for intensification of the mass transfer dependent processes such as distillation, absorption and stripping, under a centrifugal force field. This centrifugal force field was several times higher than the gravitational force; therefore, it was denoted as high gravimetric technology or HIGEE (Ramshaw and Mallinson, 1981; Rao et al., 2004; Zhao et al., 2010). Typically, RPB reactor is used in processes where mass transfer is crucial, such as absorption, distillation, stripping, heat transfer, extraction and nanoparticles preparation (Kelleher and Fair, 1996; Mondal et al., 2012).

The RPB was constructed as a doughnut shape rotor, which was mounted on a shaft and was filled with high specific area packing materials such as glass beads. The liquid was injected through an injector at the eye of the rotor and the liquid flowed outwards through the packing while the gas was introduced from the periphery inwards, thereby a concurrent flow took place, enhancing mass transfer rate (Ramshaw and Mallinson, 1981). A noticeable enhancement of the overall mass transfer rate was observed in comparison to a stationary column. As shown in Fig. 2.2, the RPB was constructed both horizontally as well as vertically with respect to the axis of rotation.

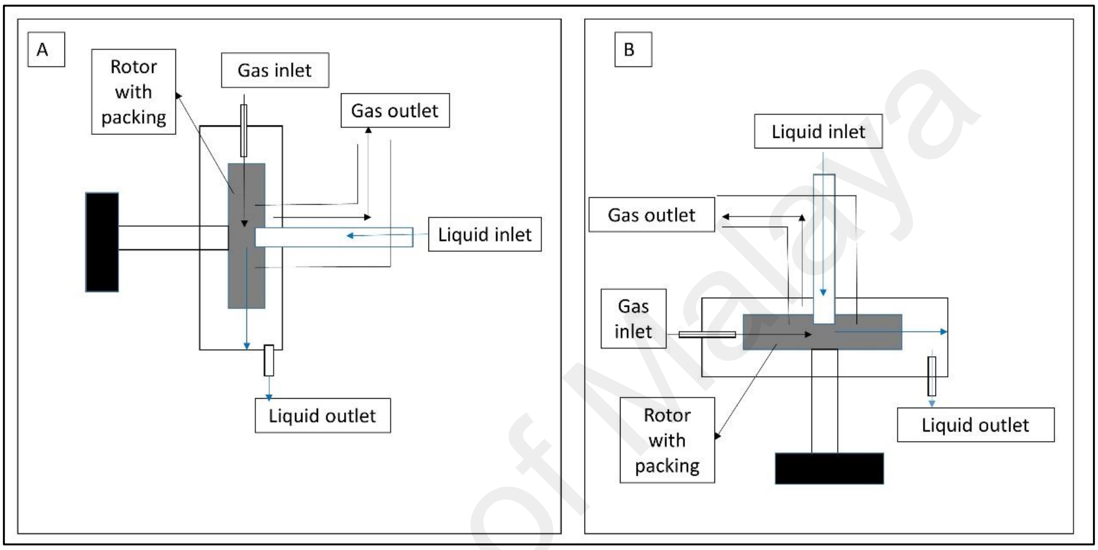

Figure 2.2 Schematic diagram of RPB (A) horizontal axis, (B) vertical axis [adopted from (Rao, et al., 2004)]

Tung and Mah (1985) opined that the liquid mass transfer behaviour in RPB system was governed by the penetration theory. Kelleher and Fair (1996) modelled the mass transfer efficiency, pressure drop and hydraulic capacity of the distillation of cyclohexane/n-heptane in a RPB contactor. Burns and Ramshaw (1996) visually inspected the pattern of liquid flow determined by the centrifugal acceleration in a RPB system. It was observed that at low rotational speed of 300-600 rpm, the liquid travelled in rivulet flow while at higher rotational speed of 600-800 rpm, the flow pattern was droplet flow. The droplet flow aided the wetting of the packed bed.

In the last few years, high gravimetric technology has been used for many different processes. Utilisation of the RPB has been observed mostly for solid-gas or liquid-gas mass transfer processes (Chiang et al., 2009; Hsu and Lin, 2012; Zhang et al., 2011). It has hardly been used for adsorption of contaminants from wastewater (Chang and Lee, 2012; Panda et al., 2011) and still less for carrying out desorption (Jassim et al., 2007). The RPB reactor has every potential to be applied as a multi-phase contactor, e.g. for use in a gas-liquid-solid or a liquid solid system. In their review on the use of RPB and HIGEE technology, Zhao, et al. (2010) elaborated the concept and fundamental issues such as liquid flow, gas–liquid mass transfer, residence time distribution and micromixing.

2.5.1 Removal of CO_2

Lin et al. (2010a) investigated CO_2 removal from a 10 vol% CO_2 gas by chemical absorption with 30 wt% alkanolamine solution in a cross-flow RPB reactor. The composition of the solution was monoethanolamine (MEA), piperazine (PZ) and 2-amino-2-methyl-1-propanol (AMP). CO_2 removal efficiency of more than 90% at a liquid flow rate of 0.54 L/min was achieved.

RPB reactor was used to capture CO_2 with the aid of ionic liquids (Zhang, et al., 2011). Ionic liquids are very viscous solution and the low gas–liquid mass transfer rates in conventional gas–liquid contactors is a hindrance for large-scale application of CO_2 capture using ionic liquids. A saturation ratio of 60% was obtained with only one cycle of gas–liquid contact in the RPB. The value of liquid side volumetric mass transfer coefficient ($k_L\alpha$) in the RPB was (0.95–3.9) × 10^{-2} s^{-1}, which was an order of magnitude higher than that in a conventional packed tower. A model was proposed based on penetration theory explaining the mechanism of gas–liquid mass transfer in a RPB, which indicated that the large gas–liquid interfacial area and its frequent renewal on the packing surface generated large $k_L\alpha$ value inside the RPB. It showed good agreement with the experimental data, with a maximum relative error of less than 15%.

Viability of applying the cross-flow RPB to remove CO_2 by absorption in monoethanolamine, NaOH and 2-amino-2-methyl-1-propanol from gaseous streams was investigated by Lin and Chen (2011). They compared the efficiency of a RPB with a conventional packed bed column. The height of the conventional packed bed was 110 cm and that of the cross flow RPB was only 12 cm. However, the cross-flow RPB had better experimental overall volumetric gas-phase mass transfer coefficients (K_Ga) value ($1.42\ s^{-1}$) in comparison to the conventional packed bed ($0.93\ s^{-1}$). They concluded that the cross-flow RPB was a better alternative as gas liquid contactor for CO_2 removal.

Chemisorption of CO_2 to NaOH solution was investigated by Luo et al. (2012). Mass transfer characteristics, such as effective interfacial area (a_e) and liquid side mass transfer coefficient (k_L) were determined for the RPB contactor with 5 novel rotors equipped with blades in the packing section as well as one conventional rotor without blades and fully filled with the same packing. The mass transfer was significantly enhanced and it was about 8% to 68% higher in the rotors with blades than the rotor without any blade. This enhancement was due to the increase in the effective interfacial area. In this study, a model was also developed based on Danckwerts surface renewal theory to calculate the liquid side volumetric mass transfer coefficient (k_La_e). The model predicted the k_La_e value, which was in good agreement with the experimental value.

2.5.2 Preparation of nano-particles

RPB has been extensively used for the preparation of nano particles in last decade. Zhao, et al. (2010) reviewed the use of RPB in nano-particle preparation. In very recent years, Sun et al. (2011) prepared nano-$CaCO_3$ by simultaneous absorption of CO_2 and NH_3 into $CaCl_2$ solution in a RPB. It was observed that smaller particle size was obtained at 500-1200 rpm. Higher gravity ensures stronger collision between liquid particles and the packing, thereby enhancing the gas–liquid mass transfer and the rapid formation of the supersaturated solution of $CaCO_3$. This situation is favourable for the generation of smaller $CaCO_3$ particles. The mean particle size was 50 nm, with a particle size distribution of 10–80 nm.

Ng et al. (2012) used superior micromixing ability of the high gravity technology to eradicate the problem in synthesising silver nano particles by precipitation in the conventional stirring system, which has poor macro- and micromixing efficiency. Taguchi optimisation approach was adopted to find the optimum operating condition for each parameter for small particle size and high product yield. The particle size obtained in the RPB was 24.83 nm, which was much smaller than the observed size (47.8mm) when a conventional magnetic stirrer was used, keeping all other experimental parameters constant. It was also reported that the complete formation of silver nanoparticles occurred within 5 min.

RPB was used to prepare Fe_3O_4 nanoparticles from solutions of $FeCl_3$/$FeCl_2$. At rotational speed of 1800 rpm, liquid flow rate of 500 mL/min and a temperature of 60 °C, the average diameter was 6.4 nm with a production rate of 17 kg/day. The nanoparticle prepared in RPB showed much better performance for H_2O_2-activating capacity of Fe_3O_4 nanoparticles for Rhodamine B removal. The prepared Fe_3O_4 nanoparticles had a decolourisation efficiency of 99% after 120 min, which is much higher than the 47% efficiency obtained from the commercially available Fe_3O_4 nanoparticles when used under similar reaction conditions (Lin et al., 2012).

2.5.3 SO_x and NO_x removal

SOx and NOx could be removed from flue gases in a column packed with various packing materials (Kiil et al., 1998), spray tower (Scala et al., 2004) or a rotating-stream tray scrubber (Sun et al., 2002). However, poor mass transfer efficiency and large size of the columns make this conventional processes expensive and difficult to handle (Jiang et al., 2011). RPB with higher mass transfer efficiency could be used to solve this problem. In recent years, high gravity technology has been used for removal of SOx and NOx from flue gas.

Sodium citrate buffer solution was used by Jiang et al. (2011) for absorption of SO_2 in a RPB of laboratory scale. They reported that a rotating speed of 700 to 900 rpm was more favourable for SO_2 absorption in terms of efficiency and operating time. It was observed that the SO_2 removal was above 97.30% at rotating speed of 700 rpm and above 98% at 900 rpm.

Li et al. (2010b) studied the absorption of NOx in nitric acid solution in the presence of ozone in a RPB reactor. They reported that higher gravity number, which was obtained at higher rpm was favourable for NOx absorption. The removal efficiency of NOx is higher than 90% at the optimal operating condition, i.e. at gas velocity less than 800 m^3/m^2 h, the gravity number larger than 110 and the liquid spray density higher than 20 m^3/m^2 h.

RPB was employed to enhance the gas–liquid mass transfer between NO and Fe^{II}(EDTA) by Zhang et al. (2012). A horizontal RPB reactor was used to facilitate the removal. A removal of 87% was obtained at gravity level of 150g. The gravity level was measured by the following equation:

$$Gravity\ level = \frac{\omega^2\, r}{g} \qquad (2.2)$$

Tit was opined that the possible reason for higher adsorption at higher gravity level was reduction of mass transfer resistance. The reduction of mass transfer resistance at a higher rotating speed compensated the reduction of the retention time, which is unfavourable to chemical absorption.

The dimensions of the recently used lab scale RPB reactors for different applications are given in Table 2.3. It is observed from the Table 2.3 that the height of the reactor is considerably small.

Table 2.3 Dimensions of the RPB reactors used for different purposes

Used in	**Outer radius (cm)**	**Inner radius (cm)**	**Axial height (cm)**	**Reference**
Bio-diesel	6.35	1.15	2	(Chen et al., 2010)
CO_2 absorption	4.4	2.4	12	(Lin, et al., 2010a)
CO_2 absorption	6	2	2	(Zhang, et al., 2011)
CO_2 absorption	4.4	2.4	12	(Lin and Chen, 2011)
CO_2 absorption	15.3	7.8	5	(Luo, et al., 2012)
CO_2 absorption	16	7.6	2	(Yu et al., 2012a)
$CaCO_3$ nanoparticle	10	4	1.2	(Sun, et al., 2011)
Fe_3O_4 nanoparticles	3.9	2.9	2.2	(Ng, et al., 2012)
SO_2 absorption	13.2	5.9	4	(Jiang, et al., 2011)
NOx absorption	29	10	20	(Li, et al., 2010b)
NOx absorption	6	2	2	(Zhang et al., 2012)

2.5.4 Adsorption

Adsorption on activated carbon is a very effective method for heavy metal removal. However, the size of the reactor is generally large to facilitate the treatment of the high volume of effluent generated by the industries. Adsorption and desorption, being mass transfer processes occurring between liquid and solid phases, can be significantly enhanced in a RPB contactor. The high throughput also makes the RPB useful in treating high volume of wastewater.

Lin and Liu (1999) studied the adsorption of Basic Yellow 2 dye on activated carbon in a centrifugal adsorption bed and found that the adsorption of the dye was influenced by centrifugal acceleration. It was also observed by them that a pseudo-first-order model could describe the mechanism of adsorption, while the intraparticle diffusion model could govern the rate-limiting step at the initial stages of adsorption.

Das et al. (2008) explored the mass transfer characteristics of continuous biosorption of Cu (II) ions on *Catla catla* fish scale under centrifugal acceleration in a rotating packed-bed (RPB) contactor. They observed an increase in adsorption of Cu(II) as well as an enhancement in volumetric mass transfer coefficient with increasing rotor speed.

Panda et al. (2011) used crude tamarind (*Tamarindus indica*) fruit shell (TFS) to remove hexavalent chromium ions from an aqueous solution in a RPB contactor by continuously recirculating a given volume of solution through the bed. In this study, it was reported that the mass transfer rate of Cr (VI) ions increases with rotational speed due to a reduction in mass transfer resistance. However, a study for optimisation of the operating parameters in a RPB-HIGEE for removal of pollutants from liquid effluents is required.

2.6 Summary

From the literature review, it is evident that the wastewater treatment has received ample attention from the researchers worldwide. However, the complexity of the technology used, higher initial cost, high operational cost, larger size of the facilities, long treatment time have made the wastewater treatment a troublesome issue for the industries. Thus, this research was conceptualised to alleviate these problems through the application of advanced technology such as microwave heating and process intensification by using HIGEE technology in rotating packed bed system. A robust optimisation for both the processes of preparation of activated carbon as well as application for the removal of heavy metal and dye is necessary. Hence, this will enable us to find information which will be useful for application of RPB in adsorption of heavy metal and dye. The following chapter describes the methodology adopted in order to fulfil the aim and objectives of the study.

CHAPTER 3: METHODOLOGY

The purpose of this chapter is to describe the method, strategies and empirical techniques applied to fulfil the objective of the research. Materials used, method for activated carbon preparation, process optimisation, RPB-HIGEE equipment construction as well as validation of the system for the wastewater treatment are described in detail. The research was performed according to the schematic diagram presented in Figure 3.1. There are two main segments of the thesis e.g. preparation of activated carbon and its application for heavy metal and dye removal.

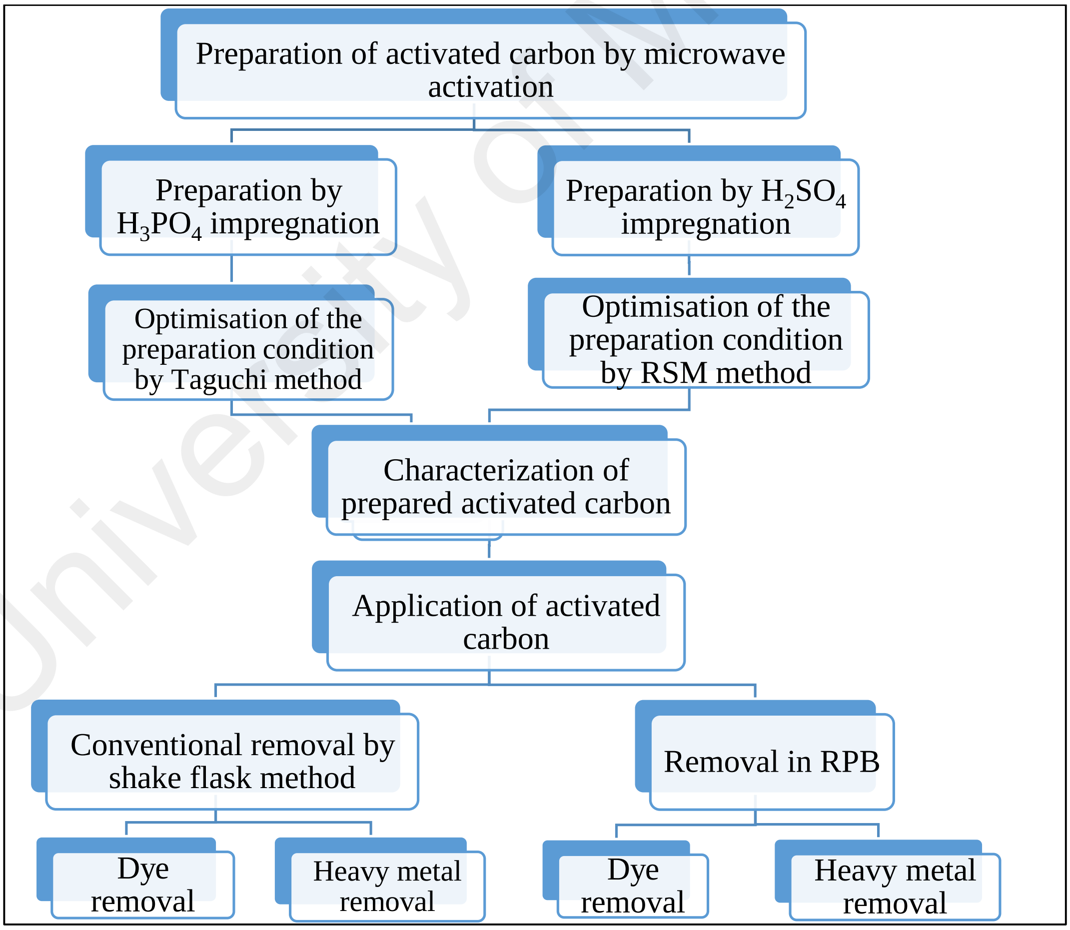

Figure 3.1 Schematic diagram of the methodology adopted

To establish the efficiency of the microwave heating activated carbon was prepared first varying the impregnation ratio of H_3PO_4. Later, two very established process for optimisation such as Taguchi method and response surface methodology (RSM) were applied to optimise the process parameters. However, these two methods are based on different philosophy and mathematical algorithm to optimise the process parameters. This makes the selection random and still provides valuable information on the effectiveness of the microwave heating. During the preparation, methylene blue (MB) and Zn was used to assess the quality of the different activated carbon prepared according to the different combination of parameter suggested by the optimisation methods. The activated carbon prepared in the optimised conditions were characterised and the activated carbon having the best adsorptive characteristics was used further for Direct Red 23 dye removal and heavy metal (Cr) removal in shake flask as well as in the RPB to optimise the process parameter and to check the efficiency of the HIGEE technology.

3.1 Materials

The chemicals used in this work were of analytical grade and obtained from R&M Chemicals, Fluka Chemicals and Sigma-Aldrich, respectively. The acids used were *O*-phosphoric acid (H_3PO_4) and sulphuric acid (H_2SO_4). The stock solutions of chromium and zinc were prepared by dissolving potassium dichromate ($K_2Cr_2O_7$) and zinc nitrate hexa-hydrate ($Zn(NO_3)_2$, $6H_2O$), respectively, in distilled water. Stock solutions of Methylene blue (MB) and Direct red 23 (DR23) were prepared by dissolving solid MB and DR23 into distilled water. The concentration of all the stock solutions were 1000 mg/L. Palm kernel shells (PKS), which were used as raw material for the preparation of activated carbon, were obtained from a local palm oil mill near Kuala Lumpur.

3.2 Proximate and ultimate analyses of the palm kernel shells

Proximate and ultimate analyses were performed to understand the chemical composition of the PKS. The parameters measured in proximate analyses were moisture, volatile matter, ash and fixed carbon. Ultimate analyses measured the elemental composition by quantitative determination of carbon, hydrogen, nitrogen, sulphur and oxygen within the PKS. Proximate analyses of PKS were carried out according to the ASTM D 7582-10. Ultimate analyses were performed using a Perkin-Elmer 2400 Series II CHNS/O analyser.

3.3 Preparation of activated carbon

Preparation of the activated carbon was prepared from locally available low cost agricultural material PKS and using microwave technology for heating. Production parameters were also optimised with the aid of Taguchi method and Central Composite Design (CCD) for Response Surface Methodology (RSM). The details are given in the following subsections. The raw material (PKS) was ground into fine powder in the size range 1400-2000 µm and washed thoroughly with distilled water.

3.3.1 Using different impregnation ratios of H_3PO_4 and microwave heating

The ground PKS were impregnated with phosphoric acid at three different ratios, which are 1:1, 1:2 and 1:3. Twenty grams of the impregnated raw material was mixed with required amount of phosphoric acid for 4 hours with constant stirring at 120 rpm at 27 ^oC. The slurry was then dried in a vacuum oven at 100 ^oC for 24 hours. The resultant impregnated sample was placed in a specially designed quartz tube. The tube was placed vertically in a microwave oven with frequency 2.450 GHz (SYNOTHERM corporation, model HAMiLab-C). The microwave power and irradiation time were set at 900 W and 15 min, respectively, based on some preliminary runs. The tube was purged with nitrogen gas at a flow of 0.2 L/m for 5 min before microwave treatment to outgas air. This flow rate was maintained during the activation and cooling stages. The product obtained was then washed thoroughly with distilled water until the pH of the washing solution became stable. The activated carbon samples were denoted as MWAC 1, MWAC 2 and MWAC 3 according to the ratio 1:1, 1:2 and 1:3, respectively.

3.3.2 Optimising the production of activated carbon using Taguchi method

Production of high quality products can be facilitated by a statistical approach. This can be addressed by a combination of methods namely Taguchi method, design of experiments and multiple regression analyses (Phadke, 2009). In Taguchi method, a set of response variables are tested against a set of control parameters or independent variables with the aid of experiments arranged in “orthogonal array” to obtain the most suitable combination of the control parameters. Orthogonal arrays provide a best set of well-balanced but minimum number experiments required to identify the optimum conditions. The log functions of desired output known as the signal to noise ratios (S/N), serve as the objective functions for optimisation. The S/N also is used in data analyses and in the prediction of the optimum results. The target of a process as defined here is the numerical value that is preferred for the quality characteristic of interest. Depending upon the target value, there are three forms of S/N ratio, such as smaller-the-better, larger-the-better, and nominal-the-best, which are of common interest for optimisation of static problems expressed by equation 3.1, 3.2 and 3.3, respectively.

$$n = -\log[\,mean\ of\ sum\ of\ squares\ of\ measured\ data] \quad (3.1)$$

$$n = -10\log[\,mean\ of\ sum\ of\ squares\ of\ reciprocal\ of\ measured\ data](3.2)$$

$$n = -10\log[\frac{square\ of\ mean}{variances}] \quad (3.3)$$

The smaller-the-better S/N ratio is chosen for the problems where the desired output value should be as low as possible, ideally zero. Common examples of such problem are number of defective products, waste generation and number of delayed flight departure. In all these situations, there is always some upper specification limit of the target value. Whereas, the larger-the-better S/N ratio signifies that the output should be as high as possible, as in the case of number of perfect products or longevity of a product. The nominal-the-best S/N ratio is considered for problems where a particular output is desired instead of some higher or lower value. For example, thickness of deposition in metal plating or the amount of lubricant required to run a machine smoothly requires a particular amount; too much or too little may create defect in product.

The algorithm for larger-the-better S/N ratio was chosen for the optimisation in this study because adsorption capacity of the adsorbent should be as high as possible at the optimum condition (Aber et al., 2009; Li et al., 2010a). To choose an appropriate orthogonal array, the total degrees of freedom of the orthogonal array must be considered. The degrees of freedom for the selected orthogonal array should be greater than or at least equal to those for the process parameters (Athreya and Venkatesh, 2012).

The optimisation for the production of activated carbon was carried out in two stages. At the initial stage, known as the coarse optimisation, the full possible range was considered for each of the control factors important for the production of activated carbon. In this stage, the significance and contribution of the factors towards the optimisation was identified. However, as the levels chosen in this stage were very wide, the optimum point obtained might not be very accurate. Thus, in the second stage, the levels chosen were in the near vicinity of the initial optimum points. Thereby, a more accurate optimum point was derived. This stage is known as the fine-tuning stage.

3.3.2.1 Initial parameter optimisation

An L16 orthogonal array was chosen for the coarse optimisation, where 16 different experiments had to be carried out. The experiments were performed with different combination of four operational parameters known as control factors, namely microwave power (W) in watt, irradiation time (t) in min, impregnation ratio (IR) indicating the amount of acid to amount of PKS, and concentration of acid in %, with four levels for each. These are illustrated in Table 3.1. The noise factor taken in this study was the particle size of the raw material. The particle size range of 0.5 mm to 1 mm was considered as the noise factor 1 (NF1), and the range between 1 mm to 2 mm was taken as noise factor 2 (NF2). A separate outer array was constructed to include the noise factors that required replication of each run in the orthogonal array for each noise condition. Table 3.2 shows the L16 orthogonal array including the noise factors. Minitab 16 software was used to formulate the Taguchi orthogonal array as well as for the computation of ANOVA and level averages. MB was used as the adsorbate to investigate the adsorption capacity of the prepared activated carbon. Adsorption capacity was used as the indicator of quality, such as the higher the adsorption capacity, the better was the quality of the activated carbon. Both isotherm and kinetic studies were performed for MB adsorption.

Table 3.1: Levels of the control factors used in preparation

Investigating parameters	**Level 1**	**Level 2**	**Level 3**	**Level 4**
Microwave Power (W)	400	600	800	1000
Time (min)	3	10	17	24
Impregnation ratio (acid:pks)	0.5	1	1.5	2
Conc. of acid (H_3PO_4) (%)	42.5		85	

PKS were ground and sieved into two different particle size ranges, namely 1000-2000 µm and 500-1000 µm. These were then washed several times with distilled water and air dried in a vacuum oven. The ground PKS were impregnated with phosphoric acid at different levels, according to the Table 3.1.

Table 3.2 L16 experimental design with the noise factors according to Taguchi method

Inner control factor array					Outer noise factor array	
Experiment No	**Microwave Power (W)**	**Time (min)**	**Impregnation ratio (acid:pks)**	**Conc. of acid (H_3PO_4) (%)**		
1	400	3	0.5	42.5	NF1 (0.5-1 mm)	NF2 (1-2 mm)
2	400	10	1	42.5		
3	400	17	1.5	85		
4	400	24	2	85		
5	600	3	1	85		
6	600	10	0.5	85		
7	600	17	2	42.5		
8	600	24	1.5	42.5		
9	800	3	1.5	85		
10	800	10	2	85		
11	800	17	0.5	42.5		
12	800	24	1	42.5		
13	1000	3	2	42.5		
14	1000	10	1.5	42.5		
15	1000	17	1	85		
16	1000	24	0.5	85		

Forty grams of PKS were mixed with the requisite amount of phosphoric acid for four hours with constant stirring at 120 rpm under 27 °C. The slurry was then dried in a vacuum oven at 100 °C for 24 h. The impregnated sample was placed in a specially designed quartz tube. The tube was placed vertically in a microwave oven with a frequency of 2450 MHz (SYNOTHERM corporation, model HAMiLab-C), as shown in Figure 3.2. The microwave power and irradiation time were set at the values assigned to the specific experimental run. The microwave was preheated at 100 W for five minutes to heat up the magnetron inside the instrument. The tube was purged with nitrogen gas at a flowrate of 0.5 L/m for five minutes before microwave treatment to remove air. This flow rate was maintained during the activation as well as cooling stages. The activated carbon obtained was then washed meticulously with distilled water until a stable pH of the washing solution was obtained. The activated carbon was denoted as $MWAC_T$. During the MB adsorption tests 100 mL of 100mg/L solution of MB was taken in a conical flask and 0.1g activated carbon added to it. The flasks were shaken at 120rpm for 24h at room temperature, which was 30 ^{o}C.

Figure 3.2 (A) Microwave oven (SYNOTHERM corporation, model HAMiLab-C) and (B) the quartz tube

3.3.2.2 Fine tuning the initial optimum condition

The results of the initial optimisation method could be used to reveal the significance of each factor by ranking them according to their significance. The ranking was based on the delta values. These values were calculated as the difference of highest and lowest mean S/N ratio values of each factor. Depending upon the rank obtained, the most important factors influencing the quality of the activated carbon was selected and a fine-tuning experiment was conducted to obtain result that is more accurate. The most insignificant factor was kept at a constant value as suggested by the initial optimum experiment. From Table 4.4 in Section 4, it can be observed that microwave power, irradiation time and impregnation ratio had significant effect on the quality of the prepared activated carbon. Therefore, in the fine tuning stage, only these three factors were taken into consideration and the experiment was designed for a standard L9 orthogonal array with three different levels. The ranges of the values were narrowed down around the initial optimum conditions. This experiment was conducted to investigate whether the actual optimum points coincide with the points indicated in the initial optimum process or it exists at some other point near to the initial optimum point. BET surface area of the prepared activated carbons were considered as the response for the experiments performed. The factors were investigated and their levels are given in Table 3.3 while the L9 array is shown in Table 3.4.

Table 3.3 Levels of the control factors used in fine-tuning experiment.

Investigating parameters	Level 1	Level 2	Level 3
Microwave Power (W)	700	800	900
Irradiation Time (min)	13	17	21
Impregnation ratio (acid:pks)	1	2	3

Table 3.4 L9 experimental design for fine-tuning experiment

Impregnation ratio	Microwave Power	Time
1	700	13
1	800	17
1	900	21
2	700	17
2	800	21
2	900	13
3	700	21
3	800	13
3	900	17

3.3.3 Parameter optimisation by central composite design in response surface methodology

RSM was applied as the second optimisation method to obtain the optimised condition for production of activated carbon from PKS by sulphuric acid impregnation and microwave heating. CCD was chosen to design different combinations of the operating variables for the experiments and to find out the best suitable combination of the operating variables. CCD method allows a quadratic surface to be fitted with the response with minimum number of experiments and assists in analysing the interaction among the effective process parameters. CCD aided to decide the factor settings that optimised the response. The most effective parameters responsible for the quality of the activated carbons were considered at various levels. The operating variables were irradiation time (T) coded as Factor A, microwave power (P) coded as Factor B, impregnation ratio (IR) coded as Factor C and sulphuric acid concentration coded as Factor D. The ranges and the level of independent variables used in this study are mentioned in

Table 3.5. The undiluted acid was considered as 100% and subsequent concentration was obtained by dilution of this 100% acid. In this design, low and high actual values of the factors were coded as -1 and +1, respectively. The total number of runs in CCD consisted of factorial runs, axial runs and centre runs according to the equation 3.4 where n is the number of independent variables.

$$N = 2^n + 2n + n_c \tag{3.4}$$

Table 3.5 Summary of experimental design of preparation of activated carbon

Factor	Name	Unit	Type	Low Actual	High Actual	Low Coded	High Coded	Mean
A	Time	min	Numeric	5	20	-1	1	12.5
B	Power	W	Numeric	600	1000	-1	1	800
C	IR		Numeric	0.5	2	-1	1	1.25
D	Conc. of acid	%	Numeric	20	100	-1	1	60

In this study, a face centred CCD was applied to find the optimum condition for four variables consisting of 16 factorial points, eight axial points and four replicates at the centre points with a total number of 28 runs. Experimental error and duplicability of the obtained data could be estimated with the aid of the four replicate experiments at the centre point. Table 3.6 shows the different combinations of the independent variables suggested by the Design Expert software (version 7.1.6, Stat-Ease, Inc.) in accordance with the CCD (Abnisa et al., 2011; Karacan et al., 2007).

Table 3.6 Experimental matrix for the preparation of activated carbon

Std	Run	Type	Factor 1 A:Time (min)	Factor 2 B:Power (W)	Factor 3 C:IR	Factor 4 D:conc of acid (%)
4	1	Fact	20	1000	0.5	20
6	2	Fact	20	600	2	20
28	3	Centre	12.5	800	1.25	60
21	4	Axial	12.5	800	0.5	60
22	5	Axial	12.5	800	2	60
1	6	Fact	5	600	0.5	20
9	7	Fact	5	600	0.5	100

Std	Run	Type	Factor 1 A:Time (min)	Factor 2 B:Power (W)	Factor 3 C:IR	Factor 4 D:conc of acid (%)
10	8	Fact	20	600	0.5	100
16	9	Fact	20	1000	2	100
24	10	Axial	12.5	800	1.25	100
17	11	Axial	5	800	1.25	60
8	12	Fact	20	1000	2	20
20	13	Axial	12.5	1000	1.25	60
7	14	Fact	5	1000	2	20
11	15	Fact	5	1000	0.5	100
26	16	Centre	12.5	800	1.25	60
5	17	Fact	5	600	2	20
27	18	Centre	12.5	800	1.25	60
19	19	Axial	12.5	600	1.25	60
18	20	Axial	20	800	1.25	60
23	21	Axial	12.5	800	1.25	20
25	22	Centre	12.5	800	1.25	60
14	23	Fact	20	600	2	100
2	24	Fact	20	600	0.5	20
3	25	Fact	5	1000	0.5	20
15	26	Fact	5	1000	2	100
13	27	Fact	5	600	2	100
12	28	Fact	20	1000	0.5	100

Yield of activated carbon (y_1) and the adsorption of zinc (y_2) were taken as the response of the processes. ANOVA, regression analysis and the interaction among the parameters were studied with aid of the same Design Expert software. A second order polynomial equation as shown in equation 3.5 was used to model the relationship between the process variables and the response (Bayraktar, 2001; Montgomery et al., 1984).

$$\boldsymbol{y = \beta_\circ + \sum_{i=l}^{k} \beta_i X_i + \sum_{i=l}^{k} \beta_{ii} X_i^2 + \sum_{i\leq j}^{k} \sum_{j}^{k} \beta_{ij} X_i X_j + \varepsilon} \tag{3.5}$$

where y represents the response or dependent variable, i and j represent linear and quadratic coefficients, respectively; β is the regression coefficient; k is the number of factors studied and optimised in the experiment; $\boldsymbol{\varepsilon}$ is the random error. The name of this activated carbon was kept MWAC.

3.3.4 Physical and chemical characterizations of the activated carbons prepared

The physical and chemical analyses of the prepared activated carbon were performed for the surface morphology and pore structure, functional group analyses and particle analyses. These physical and chemical characterisations aided the determination of the quality of the activated carbon prepared according to the above-mentioned methods.

3.3.4.1 Analyses of surface morphology and pore structure

The physical and chemical properties of the activated carbon are used to assess its performance capability. Specific surface area, pore structure, surface morphology and analysis of surface functional groups are important in understanding the adsorption capacity as well as the mechanism of adsorption. The pore structures of the prepared activated carbons were analysed using N_2 adsorption/desorption isotherm and scanning electron microscopy (SEM). Nitrogen adsorption/desorption isotherms were used to measure the Brunauer, Emmett and Teller (BET) surface area, total pore volume and density functional theory (DFT) pore size distribution at 77K by a Quantachrome Autosorb-6B. Initially, the activated carbon was degassed at 200 °C under vacuum for a period of 4 hours. The surface area was calculated by the standard BET equation. Calculation of total pore volume was carried out at a relative pressure of approximately 0.98, which was sufficient to fill all pores completely with the nitrogen gas. Nitrogen adsorption isotherm provided the DFT pore size distribution of activated carbon sample with the help of Autosorb software package with medium regularisation.

Field Emission Scanning Electron Microscopy (FESEM) (Brand: Zeiss Model: Auriga) was applied to study the surface morphology and pore development. For dissipation of charge during the process, the sample was sputter-coated with a thin layer of platinum. The sputter-coating was done with the help of a current of 6 mA in an argon atmosphere. The coated samples were transferred to the SEM specimen chamber for analyses.

3.3.4.2 Functional group analyses

Fourier Transform Infrared (FTIR) spectroscopy was used to analyse the surface functional groups of the precursor material as well as the prepared activated carbon. Bruker, IFS66v/S FTIR spectroscope was used for this purpose. Spectra were recorded at a range of 400 to 4000 cm^{-1}.

3.3.4.3 Particle size analyses

The size of the activated carbon particles were measured by Malvern Mastersizer 2000. The instrument uses laser diffraction technology based on the principle that laser scattering occurs when it hits a particle and the angle of scattering is directly related to the particle size.

3.4 Testing of the prepared activated carbon for adsorption

The activated carbons prepared in this study were used to remove heavy metals and dye from synthetic wastewater. Both conventional shake-flask experiments and experiments in RPB were conducted.

3.4.1 Removal of dye and heavy metal by conventional batch shake flask experiments

Batch shake-flask experiments were conducted to assess the removal efficiency of the prepared activated carbon for the removal of dye and heavy metal. Experiments were performed in 250 mL Erlenmeyer flasks containing 100 mL of the metal or dye solution with constant agitation at 120 rpm until the equilibrium was reached. Following the adsorption stage, all the samples containing heavy metals were filtered through Fioroni 601 filter paper. The solutions were centrifuged at 2000 rpm to separate the solid activated carbon from liquid. The final concentrations of metal in the filtrate were measured by ICP-OES (Perkin-Elmer 7000DV) while the final dye concentrations were measured with the aid of Perkin-Elmer Lambda 35 UV/VIS spectrophotometer. The following equation was applied to calculate the amount of metal or dye adsorbed:

$$\mathrm{q} = \frac{(C_o - C_f)\mathrm{V}}{\mathrm{m}} \tag{3.6}$$

where C_o and C_f are the initial and final concentrations of chromium at equilibrium in mg/L, respectively, m is the mass of adsorbent in grams and V is the volume of the solution in L.

3.4.1.1 Kinetic Study for batch adsorption

In another experiment for kinetic studies, samples were collected at particular time intervals and the amount of metal or dye adsorbed was found using equation. 3.6. The adsorption data were fitted to equation. 3.7 and 3.8, which are the standard linearised-integral forms of pseudo-first-order and pseudo-second-order kinetic models, respectively (Kundu et al., 2014a; Kundu et al., 2014b).

$$ln(q_e - q_t) = \ ln\, q_e - \ k_1 t \tag{3.7}$$

where k_l is the Lagergren rate constant of adsorption (min^{-1}). The values of q_e and k_l were determined from the plot of ln ($q_e - q_t$) against t.

$$\frac{t}{q_t} = \frac{1}{k_2} \frac{1}{q_e^2} + \ \frac{t}{q_e} \tag{3.8}$$

where k_2 is the pseudo second-order rate constant of adsorption (g/mg min). The values of the pseudo-second-order rate constants q_e and k_2 were calculated from the slopes and intercepts of the straight portion of the linear plots obtained by plotting t/q_t *vs* t.

3.4.1.2 Isotherm Study during the batch adsorption

The isotherm study was conducted with the metal or dye solution with an initial concentration of 20 to 100 mg/L. The same amount of adsorbent was added to 100 mL of solution of different concentrations and the pH was adjusted if required. The adsorption process was carried out in 250-mL Erlenmeyer flasks for 24 h at 120 rpm at the temperature obtained either by the optimisation process or at room temperature of 30 ^{o}C as required. To understand the interaction between ions and the adsorbent, most widely accepted mechanisms namely the Langmuir Isotherm, the Freundlich Isotherm, Temkin isotherm and Dubinin–Radushkevich isotherms were applied (Kundu, et al., 2014a).

The assumptions made in the Langmuir isotherm were that the surface with homogeneous binding sites and equivalent sorption energies did not interact between the adsorbed species. The linearised form of the Langmuir equation can be expressed as follows:

$$\frac{1}{q_e} = \frac{1}{q_{max} C_e} + \frac{1}{C_e q_{max}\, b} \qquad (3.9)$$

where $q_{\max}$ and b represent the maximum adsorption capacity for the adsorbent and the energy constant related to the heat of adsorption, respectively. The values of $q_{\max}$ and b were calculated from the slopes and intercepts of the straight line that was obtained by plotting $1/q_e$ *vs*. $1/C_e$.

The Freundlich Isotherm is an empirical equation based on an exponential distribution of adsorption sites and energies. The linear form of the equation is represented as follows:

$$\ln q_e = \ln K_f + \frac{1}{n} \ln C_e \qquad (3.10)$$

where K_F (L/g) and n are Freundlich constants related to the adsorption capacity and intensity, respectively. The values of Freundlich constants were obtained from the slope and intercept of the straight line obtained by plotting ln q_e against ln C_e.

The Temkin isotherm model assumed linear decrease in the heat of adsorption with increasing coverage (Dada et al., 2012). The isotherm can be represented by the following equation:

$$q_e = \left(\frac{RT}{b}\right) Ln\ A + \left(\frac{RT}{b}\right) Ln\ C_e \tag{3.11}$$

where A, b, R, and T represent Temkin isotherm equilibrium binding constant (L/g), Temkin isotherm constant, universal gas constant (8.314J/mol K) and Temperature (25 ^{o}C or 298K), respectively. The constants A and b were calculated from the slope and intercept of the q_e against Ln C_e plot.

Dubinin–Radushkevich isotherm model was used to study the adsorption mechanism with a Gaussian energy distribution on a heterogeneous surface. The model often successfully related high solute activities and the intermediate range of concentration data (Günay et al., 2007). The isotherm can be expressed by the following equation:

$$Ln\ q_e = Ln\ q_m - K\varepsilon^2 \tag{3.12}$$

where K (mol^2 k/J^2) and ε^2 are Dubinin–Radushkevich isotherm constants. The saturation adsorption capacity q_m and K were calculated from the interception and slope of Ln q_e against ε^2 plot.

3.4.2 Removal of heavy metal and dye by RPB-HIGEE system

RPB-HIGEE system is a special type of reactor in which a doughnut shaped packed bed is rotated with the help of a motor, as shown in the schematic diagram in Figure 3.3.

In this experimental set-up, the rotor was annular shaped and packed with activated carbon. The activated carbon was placed in the annular space at various packing density. Liquid was injected through the liquid injector to the inner wall of the rotor. As the rotor spun at high speed, the liquid was ejected from the outer wall. The inner as well as outer wall was made of stainless steel mesh of 45 µm, such that the packed material will not be released with the liquid. The liquid that was released from the outer wall collided with the wall of the casing and the water was collected from the liquid outlet tube located at the bottom of the casing. In this study, the packed bed spun on a vertical axis. The height of the bed was 1 cm. The inner radius of the rotor was 2 cm and the outer radius was 3 cm; therefore, the annular space was 1 cm wide. The rotor was spun with the help of a 0.5 hp motor. The rotor could be operated at a speed of 100 to 2000 rpm, thereby generating 0.3 to 112 times the gravitational force based on the arithmetic mean radius. The actual RPB system is shown in the Figure 3.4. The RPB system used in this study was specifically for liquid solid system and custom made with the help of Syarikat Get Sdn Bhd.

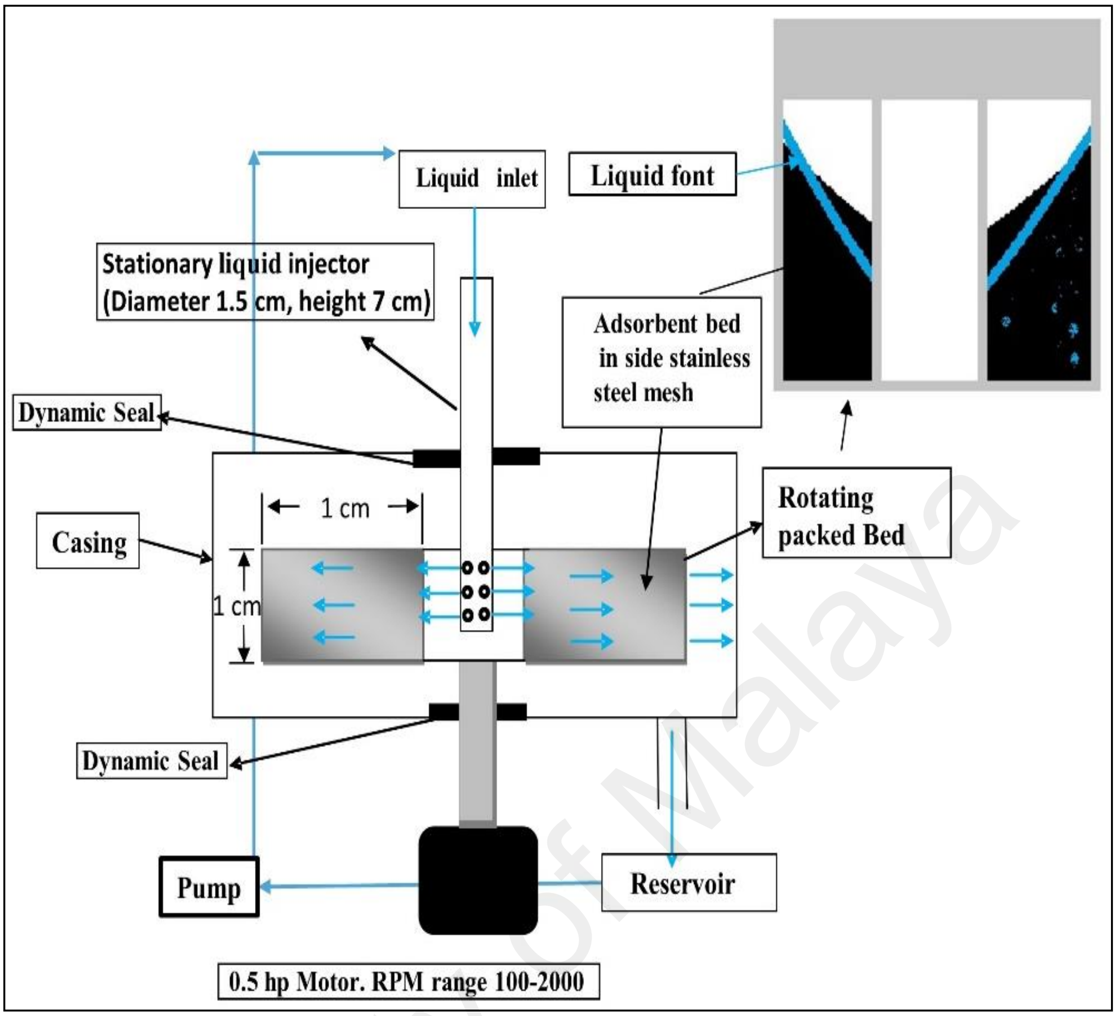

Figure 3.3 Schematic diagram of RPB

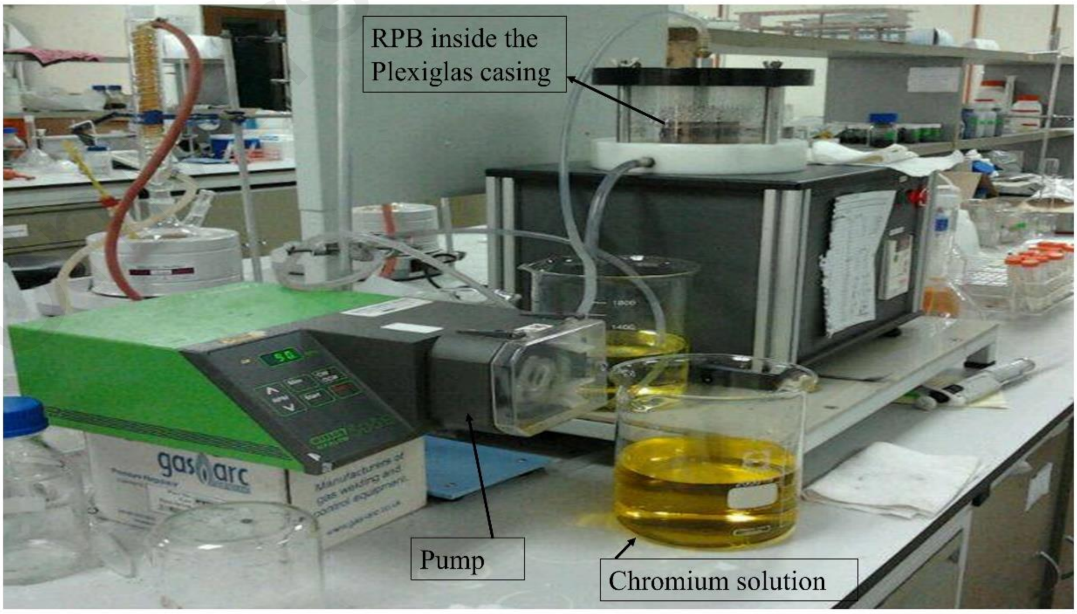

Figure 3.4 The real time diagram of RPB instrument used for experimental purpose.

A litre of sample solution at different concentrations of the heavy metal and dye was used in each RPB experiment. The heavy metal and dye solution was recirculated with the help of a pump at various feed rate to the RPB. The concentration of dye samples was determined by the absorbance obtained from the Perkin Elmer Lambda 35 UV/VIS spectrophotometer at the desired wavelength. The concentration of the heavy metal was measured with ICP-OES (Perkin-Elmer 7000DV).

3.4.3 Optimisation of heavy metal adsorption by MWAC2 using Cr(VI)

The experimental design, numerical modelling and optimisation studies were completed using Design Expert 7 software. The Box Behnken design was used to model the experiments and the design summary is as presented in Table 3.7. The independent variables used in this study were initial adsorbate concentration, initial operating pH and operating temperature. The three variables were coded as A, B and C respectively, as shown in Table 3.7. The ranges of independent variables were designated by -1, 0 and +1 respectively, and were fixed based on preliminary experiments and literature survey. The experimental design data, as provided by the software, are given in Table 3.8.

The interactions between process variables and the response were determined by analyses of variance (ANOVA) with the aid of the same software. The same programme determined the quality of fit of the polynomial model, expressed by the coefficient of regression, R^2, while its statistical significance was checked by the Fisher F-test (Fisher variation ratio). Model terms were accepted or rejected based on the P value (probability) with a 95% confidence level. The interaction among three factors, i.e. initial concentration, pH and temperature were shown in three-dimensional plots. The nature of interaction between two factors were also represented by three-dimensional plots.

The first step of RSM required the addition of appropriate approximation, with the purpose of finding a true relationship between the set of independent variables (factors) and the dependent variable, i.e. the response. According to Bayraktar (2001) a mathematical linear model which was insufficient to explain the shape of the response surface can be upgraded by adding higher order terms to the preliminary linear equation. Thus, the model can be explained by a quadratic equation defined in equation 3.13 suggested by the Design expert software (Adinarayana and Ellaiah, 2002; Bayraktar, 2001; Mukherjee et al., 2013).

$$y = \beta_{\circ} + \sum_{i=l}^{k} \beta_i X_i + \sum_{i=l}^{k} \beta_{ii} X_i^2 + \sum_{i\leq j}^{k} \sum_{j}^{k} \beta_{ij} X_i X_j + \varepsilon \qquad (3.13)$$

where y = the response or dependent variable,

i and j = linear and quadratic coefficients,

β = the regression coefficient,

k = the number of factors studied and optimised in the experiment, and

ε = the random error.

Table 3.7 Experimental Design Summary for heavy metal adsorption using Cr(VI)

Factor	**Name**	**Type**	**Low Actual**	**High Actual**	**Central Values (Zero level)**
A	Initial Conc	Numeric	20	60	40
B	pH	Numeric	1	5	3
C	Temp	Numeric	20	50	35

Table 3.8 Experimental Design according to Box Behnken model for heavy metal adsorption using Cr(VI)

Run	**Type**	**Factor 1 A:Intical Conc. (mg/L)**	**Factor 2 B:pH**	**Factor 3 C:Temp (ºC)**
1	IB Fact	40	5	20
2	IB Fact	20	3	50
3	IB Fact	40	5	50
4	Center	40	3	35
5	IB Fact	60	3	50
6	IB Fact	60	5	35
7	IB Fact	60	1	35
8	Center	40	3	35
9	IB Fact	20	3	20
10	IB Fact	40	1	20
11	IB Fact	20	5	35
12	Center	40	3	35
13	Center	40	3	35
14	IB Fact	60	3	20
15	Center	40	3	35
16	IB Fact	40	1	50
17	IB Fact	20	1	35
18	Center	40	3	35

3.4.4 Optimisation of dye removal by Taguchi method using Direct Red 23

Four operating variables namely initial concentration, pH, activated carbon loading and temperature were considered for this experiment. The design of experiments was constructed according to an L16 orthogonal array in four different levels for the four control factors. The particle size of the activated carbon was considered as the noise factor as it could affect the adsorption capacity of the activated carbon up to a considerable level and controlling the particle size was troublesome. Hence, consideration of the effect of this noise factor will reduce the variance in result. Particle size in the range of 100-500 µ was considered as noise factor 1 (NF1) while that in the range of 500-750 µ was classified as noise factor 2 (NF2) (Kundu, et al., 2014b). The control factors and their levels are given in Table 3.9 and the L16 experimental design is given in Table 3.10, respectively.

Table 3.9 Operational variables and their levels used in optimization study for dye removal using DR 23

Investigating parameters	**Level 1**	**Level 2**	**Level 3**	**Level 4**
Initial concentration (mg/L)	20	50	80	100
pH	2	5	7	10
Activated carbon dose (g/L)	1	2	3	4
Temperature (°C)	10	20	30	40

Table 3.10 Taguchi experimental matrix and result obtained from dye adsorption using DR23

Experiment no	**Initial Conc**	**pH**	**Dose**	**Temp**
1	20	2	1	10
2	20	5	2	20
3	20	7	3	30
4	20	10	4	40
5	50	2	2	30
6	50	5	1	40
7	50	7	4	10
8	50	10	3	20
9	80	2	3	40
10	80	5	4	30
11	80	7	1	20
12	80	10	2	10
13	100	2	4	20
14	100	5	3	10
15	100	7	2	40
16	100	10	1	30

For the kinetic study, 200 mL of DR23 solution with concentration of 100 mg/L was taken in the Erlenmeyer flask. Thereafter, 2 g/L of MWAC was added to the solution. The flask was placed on an orbital shaker and agitated for 24 h. Samples were drawn at 10 minutes interval for 2 h, at every half an hour interval for 1 hour, at every hour interval for 3 hours and after 24 hours. Both pseudo-first-order and pseudo-second-order kinetics, given by equation 3.7 and 3.8, respectively, were fitted to the experimental data. Weber-Morris model was used to study the rate-controlling step.

Isotherm experiments were carried out for four different concentrations; 40 mg/L, 60 mg/L, 80 mg/L and 100 mg/L. The observed data points were fitted to linear form of Langmuir, Freundlich and Temkin isotherm equations given by equation 3.9, equation 3.10 and equation 3.11, respectively.

Adsorption thermodynamics can be described by parameters of free energy change (ΔG^0), enthalpy change (ΔH^0) and entropy change (ΔS^0). Free energy change (ΔG^0) can be calculated using equation:

$$\Delta G^0 = -RT \ln K \qquad (3.14)$$

$$K = \frac{q_e}{C_e} \qquad (3.15)$$

$$\ln K = \left(-\frac{\Delta H^0}{RT}\right) + \left(\frac{\Delta S^0}{R}\right) \qquad (3.16)$$

where K is the equilibrium constant. Values of enthalpy change (ΔH^0) and entropy change (ΔS^0) were obtained from the slope and intercept of the plot of ΔG^0 vs T.

3.4.5 Dye removal onto $MWAC_T$ in RPB using DR23

DR23 dye was mixed thoroughly with distilled water to prepare solutions having concentrations 50 and 100 mg/L. The samples were marked as SF 50 and SF 100, respectively and used for shake flask experiment. For shake flask experiments, 200 mL of dye sample was taken in an Erlenmeyer flask and 2 g activated carbon added to it. The flask was agitated in an orbital shaker at 150 rpm. For analysis purpose, four-millilitre sample was collected and centrifuged at 2000 rpm to separate the solid from liquid. Dye concentration were determined by the Perkin Elmer Lambda 35 UV/VIS spectrophotometer at the required wavelength. One litre of sample solution of same two concentrations were taken in a 2L beaker for RPB experiments and marked as RPB 50 and RPB 100, respectively. To study the effect of contact time, percent removal of DR23 dye was observed for 24 hours. In this case, the rotor speed, feed rate and activated carbon loading were 1140 rpm, 40 L/h and 10 g, respectively. The ratio of solid to liquid (10g/L) was maintained for both shake flask and RPB experiments. Samples were collected for spectrophotometric analyses at ten minutes interval for the first two hours and then at every one-hour interval up to five hours followed by further collection at the 8th, 12th, 16th, and 24th hour from the start. The samples were collected from the reservoir by pipetting out 4 mL of liquid each time. The samples were returned to the reservoir as soon as measurement was done. In case of RPB, there was no need for any separation of solid and liquid as all the solid remain inside the rotor. The removal percentage of dye at time t, q_t (mg/g) was calculated by the following equation 3.17.

$$q_t = \frac{(C_0 - C_t) * 100}{C_0} \tag{3.17}$$

where C_0 (mg/L) is the initial dye concentration and C_t (mg/L) is the dye concentration at any time, t.

The data points were then fitted to the linear form of pseudo-first-order kinetics as well as pseudo-second-order kinetics as, described in the section 3.4.1.1 (Kundu, et al., 2014a). In order to check the mechanism of adsorption, the intra-particle diffusion model suggested by Webber and Morris (Kushwaha et al., 2008) was also studied. The initial rate of intra-particle diffusion was obtained by the linear form of the Webber and Morris equation (Kushwaha, et al., 2008):

$$q_t = K_t t^{0.5} \tag{3.18}$$

3.4.6 Optimisation of process parameters for removal of chromium by MWAC$_T$ in RPB

Taguchi method was used in this study to find the optimum operating condition for the removal of chromium by activated carbon in a RPB-HIGEE system. Operating parameters such as rotating speed, liquid feed rate, activated carbon packing density and initial pH of the solution were examined at different levels to obtain the optimum condition for RPB-HIGEE system. The kinetics and mechanism for the adsorption process were also examined.

Rotating speed (rpm), feed rate (L/min), packing density (kg/m^3) and initial solution pH were the most important parameters, controlling the adsorption of chromium onto activated carbon. In this experiment, there were four parameters and each has four levels. Therefore, each parameter had 3 degrees of freedom; hence, total degrees of freedom for all the parameters were 12. The standard L16 orthogonal array had 15 degrees of freedom. Therefore, L16 orthogonal array was chosen with four operating parameters known as control factors, with four levels for each, as shown in Table 3.11. Table 3.12 shows the L16 orthogonal array. Minitab 16 software was used to formulate the Taguchi orthogonal array and in the computation of ANOVA and level averages. The initial concentration of chromium in solution, considered as a noise factor in this experiment, was to reduce the variance in result. Initial concentration of 60 mg/L was considered as the noise factor 1 (NF1) while initial concentration of 80 mg/L and 100 mg mg/L were termed as noise factor 2 (NF2) and noise factor 3 (NF3), respectively.

Table 3.11 Levels of the control factors used for removal of chromium.

Investigating parameters	Level 1	Level 2	Level 3	Level 4
Rotating speed (rpm)	400	800	1200	1600
Feed rate(L/min)	20	30	40	50
Packing density (kg/m^3)	153	255	357	510
Initial Solution pH	2	3	4	5

Table 3.12 L16 experimental design for removal of chromium.

Rotating speed	Feed rate	Packing density	Initial pH
400	20	153	2
400	30	255	3
400	40	357	4
400	50	510	5
800	20	255	5
800	30	153	4
800	40	510	3
800	50	357	2
1200	20	357	3
1200	30	510	2
1200	40	153	5
1200	50	255	4
1600	20	510	4
1600	30	357	5
1600	40	255	2
1600	50	153	3

The kinetic experiment was performed with a chromium solution of initial concentration 50 mg/L. The other parameter settings were at the optimum condition as obtained by the Taguchi method. The samples were collected from the reservoir at ten minutes interval for two hours and then the collection interval was increased to 30 min and samples were collected up to four hours. The RPB was commissioned up to ten hours such that an equilibrium was achieved. The samples drawn from the reservoir were tested using ICP-OES, for the final concentration of chromium. The data obtained were analysed for the quality of fit to linear form of pseudo-first-order kinetics and pseudo-second-order kinetics as described in section 3.4.1.1. Standard linearised-integral form of pseudo-first-order and a pseudo-second-order kinetic model were represented by equation 3.7 and 3.8, respectively.

3.5 Summary

The materials and methods that were adopted to perform the experiments in order to achieve the aim and objectives of the study were described in detail in the above sections and subsections. The description of the microwave heating, physical and chemical characterisation has been described in detail. The construction and the commissioning of the RPB has also been discussed in this chapter. The following chapter critically analyse and explain the results those were obtained in the experiments mentioned in this chapter.

CHAPTER 4: RESULTS AND DISCUSSION

Adsorption on activated carbon in a high gravimetric field was the principal approach adopted for the wastewater treatment in this study. In this approach, requirement of an activated carbon, which is inexpensive and can be easily produced from locally available raw material was realised. Thus palm kernel shell (PKS), which are easily available waste material from palm oil mills were used in this work. For the efficient production of activated carbon from PKS, microwave technology was applied. According to Jones, et al. (2002), the microwave is proven to penetrate a wide variety of materials, while the microwave energy is converted to heat energy that spreads throughout the bulk of the material. This can reduce the processing time and improve the overall quality of the adsorbent by generating high surface area and pore volume. Hence, microwave heating was applied to prepare the activated carbon from impregnated PKS. The prepared activated carbon was applied to remove heavy metal and dye in conventional shake flask experiments and in a RPB, which is a high performance contactor that was used in this study. This chapter presents the experimental results and analyses of the data obtained during the experiments.

4.1 Production of activated carbon

The quality of the PKS was determined by the proximate analyses in terms of carbon, moisture, ash and volatile matter content. The proximate analyses of the PKS showed that the carbon content of the PKS was almost 50 % which made the PKS a suitable material for preparation of activated carbon. The ash content, the unwanted part, was also very low. The detailed values of the proximate and ultimate analyses are given in Table 4.1

Table 4.1 Proximate and ultimate analyses of palm shell

Parameters	Value (wt %)	Parameters	Value (wt %)
Moisture	12	C	50.68
Ash	3.1	H	5.12
Fixed carbon	19.7	N	0.18
Volatile*	65.2	O*	43.86
		S	0.16

*By difference.

4.1.1 Using different impregnation ratios of H_3PO_4 and microwave heating

Different types of activated carbon were prepared with three different impregnation ratios of H_3PO_4. The prepared activated carbon was characterised by pH, average bulk density, BET surface area, SEM and FTIR analyses. The removal efficiency could be affected by the adsorbent pH. Acidic adsorbent may affect the removal efficiency by counter reacting with the material to be removed. In this work, 3 g of the prepared activated carbon was mixed with 30 mL of distilled water and agitated. The pH was recorded after 24 h of agitation following Acharya, et al. (2009). The pH values were 5.92, 6 and 6 for MWAC 1, MWAC 2 and MWAC 3, respectively.

The average bulk density of the activated carbon was measured by water displacement method and it was found to be 0.80 g/mL, 0.86 g/mL and 0.75 g/mL, respectively, for MWAC 1, MWAC 2 and MWAC 3. It is known that higher the bulk density of the activated carbon, more will be the removal of heavy metal and dye (Acharya, et al., 2009). The BET surface areas obtained from the nitrogen adsorption-desorption isotherm were high as evident from the data tabulated in Table 4.2.

.

Table 4.2 Result of the nitrogen adsorption-desorption isotherm for the prepared activated carbon

Sample	BET surface area (m^2/g)	Total pore volume (cc/g)	Average Pore Diameter (Å)
MWAC 1	872	0.598	27.4
MWAC 2	1256	1.010	32.4
MWAC 3	952	0.778	32.7

MWAC 2 had the highest surface area of 1256 m^2/g. The average pore diameter suggested that the prepared activated carbon was mainly mesoporous. As Figure 4.1 suggests, the nitrogen adsorption-desorption isotherms were mainly type II as classified by IUPAC (Carmody et al., 2007; Rouquerol et al., 1994) with strong adsorbate-adsorbent interactions and represent unrestricted monolayer-multilayer adsorption. The activated carbons contained pore width varying from 4 to 50 Å.

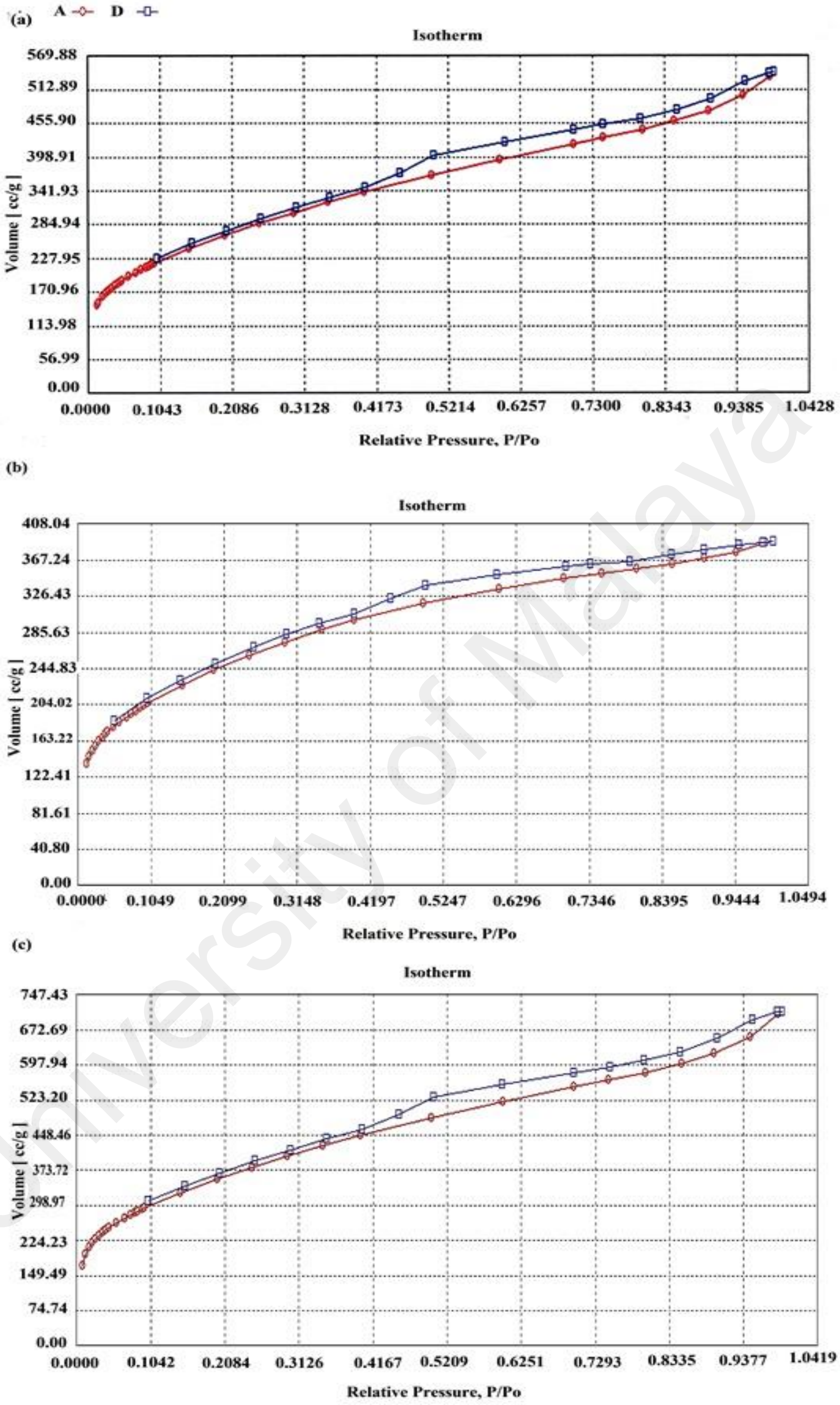

Figure 4.1 Nitrogen adsorption-desorption isotherms of A) MWAC 1, B) MWAC 2, C) MWAC 3

SEM images were used to characterise the surface morphology. Figure 4.2 depicts the surface morphology for the precursor and the three different types of prepared activated carbons. The precursor had very low porosity on the surface as can be seen from Figure 4.2A. However, development of highly porous surface due to treatment with phosphoric acid is evident from Figure 4.2B, Figure 4.2C and Figure 4.2D.

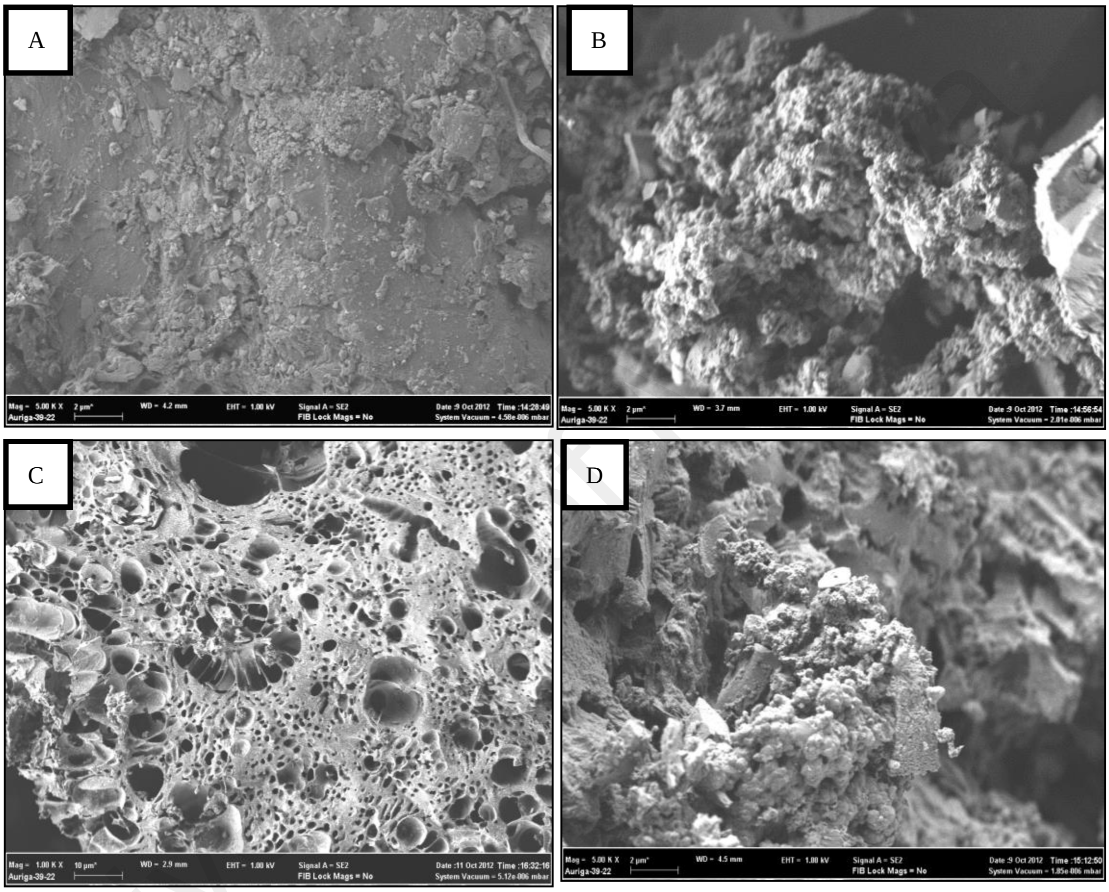

Figure 4.2 SEM images of A) precursor B) MWAC 1 C) MWAC 2 D) MWAC 3

The absence of peaks at 3452 cm^{-1} and 2923 cm^{-1} from the FTIR spectra obtained for the three different prepared activated carbons in comparison to the spectra obtained for the raw material (Figure 4.3) suggests that the hydrogen part was removed due to carbonisation. The spectra of the activated carbons shown in Figure 4.3 suggest that the carboxylic part is absent but the aromatic rings are present as peaks are observed around 1580 cm^{-1}.

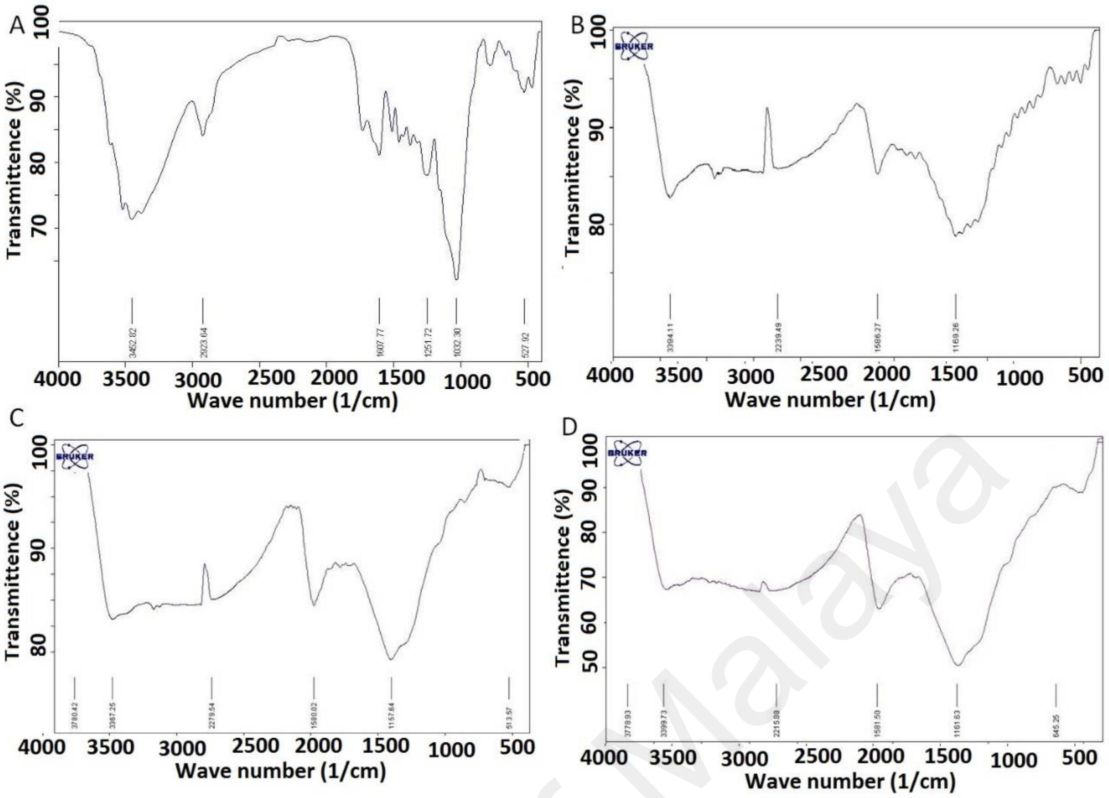

Figure 4.3 FTIR image for A) precursor B) MWAC 1, C) MWAC 2, D) MWAC 3

The results of the characterisation study suggested that MWAC 2 had the highest surface area and bulk density among the three prepared activated carbons. Hence, MWAC 2 was chosen for the removal of chromium with the help of response surface methodology.

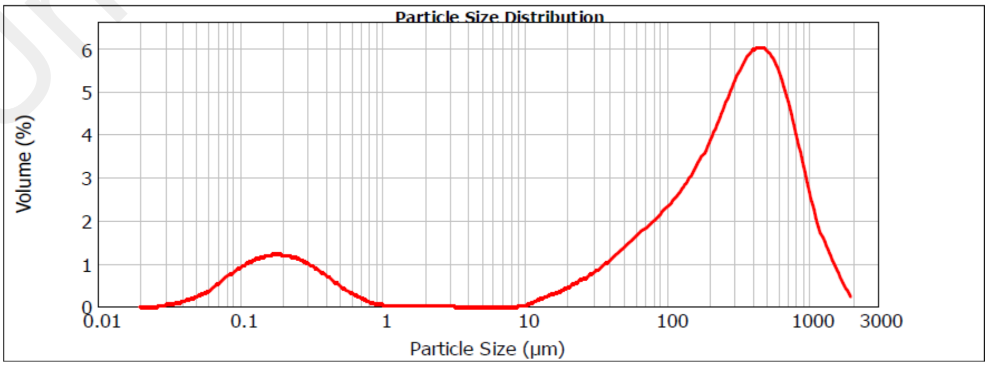

Figure 4.4 Particle size distribution of the activated carbon MWAC 2

The particle size analysis of the selected activated carbon as shown in Figure 4.4 suggests that the particle size was distributed between 100 to 1000 µm.

4.1.2 Optimising the production of activated carbon using Taguchi method

In order to obtain a robust optimised condition of the production parameters, Taguchi method was applied in this study. The optimisation was performed in two stages to obtain the most suitable operating condition.

4.1.2.1 Initial optimisation: Effects of the control factors and noise factor on the activated carbon preparation

Optimisation of the preparation conditions for activated carbon preparation were performed by Taguchi method. Thirty-two different activated carbon samples were prepared according to L16 array of Taguchi method, which considered the noise factors and tested for Methylene Blue (MB) adsorption. The adsorption capacity of the activated carbon and corresponding S/N ratio is given in Table 4.3.

Table 4.3 L16 experimental design with the noise factors, the measured value of MB adsorption and corresponding S/N ratios.

Inner control factor array					**Outer noise factor array**		
					Methylene blue adsorption (mg/g)		
Experiment No	**Microwave Power (W)**	**Time (min)**	**Impregnation ratio (acid:pks)**	**Conc. of acid (H_3PO_4) (%)**	**NF1 (0.5-1 mm)**	**NF2 (1-2 mm)**	**S/N ratio**
1	400	3	0.5	42.5	7.46	19.4	19.87
2	400	10	1	42.5	28.15	30.1	29.26
3	400	17	1.5	85	100	100	40
4	400	24	2	85	100	100	40
5	600	3	1	85	84.43	81.59	38.37
6	600	10	0.5	85	18.85	41.26	27.69
7	600	17	2	42.5	100	100	40
8	600	24	1.5	42.5	100	87.6	39.38
9	800	3	1.5	85	100	67.74	37.98
10	800	10	2	85	100	100	40
11	800	17	0.5	42.5	77.81	63.26	38.53

Inner control factor array					**Outer noise factor array**		
					Methylene blue adsorption (mg/g)		
Experiment No	**Microwave Power (W)**	**Time (min)**	**Impregnation ratio (acid:pks)**	**Conc. of acid (H_3PO_4) (%)**	**NF1 (0.5-1 mm)**	**NF2 (1-2 mm)**	**S/N ratio**
12	800	24	1	42.5	85.74	78.91	38.28
13	1000	3	2	42.5	100	100	40
14	1000	10	1.5	42.5	100	100	40
15	1000	17	1	85	100	100	40
16	1000	24	0.5	85	26.08	59.19	30.56

The S/N ratio was tested by ANOVA to determine the significance of the S/N data obtained. ANOVA determines the impact of the independent variables on the dependent variables in a regression analysis. ANOVA results of the S/N ratio is given in Table 4.4. Effects of control factors on the S/N ratio of the MB adsorption of the prepared activated carbon can be observed in Figure 4.5.

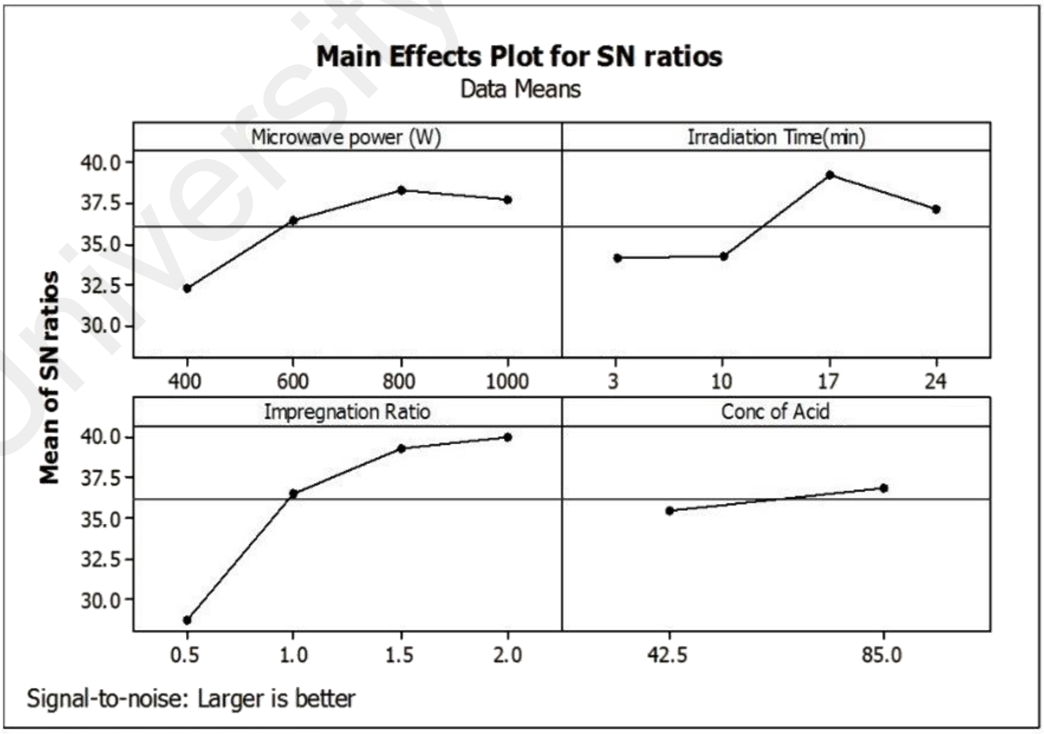

Figure 4.5. The effect of control factors on the S/N ratio of the MB adsorption by the prepared activated carbon sample

Bold values in Table 4.4 are the maximum average S/N performances of each factor in the four different levels. The largest S/N performance corresponds to the best performance characteristic. According to Kirby (2006), the F-ratio can indicate the effect of the control factor on the observed result. An F-ratio less than one suggests insignificant effect while a value near about two suggests moderate effect and if the F-ratio is more than four, the control factor has a strong and significant effect. From Table 4.4, it can be observed that microwave power as well as irradiation time had moderate effect on the preparation with F-ratio 2.62 and 2.20, respectively, whereas impregnation ratio clearly had very significant effect on the preparation of activated carbon. Concentration of the acid had no such significant impact on the quality of the activated carbon in terms of MB adsorption.

Table 4.4 ANOVA of the S/N ratios for MB adsorption of the prepared activated carbons

Source	DF[a]	Seq SS[b]	Adj SS[c]	Adj MS[d]	F	P	Level average				Delta	Rank
							Level 1	Level 2	Level 3	Level 4		
Microwave power (W)	3	86.99	86.99	28.99	2.62	0.16	32.28	36.36	**38.28**	37.64	5.99	2
Irradiation Time(min)	3	72.82	72.82	24.27	2.20	0.20	34.06	34.24	**39.21**	37.06	5.15	3
Impregnation Ratio	3	320.20	320.20	106.73	9.65	0.01	28.74	36.48	39.34	**40.00**	11.26	1
Conc of Acid	1	7.55	7.55	7.55	0.68	0.45	35.45		**36.83**		1.37	4
Residual Error	5	55.28	55.28	11.06								
Total	15	542.85										

[a]DF: degree of freedom, [b]Seq SS: sequential sums of squares, [c]Adj SS: adjusted sum of squares, [d]Adj MS: Adjusted mean of squares.

The S/N ratio for the microwave power increased as the level increased from 400 W to 800 W, implying that the adsorption capacity increased. However, when the power was higher than 800 W, the S/N ratio decreased indicating the decrease in adsorption capacity of the activated carbon. The initial rise in the adsorption capacity might be attributed to the formation of more pores and better pore structure. At the highest level of microwave power, the destruction of pores and burning of the raw material to ash led to the loss of adsorption sites, and thus reduced the adsorption capacity. Similar observation was reported by Deng, et al. (2010b). Practically no changes were observed in the S/N ratio for the first two levels of irradiation time of 3 min and 10 min. The S/N ratio and adsorption capacity increased steeply when the raw material was heated for 17 min but decreased when heated for 24 min. The increase in the adsorption capacity of the activated carbon at the third level was due to the formation of the pores but at higher level, the excessive exposure to the microwave might have damaged the pores, and consequently the adsorption capacity decreased. Similar trend was reported by Aber, et al. (2009). The impregnation ratio had a very significant effect on the adsorption capacity of the activated carbon. At lower level of IR, the amount of acid was too small to react with the amount of raw material adequately; therefore, the development of the micro and meso-pores were not facilitated. However, as the impregnation ratio increased, the cellular structure of PKS were attacked by the acid, which resulted in the rupture of the linkages between the lignin and cellulose during impregnation stage, followed by formation of larger structural units and strong cross linked solids (El-Hendawy et al., 2008). The concentration of the acid had no significant effect on the adsorption capacity of the activated carbon. However, it was found that the higher concentration of acid had higher S/N ratio, probably because acid that is more concentrated aided the bond breaking of lignin and cellulose.

4.1.2.2 Significance of noise factors

The significance of the effect of noise factor was analysed from t-test performed on the data set obtained for different noise conditions. A two tailed t-test to examine the equality of means, assuming equal variances, shows that the P-Value is 1.00 (Table 4.5), which is much greater than 0.05; therefore, the null hypothesis was accepted which implies that the means do not differ significantly across two samples. Consequently, we can conclude that the noise factor for particle size had no significant effect on the adsorption capacity of the activated carbon.

Table 4.5 t-Test to find the significance of noise factors

	Variable 1	**Variable 2**
Mean	76.78	76.81
Variance	1,205.88	748.99
Observations	16.00	16.00
Pooled Variance	977.44	
Hypothesized Mean Difference	0.00	
Df	30.00	
t Stat	0.00	
P(T<=t) two-tail	1.00	
t Critical two-tail	2.04	

4.1.2.3 Optimisation of the process variable and validation

The mean S/N ratio for each level of the control factors was summarised as S/N response, which is shown in Table 4.4. The S/N ratio should always be highest at the optimum condition because it is desirable that the signal is much higher than the noise. Thus, the optimum condition for activated carbon preparation corresponded to the levels having largest average S/N ratio. Therefore, it can be inferred that the optimum condition is the following: microwave power of 800 W (level 3), irradiation time of 17 min (level 3), impregnation ratio of 2 (level 4) and concentration of acid 85% (undiluted). For further study, a sample of activated carbon was prepared using these settings of the control factors.

4.1.2.4 Fine-tuning the optimum level for production of activated carbon with Taguchi method

The optimum points obtained from the initial optimisation needed to be fine-tuned in order to obtain more accurate preparation conditions. An L9 orthogonal array was applied for this purpose without considering any external noise factor as these were already considered in the initial optimisation. The data obtained in the experiment for the BET surface area and corresponding S/N ratio is presented in Table 4.6.

Table 4.6 L9 experimental design with the noise factors and the measured value of BET surface area and corresponding S/N ratios

Impregnation ratio	Microwave Power	Time	BET Surface area	S/N ratio
1	700	13	934	59.45
1	800	17	867	58.87
1	900	21	873	58.78
2	700	17	1535	63.71
2	800	21	1211	61.66
2	900	13	1136	61.1
3	700	21	1048	60.44
3	800	13	981	59.77
3	900	17	1094	60.74

The ANOVA of the obtained data for the fine-tuning experiment suggests that all the three parameters considered for the study have important role in determining the quality of the activated carbon. Table 4.7 shows that the F-value of the impregnation ratio is as high as 23.21, which is very significant. The effect of the control factors on the S/N ratio for the fine-tuning experiment is presented in the Figure 4.6. From the S/N ratio, it can be observed that the impregnation ratio of 2 (level 2) and irradiation time of 17 min (level 2) remain the same as the previous initial optimisation. However, the microwave power in case of fine-tuning was different from the initially obtained optimised value. The microwave power of 700 W had the highest S/N ratio.

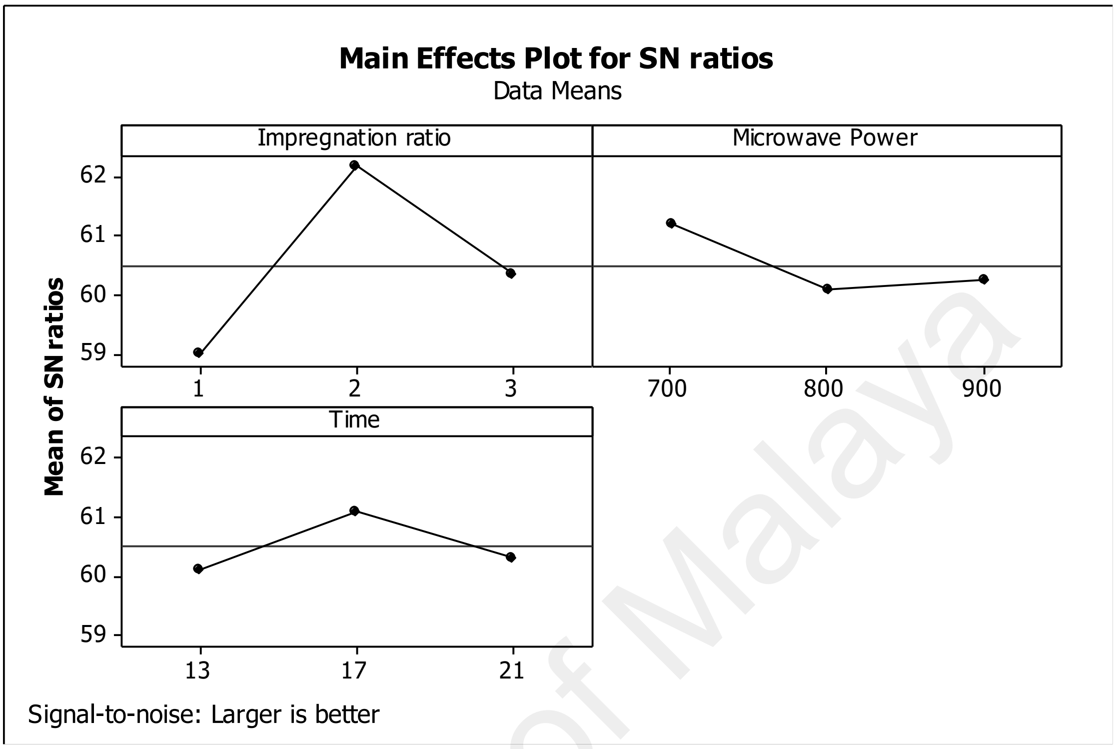

Figure 4.6 The effect of control factors on the S/N ratio of the BET surface area of the prepared activated carbon sample

The optimum conditions according to Taguchi method for the fine-tuning experiment were found to be impregnation ratio of 2 (level 2), microwave power of 700 W (level 1) and irradiation time of 17 min (level2). Here, the conditions of the optimum levels were already incorporated in the experimental matrix. Hence, separate experiment for conformation was not necessary. The BET surface area obtained in the optimum level was 1535 m^2/g. Hence, it can be concluded that the formation of pores were more prolific at 700 W rather than on 800 W, as obtained in the coarse optimisation. The BET surface area of the activated carbon prepared in the coarse optimisation method was found to be 1474 m^2/g. Hence, it can be inferred that precise result was obtained by fine-tuning the experiment.

Table 4.7 ANOVA of the S/N ratios for BET surface area of the prepared activated carbons.

Source	DF[a]	Seq SS[b]	Adj SS[c]	Adj MS[d]	F	P	Level average			Delta	Rank
							Level 1	**Level 2**	**Level 3**		
Impregnation Ratio	2	14.77	14.77	7.38	23.21	0.041	59.03	**62.15**	60.32	3.12	1
Microwave power (W)	2	2.21	2.21	1.10	3.46	0.224	**61.2**	60.10	60.20	1.10	2
Irradiation Time(min)	2	1.69	1.69	0.85	2.66	0.273	60.11	**61.11**	60.29	1.00	3
Residual Error	2	0.63	0.63	0.32							
Total	8	19.30									

[a]DF: degree of freedom, [b]Seq SS: sequential sums of squares, [c]Adj SS: adjusted sum of squares, [d]Adj MS: Adjusted mean of squares.

4.1.2.5 Characterization of the activated carbon prepared at optimum condition

The prepared activated carbon under optimum condition was labelled as $MWAC_T$. The characteristics was determined by N_2 adsorption/desorption curve with the aid of BET equation, SEM images and FTIR data. The activated carbon produced in the fine-tuning experiment was also characterised with BET surface area and SEM image.

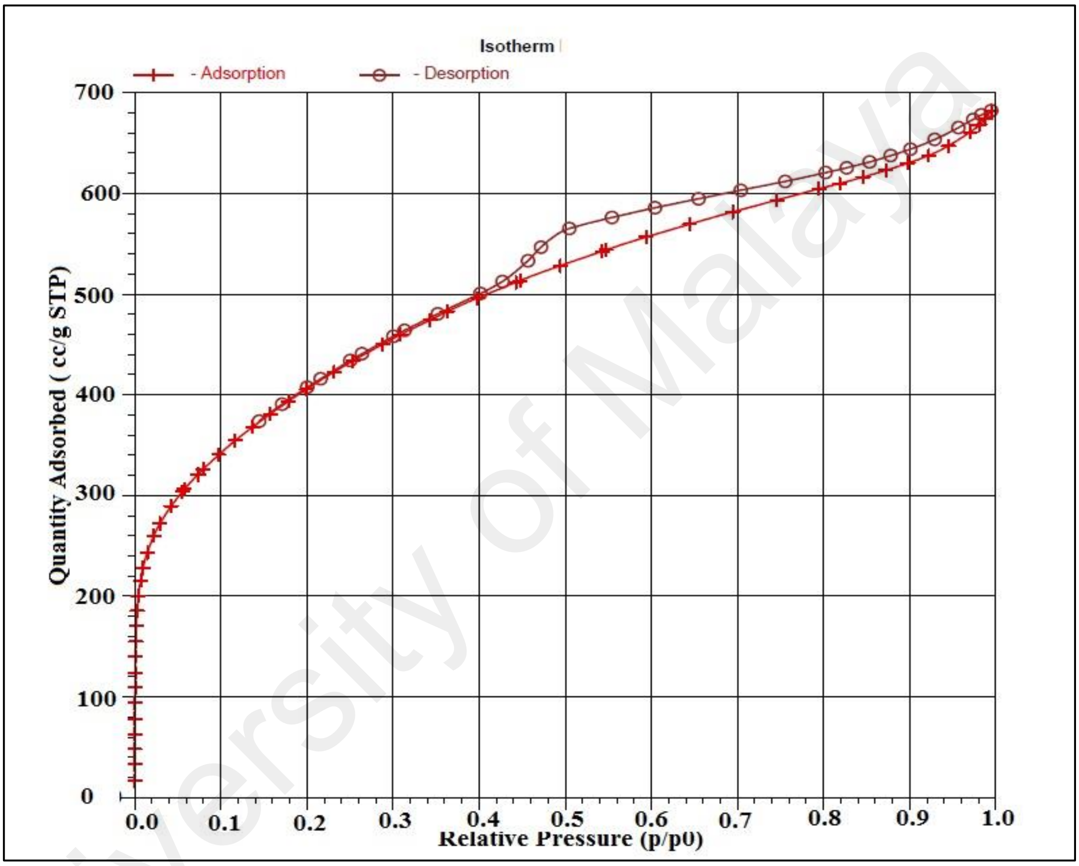

Figure 4.7 Nitrogen adsorption/desorption isotherm for the activated carbon prepared at the optimum condition showing type IV isotherm.

The BET surface area was found to be 1,474 m^2/g for the activated carbon obtained in the initial optimisation process, whereas the BET surface area of the activated carbon obtained from fine-tuning experiment was 1535 m^2/g. The nitrogen adsorption/desorption curve as shown in Figure 4.7, describes a type IV curve according to the IUPAC guideline (Rouquerol, et al., 1994) representing adsorption isotherm with hysteresis mainly associated with mesopores in the activated carbon. The sharp "knee" shape (Hoseinzadeh Hesas et al., 2013a) at the lower relative pressure suggests a considerable amount of micropores are present in the activated carbon. The average pore size was found to be 2.78 nm, which falls in the mesoporous range. According to Liu et al. (2010) intense activation reaction facilitated the formation of mesoporous activated carbon. Kubota et al. (2009) found similar mesoporous activated carbon and attributed the formation of pores to the rapid and volumetric heating, causing faster release of volatile matters from the raw material.

The raw material had much less surface roughness and porosity on the surface, as evident from the SEM image given in Figure 4.8(A). However, Figure 4.8(B) illustrates that activated carbon prepared in the optimum operating condition developed considerable amount of porosity after activation. The acid in the impregnation stage and microwave heating in the activation stage contributed towards the formation of pores and surface roughness.

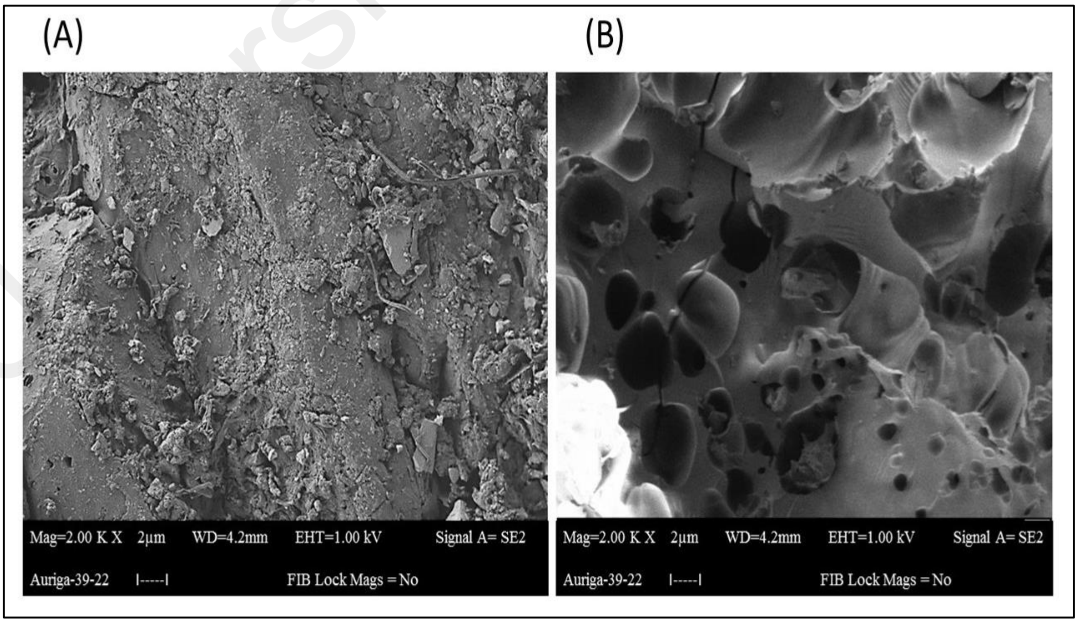

Figure 4.8 SEM micrographs (A) raw material (B) prepared activated carbon at optimised condition

The FTIR data in Figure 4.9 (A) and Figure 4.9 (B) show that the intensity of the peaks, which are between 3500 and 3200 cm^{-1} due to the O-H stretching of alcohols or phenols, decrease largely. Intensity of the band of 3000-2850 cm^{-1} corresponding to C-H stretch of alkanes has also diminished in the activated carbon. Both phenomena indicate that the phosphoric acid acted as a dehydrating agent and removed considerable amount of hydrogen from the raw material (Hesas et al., 2013) by chemical reaction. Reduction of intensity of the complex peaks around 1580-1650 cm^{-1} can be attributed to N-H bend of primary amines while the C-C stretch of aromatic ring in activated carbon is also observed. The C-O stretch for alcohols, carboxylic acids, esters and ethers corresponding to the band 1300-1000 cm^{-1} had much lower peak. These observations signifies removal of hydrogen and oxygen associated with the raw material.

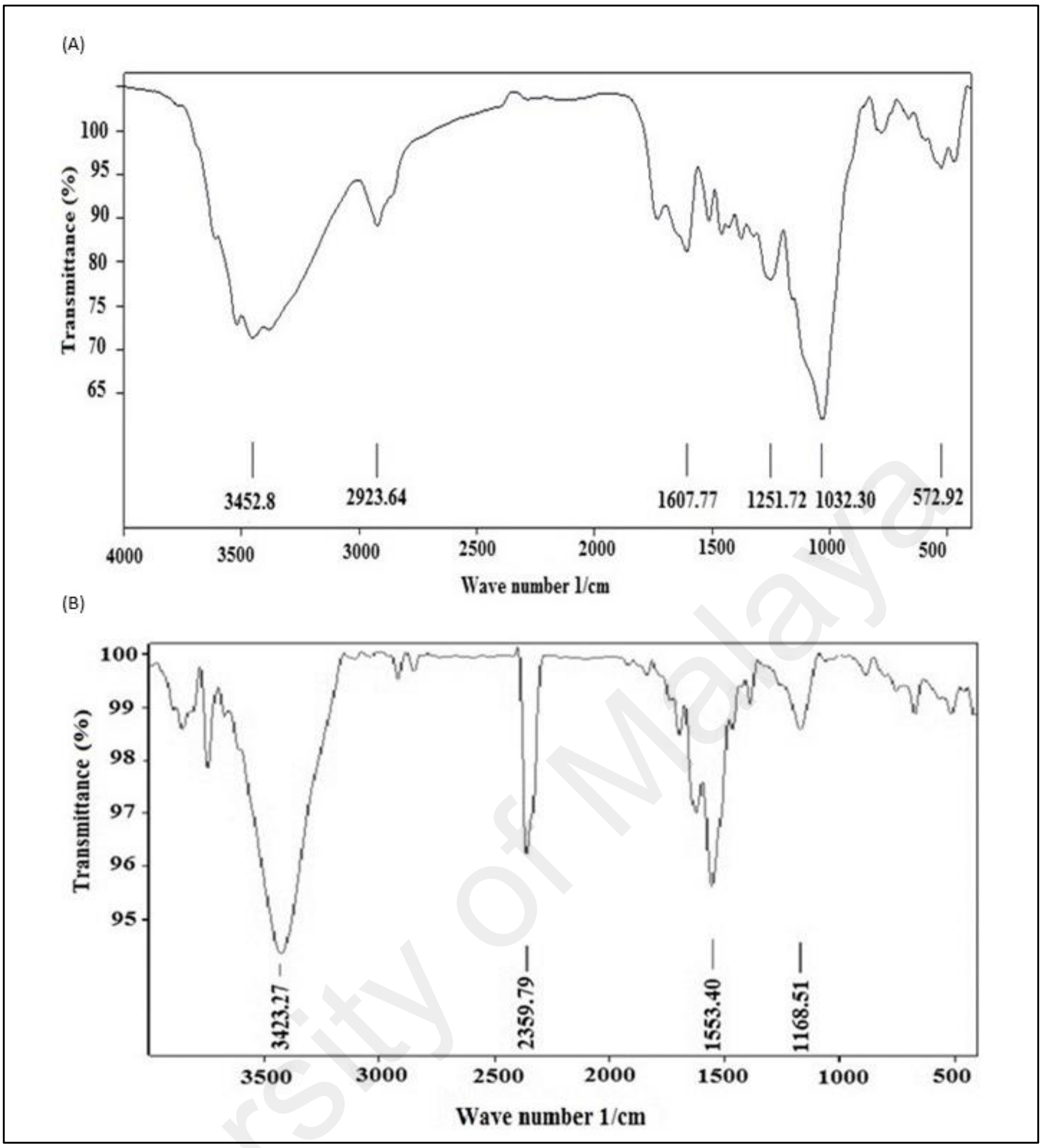

Figure 4.9 FTIR spectra of (A) the raw material and (B) prepared activated carbon at optimised condition

4.1.3 Optimising the production of activated carbon by CCD in response surface methodology

In a second optimisation study, CCD was used for RSM to optimise the production parameters. Here, the impregnation material used was H_2SO_4. The result obtained and the discussion on the statistical analyses is presented in the following subsections.

4.1.3.1 Statistical analysis and model development

Statistical analysis of the data obtained for the yield and zinc adsorption by 28 different samples prepared according to the design matrix were analysed with the help of central composite design and Design Expert software. The data were also fitted to linear, two-factor interaction (2FI), quadratic and cubic polynomials to determine the most suitable model. The quadratic model was most suitable for the data obtained according to the model fit summary. The adjusted R^2 value for the quadratic model for yield of activated carbon is 0.8889, much closer to unity than the R^2 values of linear (0.5772), 2FI (0.6494) and cubic polynomials (0.8642). The respective *p*-values for quadratic, linear, 2FI and cubic are 0.8083, 0.2326, 0.2802 and 0.6830 also support the quadratic model as the acceptable model. Data for adsorption of zinc can also be better fitted to the quadratic model. The adjusted R^2 value for the quadratic model for zinc adsorption is 0.8840, which is superior to the R^2 value of linear, 2FI and cubic polynomial model having R^2 value 0.0082, -0.2242 and 0.8435, respectively. The quadratic model equation for the zinc adsorption and the yield of activated carbon in terms of the coded factors are shown in equation 4.1 and 4.2:

$$Adsorption = 14.26 + 0.61A - 0.93B + 1.13c + 1.38D - 1.00AB - 0.18AC + 0.81AD + 0.63BC - 0.49BD - 4.98A^2 - 1.58B^2 - 1.70C^2 \qquad (4.1)$$

$$Yield = 57.92 - 12.83A - 4.67B - 9.04C - 7.09D + 1.71AB - 5.69AC - 3.81AD + 0.36BC - 5.0BD + 1.79CD + 5.34A^2 - 7.54B^2 + 4.13C^2 + 12.83D^2 \qquad (4.2)$$

ANOVA was used as a tool to test the significance of the differences between means and to understand the significance of a model (Sen and Swaminathan, 2004). ANOVA determines the impact of the independent variables on the dependent variables in regression analyses. The Fisher's F-test, where the $F_{\text{model, Adsorption}} = 18.82$ and $F_{\text{model, yield}} = 16.43$, respectively, suggested high significance of the model with a very low probability value of P model > F= 0.0001 for both the adsorption and yield (Table 4.8 and Table 4.9). A very little probability of only 0.01% was there so that a model value of this magnitude could occur due to noise. In the graph of the predicted values versus actual data, the 45-degree line should evenly split the entire data set. In this case, it is clear from Figure 4.10(A) and Figure 4.10(B) that the points are evenly distributed around the 45-degree line, which suggests that the model can closely predict the response.

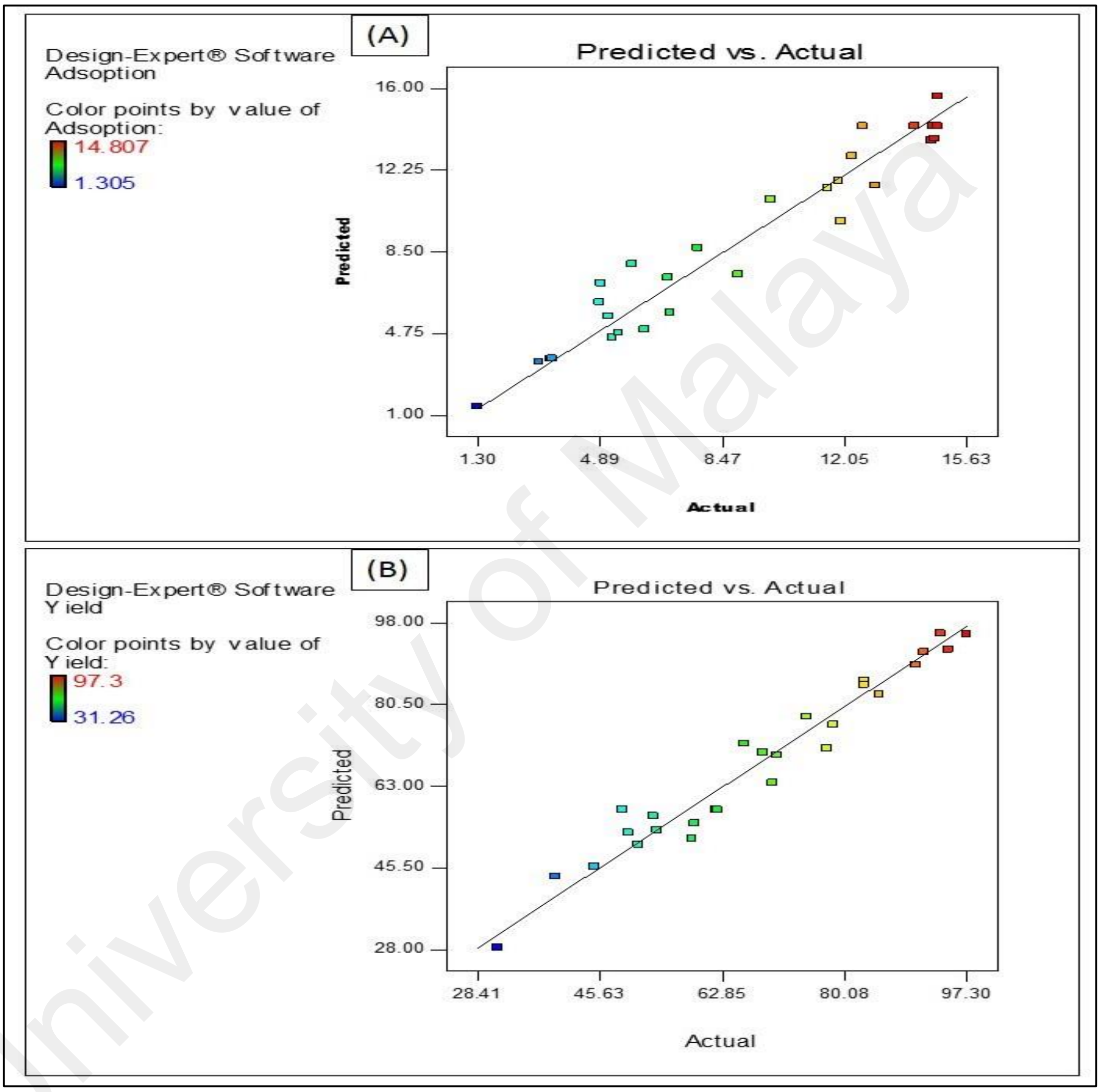

Figure 4.10 Predicted Vs Actual plot for (A) adsorption of Zn and (B) yield of activated carbon

The predicted R^2 indicates the accuracy of the prediction for a response value by the model. The predicted R^2 can prevent over fitting the model and can be more useful than adjusted R^2 for comparing models since it is calculated using observations not included in model estimation. A difference of 0.20 or less between adjusted R^2 and predicted R^2 is considered acceptable for the model to predict the response sufficiently. As evident from

Table 4.8, in the case of adsorption the predicted *R^2* value was 0.6997, which was within reasonable agreement with the adjusted *R^2* value of 0.8879. In case of yield too, the predicted *R^2* was in reasonable agreement with adjusted *R^2*, as evident from the ANOVA given in Table 4.9. Adequate precision measures the signal to noise ratio, which in turn indicates the preciseness of the model. A ratio greater than 4 is desirable. Signal to noise ratio of 14.342 in case of adsorption and 15.133 for yield of activated carbon indicated that an adequate signal was obtained. Thus, this model could be used to navigate the design space.

Table 4.8 ANOVA of regression models for adsorption

Response Adsorption
ANOVA for Response Surface Reduced Quadratic Model

Source	**Sum of Squares**	**df**	**Mean Square**	**F Value**	***p*-value Prob > F**	
Model	479.06	12	39.92	18.82	< 0.0001	significant
A-Time	6.66	1	6.66	3.14	0.0968	
B-Power	15.72	1	15.72	7.41	0.0157	
C-IR	22.85	1	22.85	10.78	0.005	
D-Conc. of acid	34.04	1	34.04	16.05	0.0011	
AB	15.97	1	15.97	7.53	0.0151	
AC	0.49	1	0.49	0.23	0.6373	
AD	10.39	1	10.39	4.9	0.0428	
BC	6.35	1	6.35	2.99	0.1042	
BD	3.9	1	3.9	1.84	0.195	
A^2	69.74	1	69.74	32.88	< 0.0001	
B^2	7.07	1	7.07	3.33	0.0879	
C^2	8.15	1	8.15	3.84	0.0688	
Residual	31.81	15	2.12			
Lack of Fit	28.78	12	2.4	2.37	0.2589	not significant
Pure Error	3.03	3	1.01			
Cor Total	510.88	27				

R^2 = 0.9377
Adj R^2 =0.8879
Pred R-Squared= 0.6997
Adeq Precision=14.342

Table 4.9 ANOVA of regression models for yield

Response Yield
ANOVA for Response Surface Quadratic Model

Source	Sum of Squares	Df	Mean Square	F Value	p-value Prob > F	
Model	8478.74	14	605.62	16.43	< 0.0001	significant
A-Time	2963.47	1	2963.4	80.38	< 0.0001	
B-Power	392.09	1	392.09	10.63	0.0062	
C-IR	1471.89	1	1471.8	39.92	< 0.0001	
D-conc of acid	903.98	1	903.98	24.52	0.0003	
AB	46.58	1	46.58	1.26	0.2813	
AC	517.79	1	517.79	14.04	0.0024	
AD	231.8	1	231.8	6.29	0.0262	
BC	2.02	1	2.02	0.055	0.8187	
BD	399.6	1	399.6	10.84	0.0058	
CD	51.41	1	51.41	1.39	0.2588	
A^2	73.58	1	73.58	2	0.1812	
B^2	146.81	1	146.81	3.98	0.0674	
C^2	43.91	1	43.91	1.19	0.295	
D^2	424.65	1	424.65	11.52	0.0048	
Residual	479.3	13	36.87			
Lack of Fit	304.62	10	30.46	0.52	0.8083	not significant
Pure Error	174.67	3	58.22			
Cor Total	8958.04	27				

R^2 = 0.9465
Adj R^2 =0.8889,
Pred R-Squared=0.7671
Adeq Precision =15.133

4.1.3.2 Effect of multiple variables during the preparation of activated carbon for the adsorption of Zn

The variables, namely irradiation time (t), microwave power (P), impregnation ratio (IR), concentration of acid and the interaction among these variables determine the quality of the activated carbon during production. ANOVA in Table 4.8 shows that P, IR and concentration of acid are very important factors as the *p*-value is less than 0.05. The interaction of irradiation time and the microwave power at lower value such as 5 min and 600 W, respectively, produced activated carbon, which had much less adsorption capacity

(6.3 mg/L). Increase in irradiation time and microwave power led to a better quality of activated carbon in terms of its adsorption capacity. At 12.5 min irradiation time and 800 W of microwave power, the adsorption capacity reached approximately 14 mg/L. However, after this level, the adsorption capacity again decreased. This trend in the adsorption capacity can be observed in the three dimensional interaction plots of the variables given in Figure 4.11 (A). The reason for such adsorption trend might be attributed to incomplete conversion of the raw material to carbonaceous activated carbon due to insufficient irradiation time and energy in the lower level of irradiation time and microwave power. When the irradiation time and the microwave power were at the higher end, the interaction among these factors led to destruction of the pore structure and burning of carbon due to over exposure and excessive energy (Deng, et al., 2010b). Thus, the lack of adsorption site could not facilitate high adsorption capacity of the activated carbon. It was observed that as the quantity of the acid, (thereby the impregnation ratio) was increased, the adsorption capacity increased at first but then decreased after a certain level.

This trend was also observed when interaction between time and impregnation ratio, as shown in Figure 4.11 (B), was studied. Lower levels as well as higher levels of IR and time produced activated carbon with low adsorption capacity of only 5.6 mg/L. At lower level of IR, the amount of acid was too small to react with the raw material adequately; therefore, the development of the micro and mesopores were not facilitated. At the high IR levels, the excess amount of sulphuric acid could break down the lignocellulose structure of the PKS and therefore the pore formation was not possible. This was reflected in the low adsorption capacity of the activated carbon.

Interactive effect of IR and power suggested that at lower impregnation ratio, the adsorption capacity was reduced with increasing power possibly due to higher burnt off the insufficiently impregnated material. Higher IR and microwave power also affected the quality of the activated carbon negatively by destroying the pore structure, as can be observed from Figure 4.11 (C).

The concentration of the acid used for impregnation had a considerable effect on the adsorption capacity of the activated carbon. With the increasing concentration of acid, the adsorption capacity was found to increase (Figure 4.11 (D)). It was highest when undiluted acid (considered as 100% acid) was used. The cellular structures of PKS were attacked by the acid that helped to rupture the linkages between the lignin and cellulose during impregnation stage. In the next stage, larger structural units and strong cross linked solids were formed by recombination reactions (El-Hendawy, et al., 2008). The undiluted acid facilitated this reaction. This adsorption behaviour at the lower levels and higher levels of the variables indicated that there existed optimum levels for these variables, which could be found out by optimisation of these variable factors.

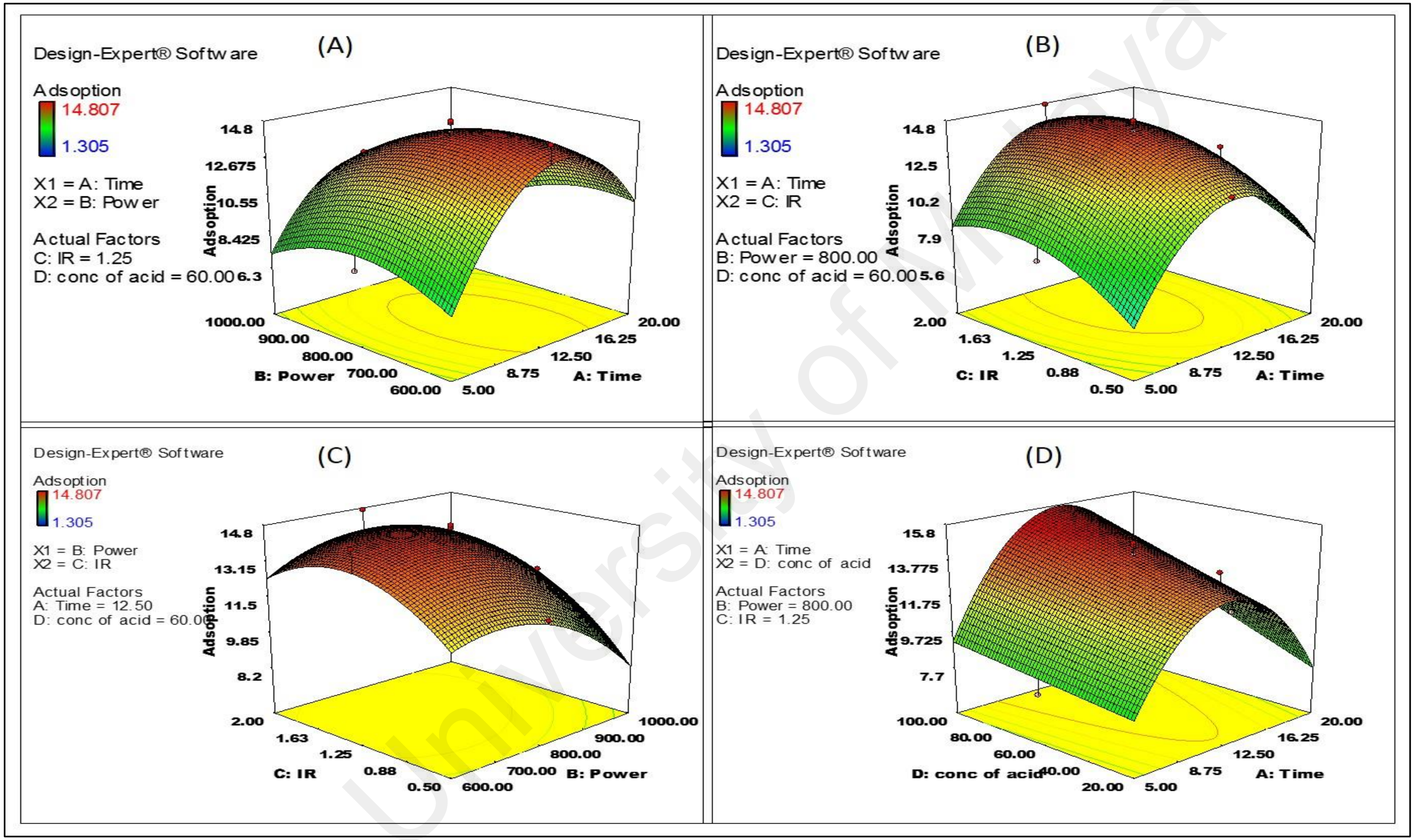

Figure 4.11 Three dimensional graphical representation of the interaction between (A) time and power, (B) time and IR, (C) power-IR, and (D) time and concentration of acid for Zn adsorption

4.1.3.3 Effect of multiple variables during the preparation of activated carbon for yield of the activated carbon

Yield of the product obtained from a process is an important factor in assessing the economic viability of the product. The selected factors T, W, IR and concentration of acid also had important effects on the yield of activated carbon. The interaction of these variables assumed important role in determining the yield of the activated carbon. It can be observed from Figure 4.12 (A) that, at high irradiation time and power, yield of activated carbon was only approximately 39 %, possibly due to burnt off and excessive release of volatile matter as well as the tar content in the raw material (Hoseinzadeh Hesas et al.). At lower irradiation time and power levels, the yield is higher, approximately 80%, due to incomplete conversion of the raw material to activated carbon.

It was also observed that high impregnation ratio caused yield to decrease from 72% to approximately 40% when interaction with time was considered, as evident from Figure 4.12 (B). At higher impregnation ratio, the cleavage of the lingo-cellulosic matter occurred in higher proportion and when exposed for a longer time, the extent of carbon-chemical reaction increased, thereby releasing more volatile matter and tar (Foo and Hameed, 2012a; Xin-hui et al., 2011).

Figure 4.12 (C) shows the trend when the interaction between irradiation time and concentration of acid was considered to assess the yield of the AC. It was observed that at low irradiation time, the yield decreased with increasing concentration of acid. After the acid concentration was more than 80%, the yield increased slightly from 70% to 81%. The reason could be that the very high concentration of acid (80 to 100%) may have blocked the pores and hindered the formation of tar (Xin-hui, et al., 2011), resulting in higher yield. Similar interaction had been observed between impregnation ratio and concentration of acid, as shown in Figure 4.12 (D). The general trend was that the yield of activated carbon decreased with increase in the level of variables used. Similar trend was also reported by XIA et al. (2007) and Xin-hui, et al. (2011).

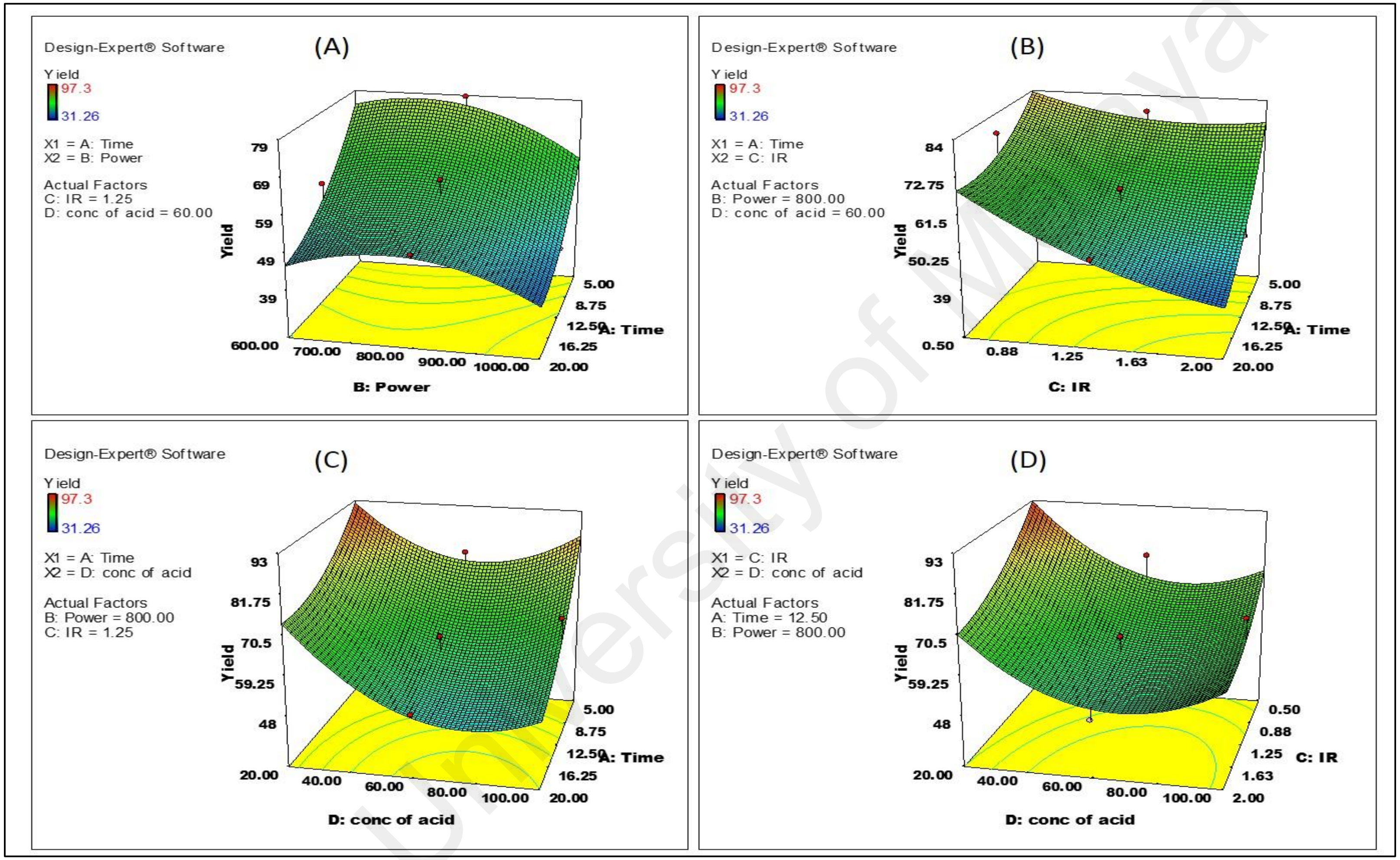

Figure 4.12 Three dimensional graphical representation of the interaction between (A) time and power, (B) time and IR, (C) time and concentration, and (D) IR and conc. of acid for yield of activated carbon

4.1.3.4 Optimisation of the preparation process

The commercial production of activated carbon demands higher product yield for economic viability while the adsorption efficiency is a critical product attribute. Hence, it is desirable to prepare activated carbon with optimum yield, maximising the adsorption capacity. However, it is not always possible that the activated carbon with highest yield would have the highest adsorption capacity. In order to compromise these two values, the desirability function is applied using the Design Expert software. The process condition which had the highest desirability was selected as the optimum condition. In order to obtain this condition, criterion was set as “in range” for the independent variables such as T, P, IR and concentration of acid. Criteria for the responses such as adsorption and yield were set as “maximise”. Based on the highest desirability value of 0.805, the optimum process condition obtained was 11.02 min of irradiation time, 676 W of microwave power, impregnation ratio of 0.68 and undiluted sulphuric acid. The predicted adsorption value was 13.73 mg/g and predicted yield was 77.73%. Validation experiments were conducted to confirm the values predicted from the model. In the validation experiment, it was found that the activated carbon prepared in the optimum condition had adsorption capacity 14.6 mg/g and yield of activated carbon was 72%. The error in prediction was 6.41% and 7.1%, respectively.

4.1.3.5 Characterisation of the activated carbon

The activated carbon prepared was characterised by SEM, BET surface area and FTIR spectroscopy. The SEM image given in Figure 4.13 (A) shows that the raw material had much less surface roughness and porosity on the surface. Activated carbon prepared in the optimum operating condition developed considerable amount of porosity after activation, as evident from Figure 4.13 (B). The acid in the impregnation stage and microwave heating in the activation stage facilitated the formation of pores.

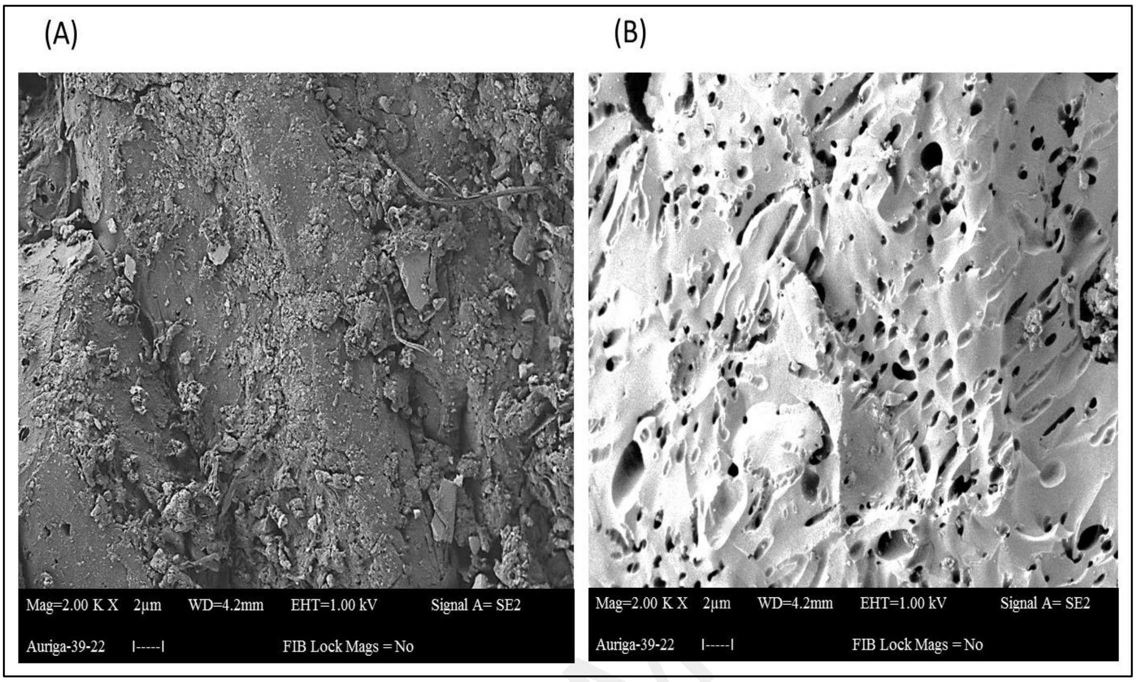

Figure 4.13 SEM image of (A) raw palm kernel shell and (B) activated carbon

FTIR data analyses showed that the intensity of the peak between 3500-3200 cm^{-1}, which is attributed to O-H stretching of alcohol or phenol groups, decreased largely. Intensity of the band of 3000-2850 cm^{-1} corresponding to C-H stretch of alkanes diminished in the activated carbon. Both of these phenomena indicate that the sulphuric acid acted as a dehydrating agent and had removed a considerable amount of hydrogen from the raw material (Hesas, et al., 2013) to convert it into activated carbon. The complex peaks around 1580-1650 cm^{-1} in raw PKS as can be seen in Figure 4.14 (A) could be attributed to N-H bend of primary amines and C-C stretch of aromatic ring. The intensity of this band had also reduced. The C-O stretch for alcohols, carboxylic acids, esters and ethers corresponding to the band 1300-1000 cm^{-1} remained in the activated carbon (Figure 4.14 (B)) as in the raw material with a much lower intensity of the peak. This also shows removal of hydrogen and oxygen parts from the raw material.

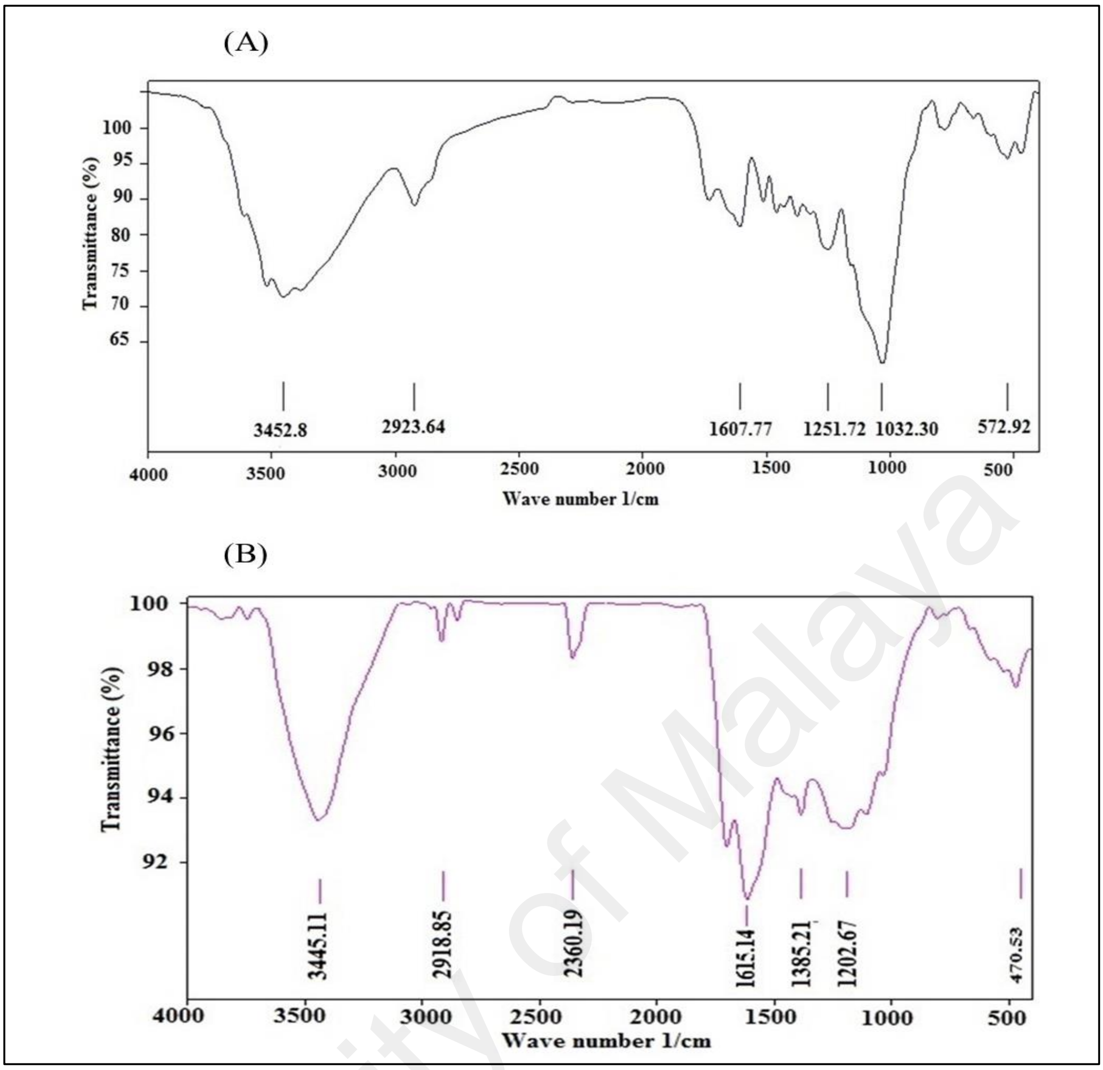

Figure 4.14 FTIR spectra of (C) Raw palm kernel shell and (D) activated carbon

Nitrogen adsorption/desorption isotherms determined the surface area through from the BET equation and was found to be 1011 m^2/g. The pore size distribution curves showed that the activated carbon contained mainly micro and meso pores, which assisted in the adsorption process. The average pore diameter of the activated carbon prepared at the optimum condition was 21.89 Å.

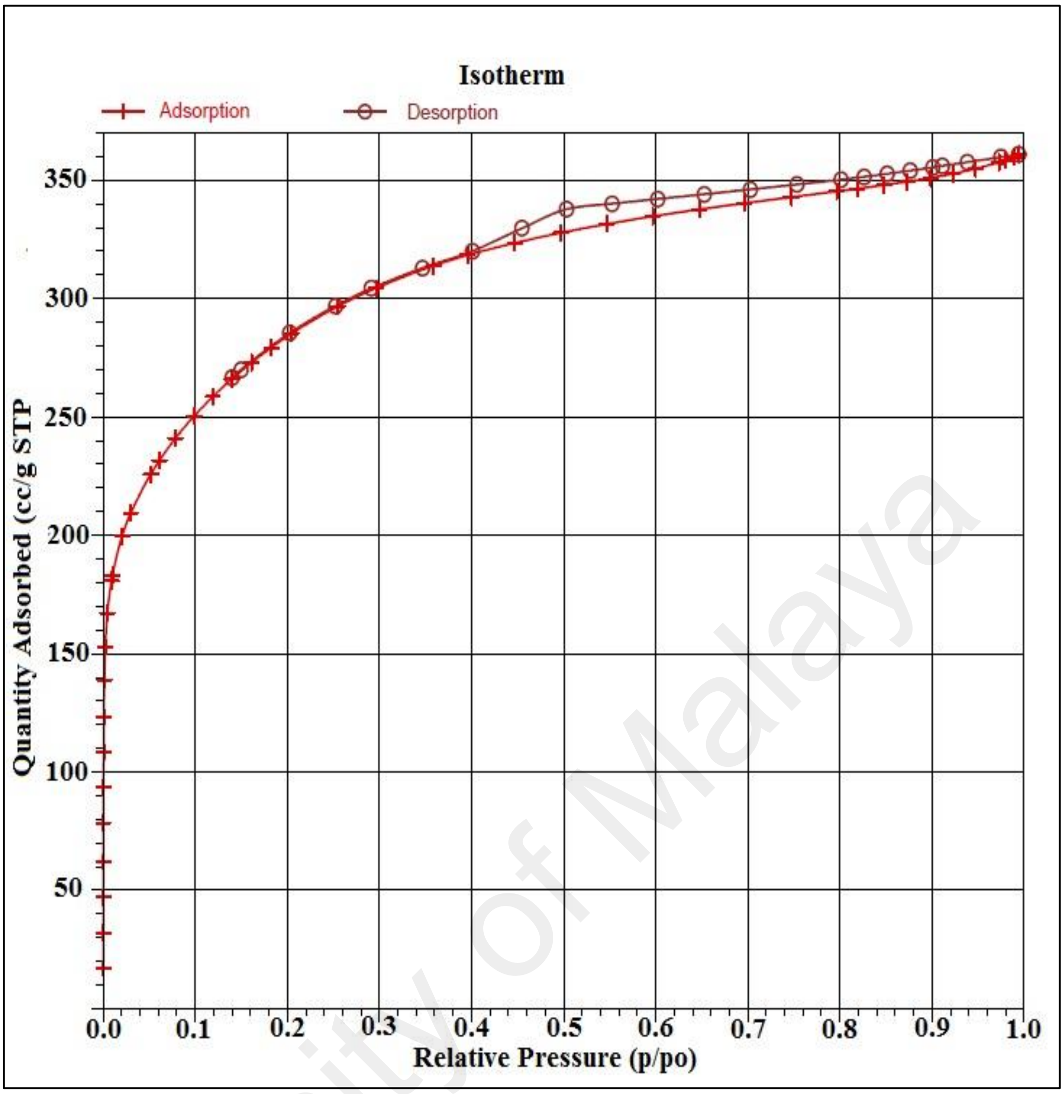

Figure 4.15 Nitrogen adsorption/desorption isotherm for the activated carbon prepared at the optimum condition showing type I isotherm.

The adsorption/desorption isotherm of the activated carbon prepared at the optimum condition, as shown in Figure 4.15, indicates that the curve is a type I isotherm, characterising micro-porous adsorbent for monolayer adsorption (Carmody, et al., 2007).

The qualities of the activated carbon prepared in this study were very much comparable to the quality of the activated carbon prepared by other researchers as mentioned in Table 2.2.

4.2 Removal of dye and heavy metal by activated carbon using conventional batch shake flask experiments

The efficacy of the activated carbon was tested by using them for adsorption of heavy metal and dye in batch shake-flask experiments. The adsorption capacity and kinetics of the activated carbon were also determined by these experiments.

4.2.1 Optimisation of Cr(VI) adsorption by activated carbon MWAC2

The activated carbon derived from H_3PO_4 impregnation and microwave activation of palm shell, namely MWAC2 was used to remove Cr(VI) from aqueous solutions. A mathematical model was developed with the aid of Box-Behnken design to optimise process parameters. ANOVA aided the evaluation of the model.

4.2.1.1 Evaluation of the model and ANOVA of the Cr(VI) adsorption process

The results of ANOVA for the response surface reduced quadratic are presented in Table 4.10. As shown in Table 4.10, ANOVA of the regression model showed that quadratic model was highly significant for assessing the metal ions removal. This is evident from the Fisher's F-test (F_{model}= 29.96), with a very low probability value (P model > F= 0.0001).This is in conformity with the analysis put forward by Liu et al. (2004). There is only a 0.01% chance that a model value of this magnitude could occur due to noise.

Table 4.10 ANOVA data of the second order polynomial equation

Source	Sum of Squares	Df	Mean Square	F Value	p-value Prob > F	
Model	295.4935	8	36.93669	29.96147	< .0001	significant
A-Initial Conc.	111.7924	1	111.7924	90.68121	< .0001	
B-pH	0.592961	1	0.592961	0.480984	0.5055	
C-Temp	2.52282	1	2.52282	2.046404	0.1864	
AB	0.661782	1	0.661782	0.53681	0.4824	
AC	1.991627	1	1.991627	1.615523	0.2356	
BC	0.472656	1	0.472656	0.383399	0.5511	
A^2	5.344921	1	5.344921	4.335572	0.0670	
B^2	164.411	1	164.411	133.3632	<0.0001	
Residual	11.09526	9	1.232806			
Lack of Fit	7.34377	4	1.835942	2.446953	0.1765	not significant
Pure Error	3.751488	5	0.750298			
Cor Total	306.5887	17				

In the graph of the predicted values versus actual data points, the 45-degree line should evenly split the data set. From Figure 4.16 it is evident that the points are evenly distributed around the 45-degree line.

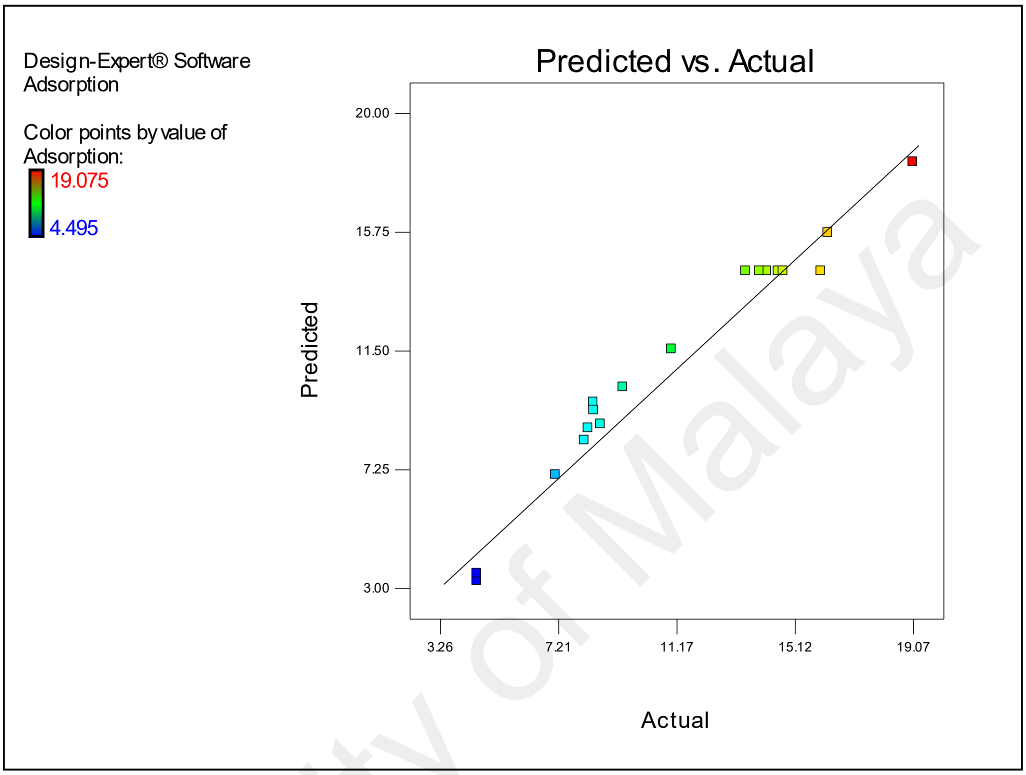

Figure 4.16 Predicted vs Actual plot for adsorption of Cr(VI)

The accuracy of prediction of a response value by a model can be measured by the Predicted R^2. For the model to be sufficient, a difference less than 0.20 is expected between the observed and the predicted data. If the predicted and adjusted R^2 values are not within approximately 0.20 then there is an error in the model or the data. In case of adsorption, the predicted R^2 value is 0.7504, which is within reasonable agreement with the adjusted R^2 value of 0.9316.

A signal to noise ratio indicates preciseness of the model. The error expressed as a percentage of the mean indicates the coefficient of variation for this model. In general, the desired value should be 4 or more (Aghamohammadi et al., 2007). In this case, the ratio of 19.094 indicates adequate signal.

4.2.1.2 Interaction effects of adsorption variables

The perturbation plot illustrates the effect of the independent factors at a particular point of the design space. The perturbation plots illustrate the change of the response while each factor moves from a chosen reference point, generally the midpoint, keeping all other factors constant at their reference value (Sen Gupta and Ako, 2005). The plot of the response (adsorption) was carried out against the deviation from the reference point by changing only one factor over its entire range while holding all other factors constant as shown in Figure 4.17. The nature of the plots of all three independent variables suggests that the adsorption was sensitive to the process variables especially initial concentration and pH.

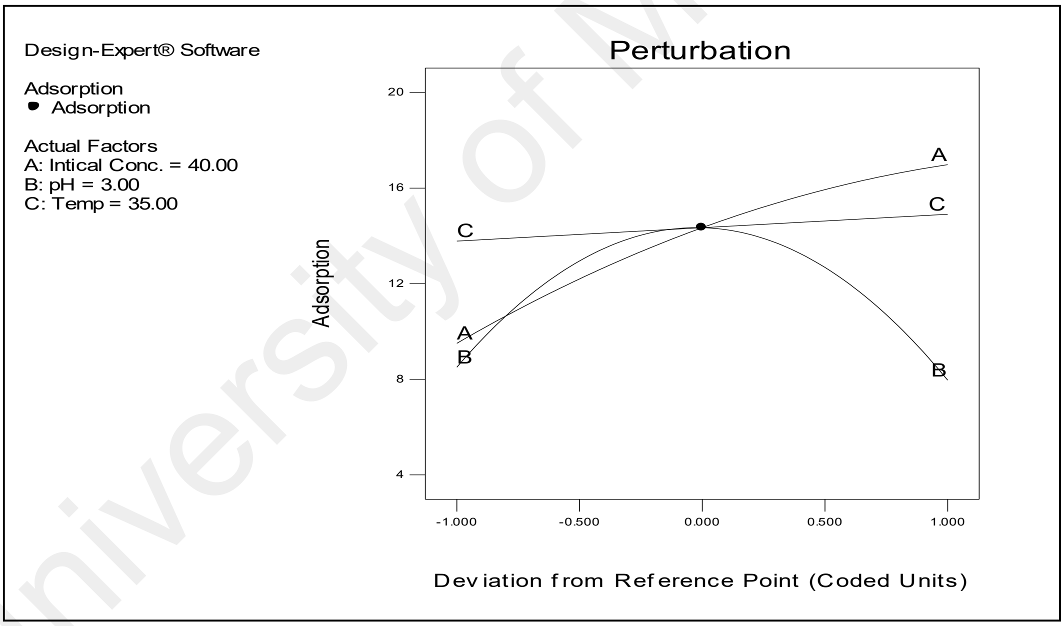

Figure 4.17 Perturbation plot, which show the effect of all variable parameters on adsorption.

4.2.1.3 Combined effect of initial concentration and pH

The three dimensional plot, as shown in Figure 4.18, illustrates interaction of initial Cr(VI) concentration and initial operating pH of the solution when temperature (35 °C) was the actual factor. It is noticed that the adsorption of Cr(VI) increases as the initial concentration increases for the entire range of pH values used in this work. The 3D plot shows the adsorption is at maximum around pH 3. This may be due to the fact that at pH 3, the negatively charged species $HCrO_4^-$ and $Cr_2O_7^{2-}$ are prevalent in the solution and are attracted to the protonated surface of the activated carbon. At lower pH neutral species H_2CrO_4 prevails, hence, the attraction by the protonated surface is minimal (Gherasim et al., 2011). The adsorption capacities were 11.54 mg/g and 10.18 mg/g at pH 1 and 5, respectively, when the initial concentration of Cr(VI) was 60 mg/L. The adsorption capacity of the adsorbent increased to 16.98 mg/g at pH 3 with the same concentration of Cr(VI). Adsorption is also reduced at higher pH due to electrostatic repulsion between the OH^- ions and negatively charged $HCrO_4^-$ and $Cr_2O_7^{2-}$ ions, as mentioned by Kiran et al. (2007).

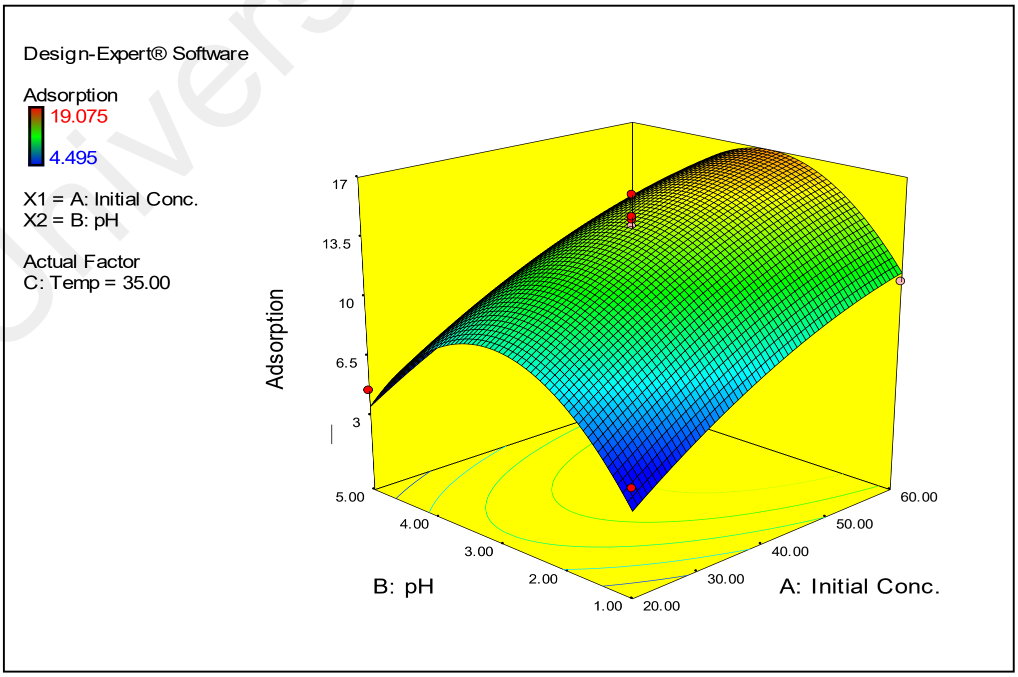

Figure 4.18 Combined effect of initial concentration and pH for Cr(VI) adsorption

4.2.1.4 Combined effect of initial concentration and temperature

The combined effect of temperature and initial Cr(VI) concentration is observed from three dimensional plot, as shown in Figure 4.19, when pH was the actual factor. It was observed that at lower concentration, temperature was not effective. However, at higher initial concentration, the temperature change has been effective for adsorption of Cr(VI). It was observed that adsorption capacity increased with the increase in temperature. The adsorption capacity increased to 19.1 mg/g from 8.39 mg/g as the temperature increased from 20 ^{o}C to 50 ^{o}C and the initial concentration increased from 20 mg/L to 60 mg/L of Cr(VI).

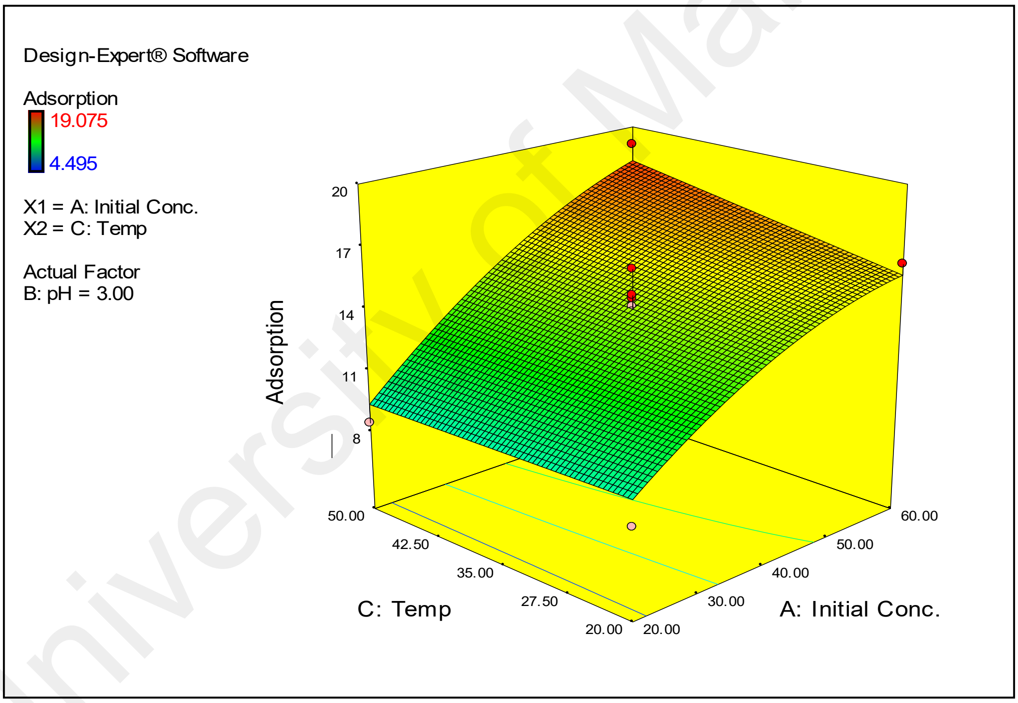

Figure 4.19 Combined effect of initial concentration and temperature for Cr(VI) adsorption

The increase in adsorption capacity with increase in temperature may be attributed to the increased adsorbate transfer within the pores of the adsorbent. It may also happen due to the increase in the number of adsorption sites generated at the surface at increased temperature (Acharya, et al., 2009).

4.2.1.5 Combined effect of pH and temperature

As evident from the three-dimensional plot in Figure 4.20, the adsorption capacity is maximum at pH 3. The adsorption capacity increases with temperature. The amount of adsorbed Cr(VI) increased from 15.71 mg/g to 18.25 mg/g as the temperature was raised to 50 ^{o}C from 20 ^{o}C at pH 3 at an initial concentration of 60 mg/L of Cr(VI).

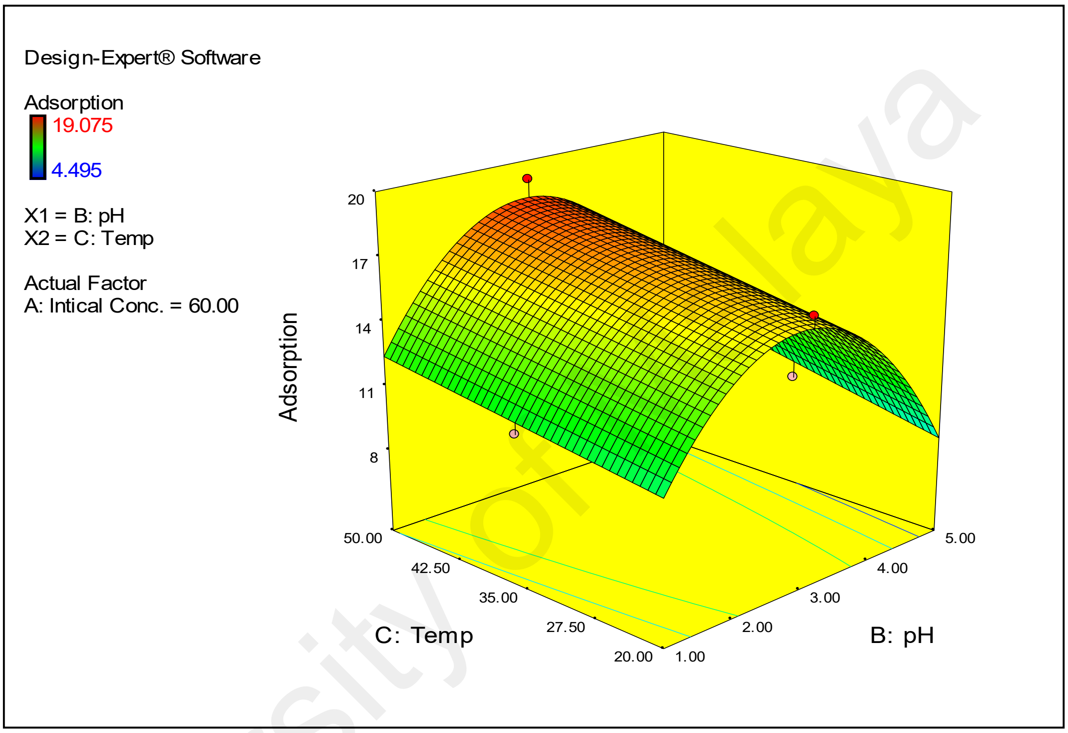

Figure 4.20 Combined effect pH and temperature for Cr(VI) adsorption

4.2.1.6 Optimisation of the adsorption process

The optimisation of the different process parameters viz., initial Cr(VI) concentration, initial operating pH and operating temperature for maximum Cr(VI) adsorption was accomplished by multiple response method known as desirability function. The criterion for the independent variables was set as "in range", while it was set as "maximum" for the dependent variable or the response, e.g., amount adsorbed (mg/g). The desirability value was found to be 0.943232 for combination of variables and 1 for individual variables, respectively, as shown in Figure 4.21.

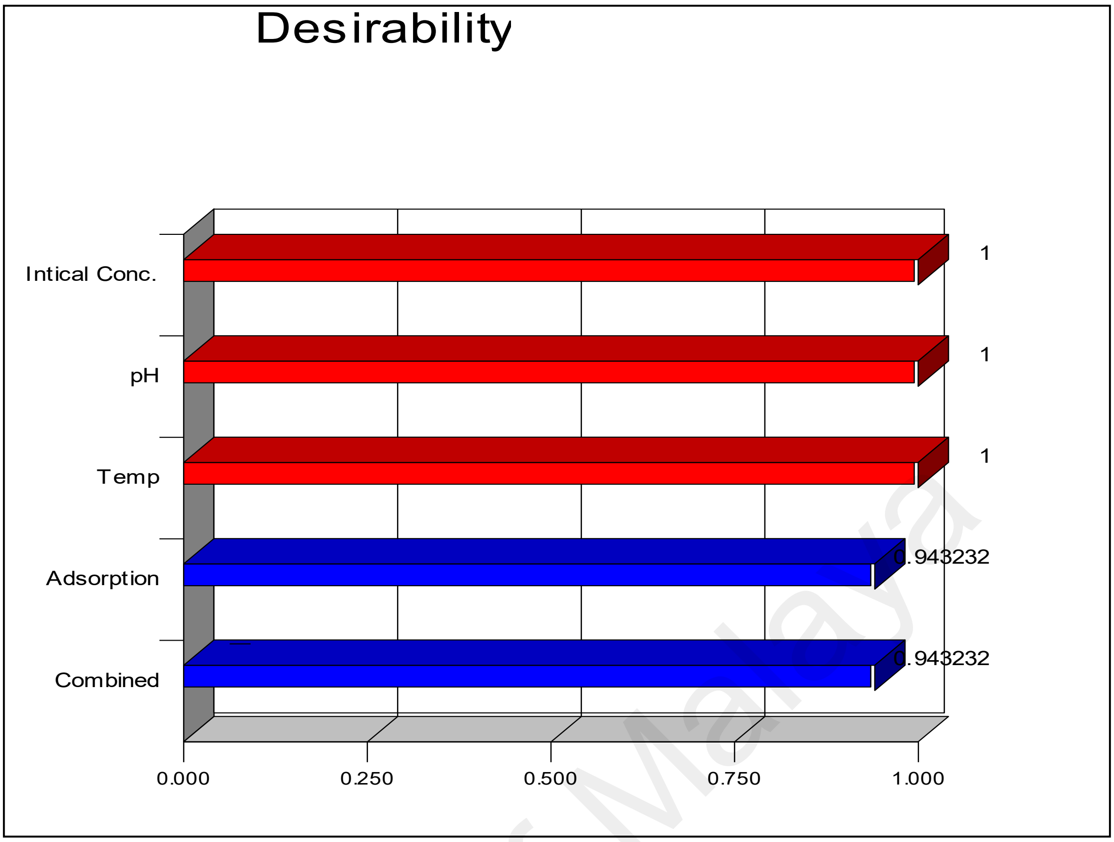

Figure 4.21 Bar graph for optimisation procedure

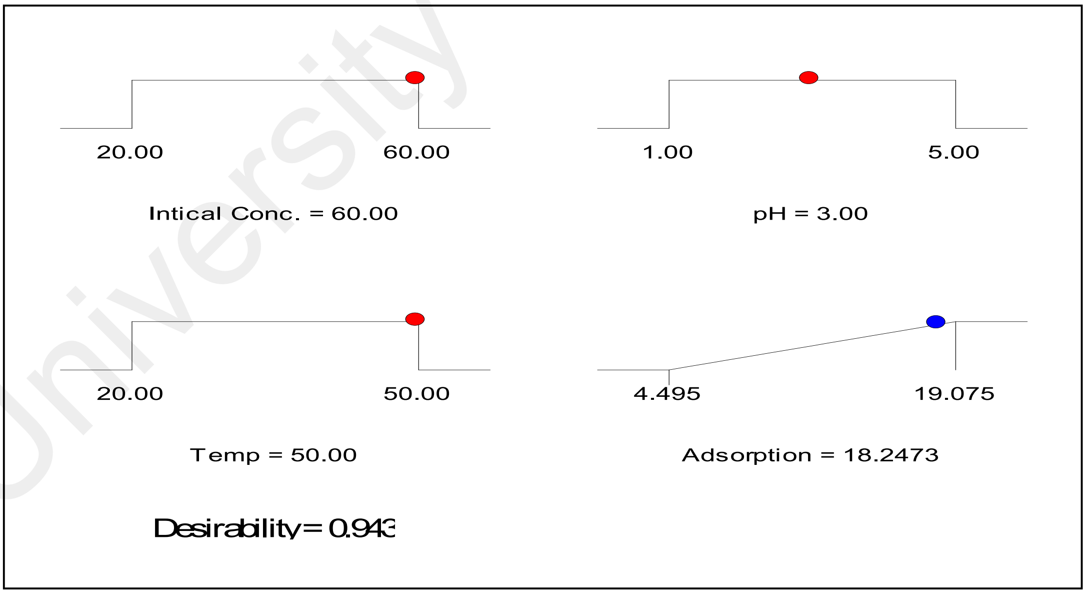

Figure 4.22 RAMP plots for the optimisation process

As illustrated in Figure 4.22, the optimum removal of Cr(VI) was 18.25 mg/g as suggested by the RAMP plots when the independent variables were set at an initial Cr(VI) concentration of 60 mg/L, pH 3 and temperature 50 ^{o}C at the maximum desirability value.

To validate the model, confirmatory experiments were performed at the optimum values of the process parameter obtained from the software. The values are tabulated in Table 4.11.

Table 4.11 Optimised values of the process parameters from the model and validation of the model

Initial Cr(VI) concentration	**pH**	**Temperature**	**Optimisation**		**Validation**	
			Adsorption (mg/g)	**Desirability**	**Adsorption (mg/g)**	**Error (%)**
60	3	50	18.25	0.943	19.1	4.65

4.2.1.7 Kinetic Study

The data obtained from the kinetic experiments conform to a pseudo-first-order kinetic equation, popularly known as Lagergren equation as well as to a pseudo-second-order kinetic equation. The results obtained after regression analysis of the data collected based on the pseudo-first-order and pseudo-second-order kinetics, as shown in Figure 4.23(a) and (b), respectively. Applicability of a particular type of rate equation is selected based on the value of regression coefficient R^2. The value of regression coefficients and rate constants are tabulated in Table 4.12. The R^2 value of pseudo-second-order equation (0.9931) suggests that this could describe the adsorption of chromium better than the pseudo-first-order equation with R^2 value 0.8046.

Table 4.12 Kinetic parameters for Cr(VI)adsorption

k_1(1/min)	***k_2(g/mg min)***	**R^2 (first order)**	**R^2 (second order)**
0.0044	0.0022	0.8046	0.9931

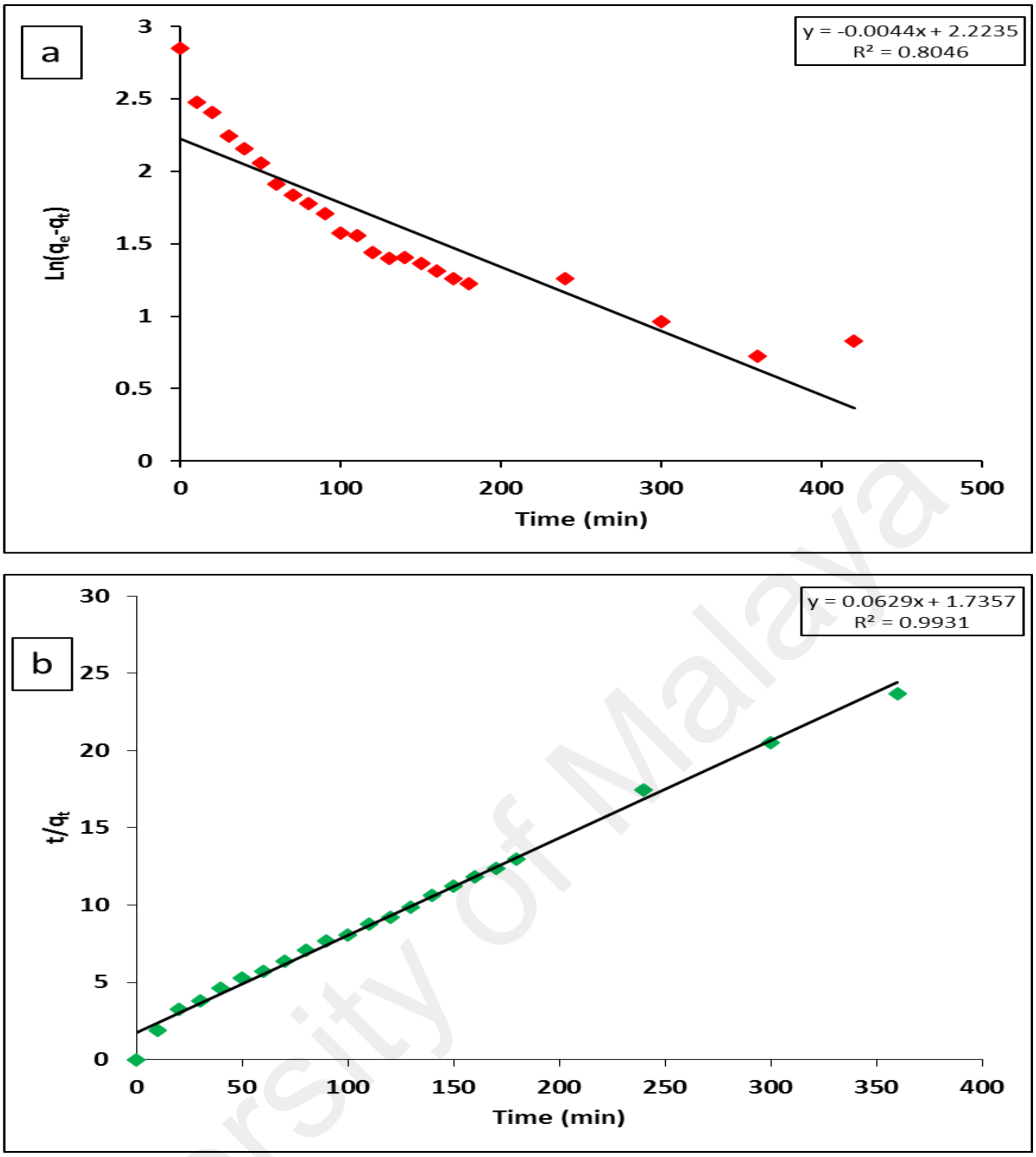

Figure 4.23 Plots of a) pseudo-first-order equation, b) pseudo-second-order equation

4.2.1.8 Adsorption Isotherm Study

In the equilibrium state, the distribution of molecules between the adsorbent and the adsorbate is generally governed by the adsorption isotherm (Hameed et al., 2007). Two most extensively used models are Langmuir and Freundlich isotherms. A monolayer adsorption onto a surface, which comprise a finite number of adsorption sites of uniform scheme of adsorption, is considered by Langmuir isotherm with no trans-migration of adsorbate in the plane of the surface. In contrast, heterogeneous surface energies are considered in Freundlich isotherm model. Here, the energy term in Langmuir equation varies as a function of the surface coverage (Weber, 1972).

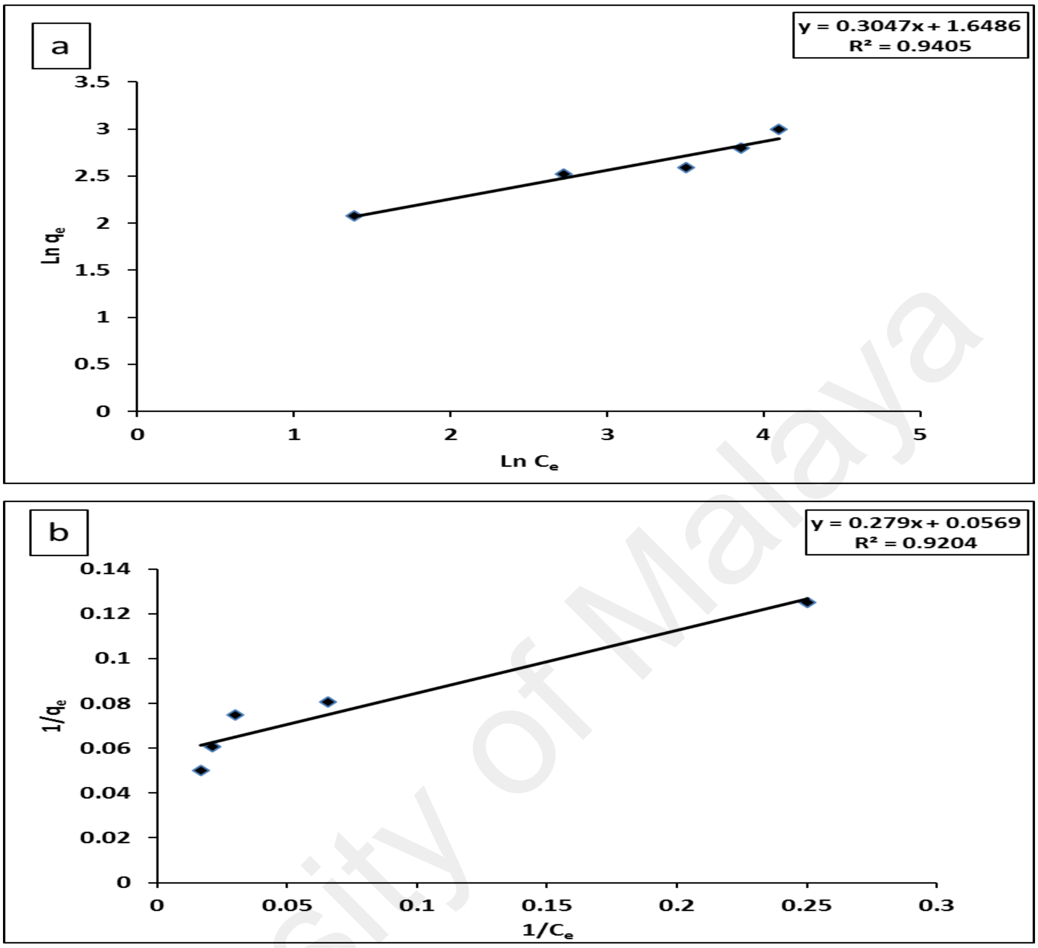

Figure 4.24 Plots of a) Freundlich isotherm, b) Langmuir isotherm at different temperature

Figure 4.24(a) and (b) represent the Freundlich and Langmuir isotherm plots, respectively. The isotherm parameters of the two models are tabulated in Table 4.13.

Table 4.13 Values of Isotherm models parameters

Temperature (K)	q_{max} **(mg/g)**	***b*** **(L/g)**	R^2	K_f **(L/g)**	**1/*n***	***n***
298	17.574	0.2039	0.9405 (Freundlich) 0.9204 (Langmuir)	5.1996	0.3047	3.282

From the R^2 values, it is suggested that the adsorption process follows Freundlich isotherm model. The value of *n* is 3.282, which suggests favourable condition for the adsorption as 1<*n*<10 (Kumar and Phanikumar, 2012). The dimensionless parameter R_L is calculated from the equation 4.3.

$$R_L = \frac{1}{1+bC_0} \tag{4.3}$$

The value of R_L suggests the favourability of adsorption. It may be noted that $R_L > 1$ suggests an unfavourable process whereas $0<R_L<1$ suggests a favourable process. The R_L values for initial concentrations of 20 mg/L , 40 mg/L , 60 mg/L , 80 mg/L and 100 mg/L are found to be 0.1969, 0.1092, 0.0755, 0.0578 and 0.0467 respectively, which also suggest that the adsorption process is favourable.

4.2.1.9 Thermodynamic study

Thermodynamic parameters such as change in free energy (ΔG^0), enthalpy change (ΔH^0) and entropy change (ΔS^0) aid to understand the nature of the adsorption fully.

The Eq 3.14- 3.16 were employed to measure the change in free energy ($\Delta G°$) for adsorption process (Hasan et al., 2000). The enthalpy change ($\Delta H°$) value was obtained from the slope while the entropy change ($\Delta S°$) value was obtained from intercept of the

ΔG° vs T plot given in Figure 4.25. The values of the thermodynamic parameters obtained are tabulated in Table 4.14.

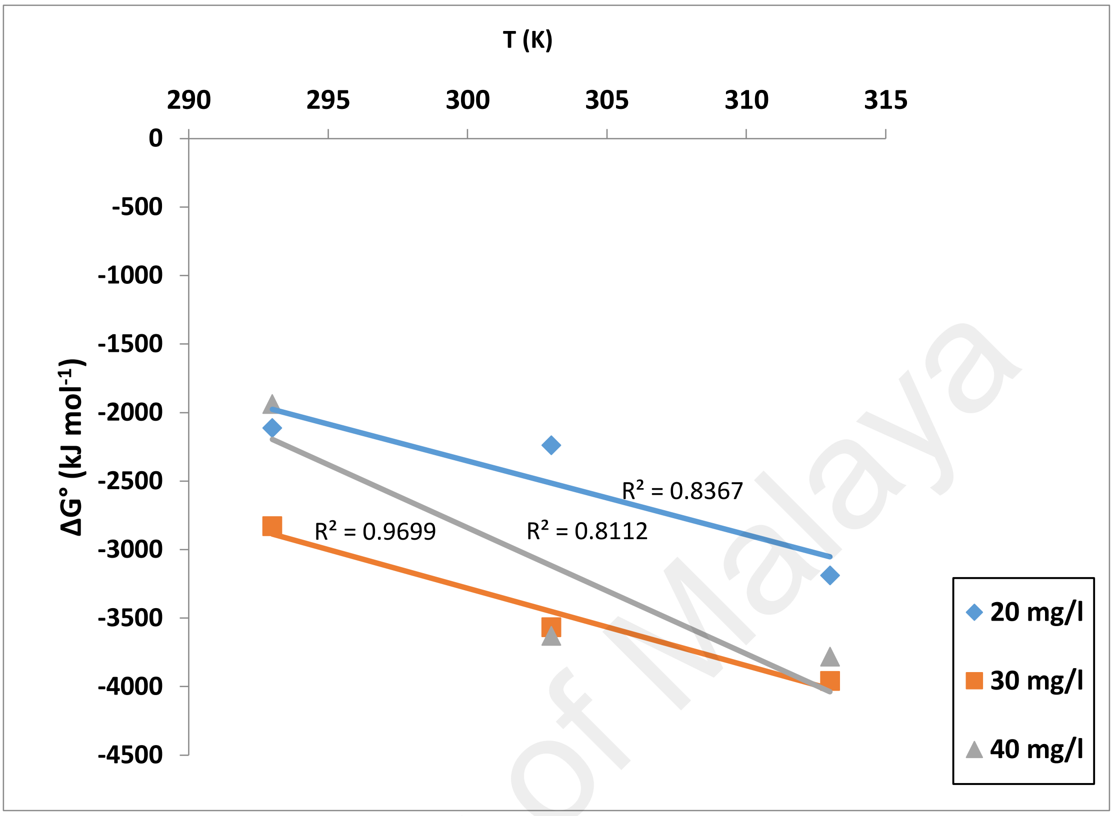

Figure 4.25 Free energy change vs temperature plot.

The value of free energy changes, as tabulated in Table 4.14, show that the adsorption process of Cr(VI) is thermodynamically favourable under the operating conditions. The positive values of ΔH° suggest that the adsorption of Cr(VI) is an endothermic process and a positive ΔS° value suggests that the randomness of the process at the solid–solution interface increased when the chromium ions were attached to the active sites of the adsorbent. (Acharya, et al., 2009).

Table 4.14 Thermodynamic parameters for adsorption of Cr(VI)

Initial Conc C_0 (mg/L)	ΔH^0 (kJ/mol)	ΔS^0 (kJ/mol K)	ΔG^0 (kJ/mol)		
			293K	**303K**	**313K**
20	13.78	0.053	-2.113	-2.239	-3.189
30	13.64	0.056	-2.83	-3.566	-3.958
40	24.79	0.092	-1.938	-3.629	-3.781

4.2.2 Optimising the adsorption of DR23 using Taguchi method by activated carbon $MWAC_T$

Taguchi optimization method was used to find the optimum conditions for adsorption process of DR23 by using $MWAC_T$. The effects of experimental variables: initial concentration (mgL^{-1}), pH, activated carbon dose (gL^{-1}) and temperature (°c) were observed using orthogonal arrays.

4.2.2.1 Effects of the control factors and noise factor on the activated carbon preparation

Thirty-two experiments were performed in three replicates according to L16 array and considering the two external arrays of noise factor. Table 4.15 shows the percent adsorption of DR23 by $MWAC_T$.

ANOVA was performed on the data obtained to determine those control factors, which have significant effect on the adsorption of the dye. F-test in statistics describes the significance of a control factor on the quality characteristic, which in this case is adsorption.

Table 4.15 Taguchi experimental matrix and obtained result for DR23 adsorption

Experiment no	Initial Conc	pH	Dose	Temp	Obs 1 (% removal)	Obs 2 (% removal)	SNRA
1	20	2	1	10	100	100	38.23
2	20	5	2	20	100	100	37.45
3	20	7	3	30	100	100	39.10
4	20	10	4	40	100	100	40.00
5	50	2	2	30	90.63	95.24	35.39
6	50	5	1	40	21.70	30.30	16.51
7	50	7	4	10	91.81	88.07	34.37
8	50	10	3	20	56.88	57.66	24.20
9	80	2	3	40	100	98.39	35.30
10	80	5	4	30	74.68	76.91	32.77
11	80	7	1	20	4.22	5.08	0.03
12	80	10	2	10	16.09	18.82	0.85
13	100	2	4	20	82.83	77.32	33.66
14	100	5	3	10	38.10	41.49	24.41
15	100	7	2	40	19.92	23.41	18.67
16	100	10	1	30	8.77	9.18	8.41

The F value for each control factor is simply the ratio of the mean of squared deviations to the mean of squared error. Usually, when F > 4, it means that the change of the control factor has a significant effect on the quality characteristic (Barman, et al., 2011). The last column of the Table 4.16, which tabulates the ANOVA results shows the “percent” contribution of each factor as the total variation, indicating its influence on the result. The F-value of 9.6 for the initial concentration ascertains that it has a significant contribution on the adsorption and the percent contribution is 38.03%. $MWAC_T$ dose also has a significant contribution with F value of 8.03 and this parameter contributes 31.8% on the removal of dye. The parameter pH also has a significant effect with F value 5.59 and its contribution towards the removal is 23.61%. Although the other three parameters have significant effect, it was found that temperature had insignificant contribution with F value of 0.66, which contributes only 2.6% in the removal of the dye by $MWAC_T$.

Table 4.16 ANOVA for SN ratios for the removal of DR23

Source	**DF**	**Seq SS**	**Adj SS**	**Adj MS**	**F**	**P**	**Percent contribution**
Initial Conc	3	1050.68	1050.68	350.23	9.6	0.048	38.03
pH	3	652.31	652.31	217.44	5.96	0.088	23.61
Dose	3	878.72	878.72	292.91	8.03	0.06	31.80
Temp	3	71.92	71.92	23.97	0.66	0.631	2.60
Residual Error	3	109.4	109.4	36.47			
Total	15	2763.04					

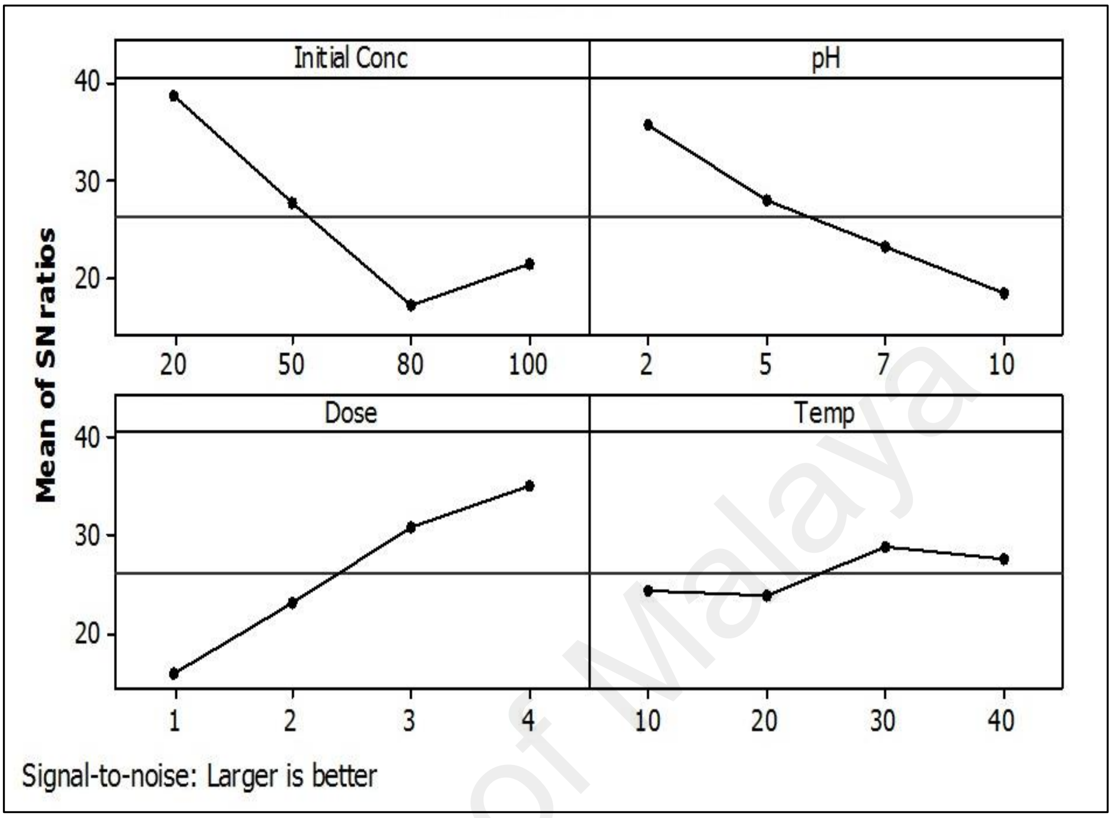

Figure 4.26 Main effect plot for S/N ratio for the removal of DR23

Effects of control factors on the S/N ratio of the dye adsorption by the prepared $MWAC_T$ can be observed in Figure 4.26. Bold values in Table 4.17 are the maximum level average S/N performances of factors in the four different levels at each factor. The largest S/N performance corresponds to the best performance characteristic. From Figure 4.26, it can be seen that with increasing initial concentration of dye, the signal to noise ratio decreases. The reason could be that as initial concentration increased, the $MWAC_T$ was saturated and thus percent removal decreased. However, the S/N ratio increased when initial concentration increased from 80 mg/L to 100 mg/L. This could be due to multilayer adsorption on the MWAC at very high concentration. The S/N ratio for pH steadily decreased when pH value increased. At lower pH, the dye molecule was stabilised by the surrounding H^+ molecules; however, at higher pH, the $[OH^-]$ ions reacted with the negatively charged SO_3^- group of the dye. The S/N ratio was highest at the highest

$MWAC_T$ loading. Higher amounts of $MWAC_T$ had more adsorption sites, which aided in the increase in the adsorption and thus the S/N ratio. S/N ratio with respect to temperature remained almost the same for first two levels and then increased at the third level. Thereafter, it remained almost constant at the fourth level. The S/N ratio was the highest at the third level. This indicates that the adsorption process was endothermic. The 'delta' value in Taguchi design denotes the difference between the maximum and minimum response across levels of a variable factor. Larger is the 'delta' value greater is the effect of that variable factor on the response. In this case, it can be seen from Table 4.17 that initial concentration had the most significant effect on the adsorption followed by activated carbon loading, pH and temperature, respectively.

Table 4.17 Response table for signal to noise ratios (larger the better)

Level	**Initial Conc.**	**pH**	**Dose**	**Temp**
1	**38.7**	**35.65**	15.79	24.47
2	27.62	27.78	23.09	23.83
3	17.24	23.04	30.75	**28.91**
4	21.29	18.37	**35.2**	27.62
Delta	21.46	17.28	19.4	5.08
Rank	1	3	2	4

Taguchi suggested that the level with highest S/N ratio in case of larger the better model should be the optimum level for that particular control factor. In this experiment, it was found that the optimum condition for DR23 adsorption with $MWAC_T$ is as follows: initial concentration of 20 mg/L, solution pH of 2, MWAC dose of 4 g/L and temperature of 30 ^{o}C. The removal percentage was almost 100% at this optimum condition.

4.2.2.2 Kinetic study

Data obtained from the kinetic experiments were fitted to the linearised form of pseudo-first-order as well as pseudo-second-order kinetic equations. The results are shown in Figure 4.27(a) and (b), respectively. The favourable kinetics of the adsorption process can be understood by the value of regression coefficient R^2. The R^2 values for both kinetic equations are tabulated in Table 4.18.

Table 4.18 Values of kinetic parameters for adsorption of DR23 on MWAC.

Initial conc (mg/L)	**$q_{e,\ exp}$ (mg/g)**	**Pseudo-first-order kinetic model**			**Pseudo-second-order kinetic model**			**Intraparticle diffusion**	
		$q_{e,\ cal}$	**k_1**	**R^2**	**$q_{e,\ cal}$**	**k_2**	**R^2**	**k_{ipd}**	**R^2**
80	40	22.44	0.0033	0.8185	30.68	0.0011	0.9873	1.221	0.8129
100	45.99	28.36	0.0029	0.83	35.59	0.0008	0.9845	1.391	0.7602

As shown in Table 4.18, R^2 values for pseudo-second-order kinetic equation are 0.9873 and 0.9845 for solution with initial concentration of 80 mg/L and 100 mg/L, respectively. These values are higher than the R^2 for pseudo-first-order kinetic equation. It indicates that pseudo-second-order kinetic equation could better describe adsorption process where chemisorption played an important role in the overall adsorption process (Kushwaha, et al., 2008).

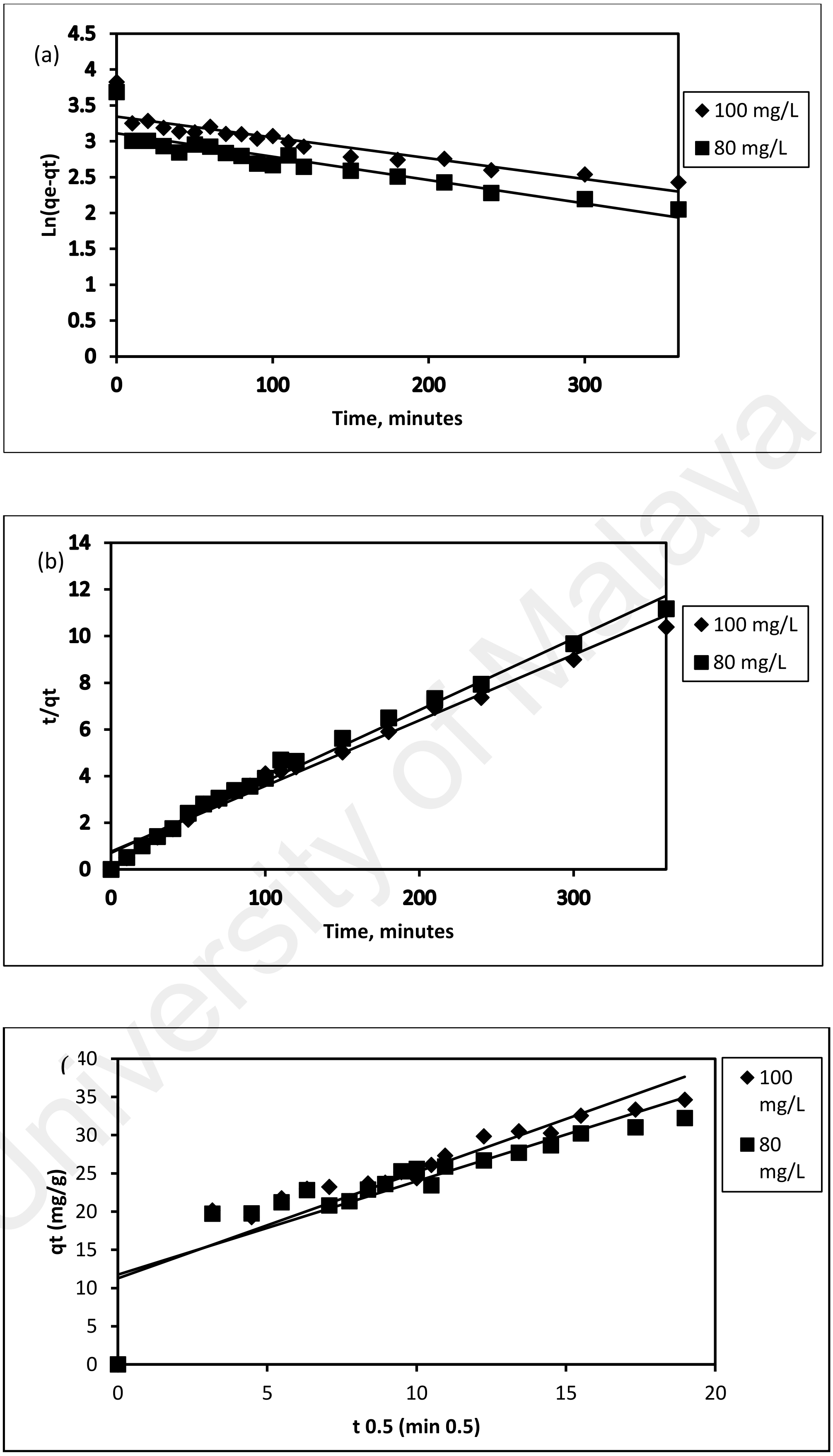

Figure 4.27 Linearized plot for (a) first order kinetics, (b) second order kinetics, (c) intraparticle diffusion model.

Weber-Morris intra-particle diffusion model was also tested to determine whether intra-particle diffusion was the rate-controlling step. The linear portion of the curve suggests that there was some diffusion; however, intra-particle diffusion was not the only rate-controlling step because it did not pass through the origin as can be seen from Figure 4.27(c).

4.2.2.3 Isotherms study

The purpose of adsorption isotherms is to describe the interaction between solutes and adsorbents. In this study, data obtained from experiments were analysed using Langmuir, Freundlich and Temkin isotherms. Summary of isotherm parameters are shown in Table 4.19. All isotherms show good regression coefficient values but the interaction process is best described by Langmuir isotherm as it has higher regression coefficient, R^2 at 0.9997. The characteristic of Langmuir isotherm can be expressed by dimensionless parameter R_L, represented in equation 4.3:

The R_L values for initial concentration of 40 mg/L, 60 mg/L , 80 mg/L and 100 mg/L were 0.0123, 0.0083, 0.0062 and 0.005, respectively. From these results, it is suggested that the adsorption process of DR23 onto $MWAC_T$ was favourable. The maximum adsorption according to Langmuir model is 24.75 mg/g, which is better than the value of 10.72 mg/g, reported by Doulati Ardejani et al. (2007).

Table 4.19 Isotherm parameters for DR23 adsorption on MWAC

Langmuir Isotherm		**Freundlich Isotherm**		**Temkin Isotherm**	
q_{max} (mg/g)	24.75	K_f (L/g)	19.8103	A (L/g)	5566620
b (L/g)	2	1/n	0.0581	b(kJ/mol)	1.9423
		n	17.2117	B (J/mol)	1.2756
R^2	0.9997	R^2	0.9831	R^2	0.9815

4.2.2.4 Thermodynamic study

Key thermodynamic parameters for the adsorption process are free energy change (ΔG^0), enthalpy change (ΔH^0) and entropy change (ΔS^0). These values are shown in Table 4.20.

Table 4.20 Thermodynamic parameters for DR23 adsorption on MWACT

Initial concentration, C_0 (mg/L)	**ΔG^0 (kJ/mol)**				**ΔH^0 (kJ/mol)**	**ΔS^0 (kJ/mol K)**
	288K	**298K**	**308K**	**318K**		
80	1.174612	-0.04036	-0.31144	-8.00376	82.376	0.2776
100	1.869018	1.537152	1.470375	-1.36967	30.494	0.0977

The positive values of enthalpy change (ΔH^0) indicate that the adsorption process was endothermic. The values of free energy (ΔG^0) obtained suggest that at the initial low temperature, the adsorption process was not favourable. However, at 45°C the process becomes spontaneous for both concentrations.

4.3 Evaluation of HIGEE technology in rotating packed bed reactor

High gravimetric or HIGEE technology is a revolutionary mechanism, which aided the achievement of the process intensification in chemical industry thus provided a competitive advantage, reduction in costs, improvement in product quality and increase in yields. Rotating packed bed (RPB) contactor is the tool to implement this technology in the field of adsorption. The high gravitational field in the RPB improves the mass transfer limited processes compared to columns. This unique feature of RPB is established for liquid-gas system. However, in-depth study and robust optimisation is required to establish the same for liquid-solid system such as adsorption of dyes and heavy metal from wastewater onto activated carbon.

4.3.1 Application of rotating packed bed contactor for removal of Direct Red 23 by adsorption

The aim of this study was to investigate the adsorption of DR23 dye on activated carbon in a RPB. This study investigated adsorption rates of the dye in a RPB and compared the results with the shake flask data for the same amount of activated carbon. Effect of operational parameters such as activated carbon loading, rotor speed and feed rate were studied to understand the influence of these parameters on dye adsorption.

4.3.1.1 Comparative study of dye removal with contact time in shake flask and in RPB

The effect of contact time on adsorption was studied for both RPB and shake flask to understand the effect of the centrifugal force on the adsorption of DR23. The data are shown in Figure 4.28. It can be observed that removal percentage in RPB is much higher than that in the shake flask experiment. In five hours, the percent removal of dye reached 93% for 50 mg/L initial concentration while 77% of the dye was removed from 100 mg/L solution in RPB. A removal of 55% for initial concentration 50 mg/L and 46% for initial concentration of 100 mg/L were observed for shake flask study, which were considerably lower than that in the RPB in 5 hour. The reason for higher removal in a RPB contactor is mainly attributed to the centrifugal force that is generated due to the rotation of the bed. This relative centrifugal force (RCF) can be several times higher than the gravitational force depending upon the rotating speed according to the following equation 4.7 (BioScience, 2014):

$$RCF = 11.18 * r * (\frac{Q}{1000})^2 \tag{4.7}$$

This high rotational speed reduces film mass transfer resistance in the packed bed, which in turn, facilitates mass transfer from liquid to activated carbon (Das et al., 2008; Panda, et al., 2011) according to equation 4.8.

$$k_s = 2.8 \left(\frac{Q_w}{\Delta X}\right) s_c^{-2/3} R_e^{-8/9} Gr_{avg}^{2/9} \tag{4.8}$$

where Q_w, Gr_{avg}, Re, Re, and Sc represent the liquid flow rate per unit width of the packed bed, Grashof number based on average bed radius, Reynolds number, and Schimdt number, respectively and ΔX is the surface renewal parameter. The Grashof number and Reynolds number are proportional to the rotational speed and liquid flow rate, respectively. According to equation 4.8 k_s increases with rotational speed. Effective solid-liquid interfacial area also increases with rotational speed and often used for estimating the same in RPB. So the increase in volumetric solid_liquid mass transfer coefficient is expected to be even larger. Tortuosity must also have some effect and therefore, the adsorption decrease after certain level.

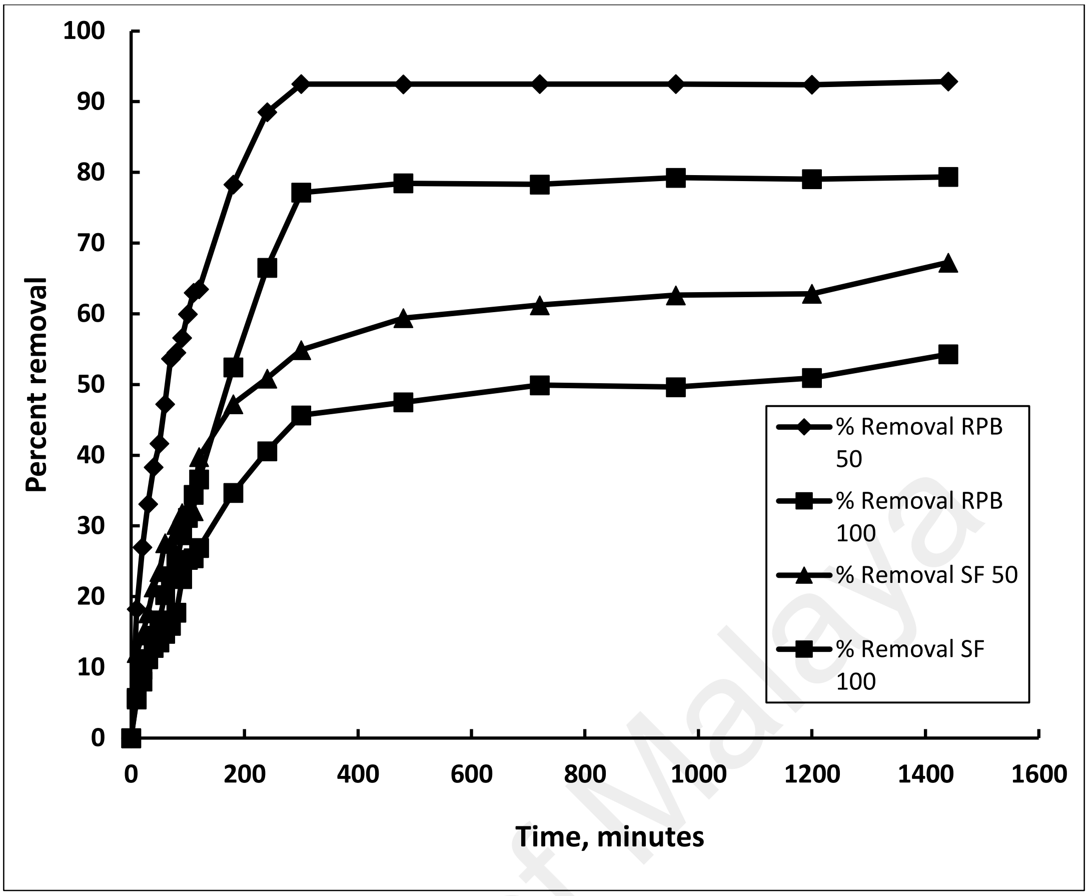

Figure 4.28 Comparison dye removal in RPB and Shake flask

4.3.1.2 Kinetic studies for the adsorption of the dye

A linearised form of pseudo-first-order kinetic equation, popularly known as the Lagergren equation, as well as a linearised form of pseudo-second-order kinetic equation was used to validate the data obtained in the kinetic experiment. The results obtained after regression analysis of the data for the pseudo-first-order and pseudo-second-order kinetics are shown in Figure 4.29 (A) and 4.29 (B), respectively. Applicability of any of the rate equation was decided based on the value of regression coefficient R^2.The R^2 value of the pseudo-first-order equation, listed in Table 4.21, having higher value suggests that this could describe the adsorption of DR23 better than the pseudo-second-order equation with lower R^2 values. This suggests that the adsorption process is dependent upon the concentration of the solute. The theoretical value of q_e calculated from the equation obtained for pseudo-first-order model showed a reasonably good agreement with experimental values of q_e. On the other hand, the difference between q_e calculated and q_e experimental values for pseudo-second-order model was quite large.

The above two models could not explain the mechanism of the adsorption process. Therefore, intra-particle diffusion model was employed to understand the mechanism of the adsorption. The higher values of correlation coefficient R^2 listed in Table 4.21 suggest intra-particle diffusion was responsible for the adsorption of the dye molecules. However, the fact that the plot does not pass through the origin, as can be seen from Figure 4.29 (C), implies it was not the only controlling factor for adsorption of DR23 dye.

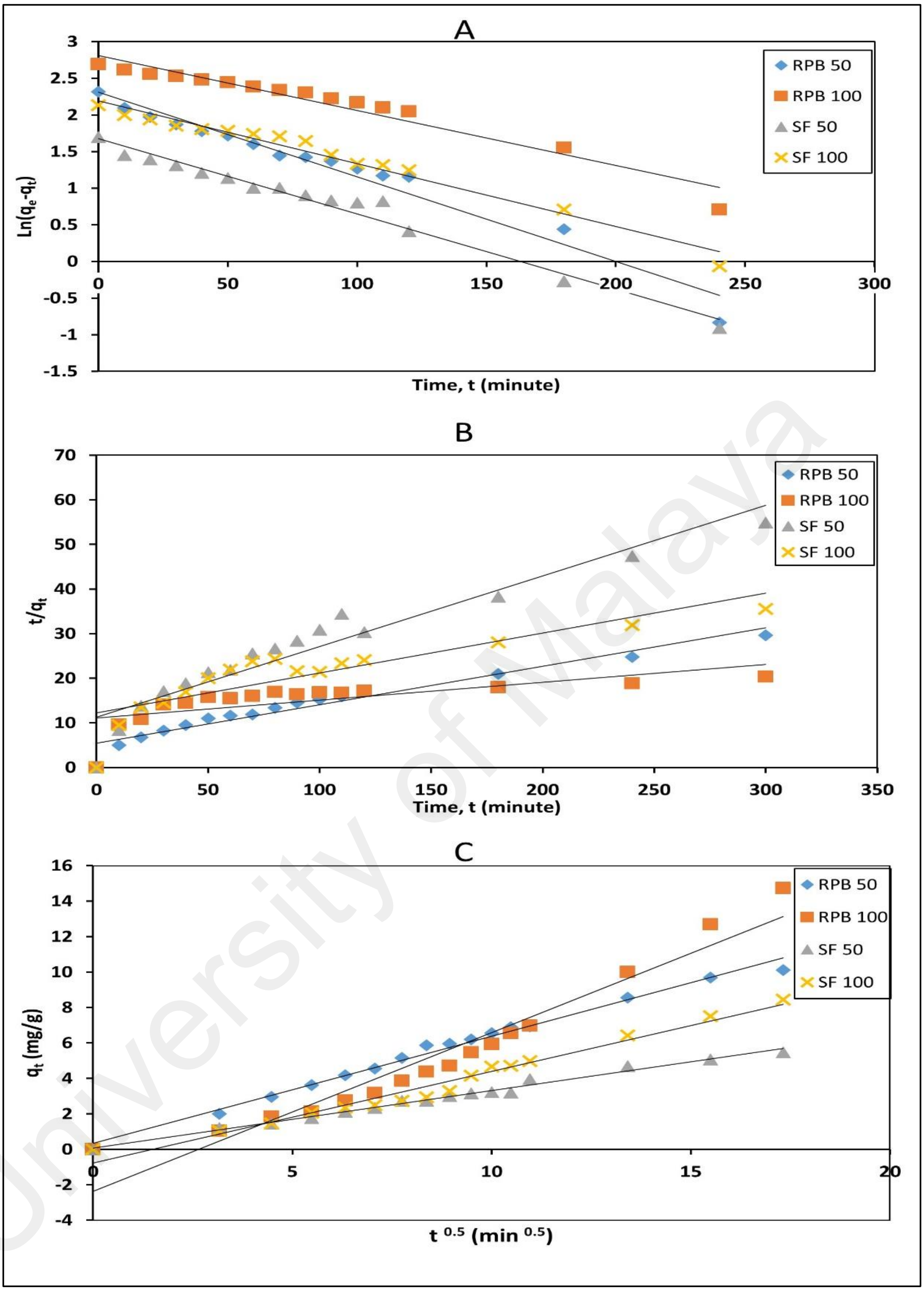

Figure 4.29 A) Pseudo-first-order kinetic model, B) Pseudo-second-order kinetic model, C) Intra-particle diffusion model for adsorption of DR23 on AC in RPB.

Table 4.21 Pseudo-first order, Pseudo-second-order and intra-particle diffusion values

Experiments	**Initial concentration (mg/L)**	**$q_{e,\ exp}$ (mg/g)**	**Pseudo-first-order kinetic model**			**Pseudo-second-order kinetic model**			**Intra-particle diffusion**	
			$q_{e,\ cal}$	**k_1**	**R^2**	**$q_{e,\ cal}$**	**k_2**	**R^2**	**k_{ipd}**	**R^2**
Rotating packed bed	50	10.12	10.1	0.012	0.9617	11.59	0.008	0.9431	0.604	0.9903
	100	14.73	16.63	0.008	0.9412	24.94	0.003	0.4866	0.896	0.9435
Shake flask	50	5.47	5.34	0.010	0.9738	6.32	0.027	0.9125	0.324	0.9878
	100	8.45	8.97	0.009	0.9728	11.17	0.011	0.757	0.517	0.9749

4.3.1.3 Effect of rotor speed on dye removal in RPB

Effect of rotor speed on the adsorption of dye could be one of the most important factors as the centrifugal force, which plays an important role in the mass transfer process in RPB, varies with the speed at which the rotor spins. In order to study the effect of rotor speed, the rotor was spun at different speeds of 628 rpm, 855 rpm and 1140 rpm at a constant feed rate of 20 L/h and 5 g of activated carbon loading. The result showed almost similar percent removal of dye except at 855 rpm after 2 hours. Percent removal slightly decreased at rotor speed 855 rpm and it had the lowest adsorption capacity of 6.9 mg/g, as evident from Figure 4.30 (A). Although percent removal at 628 and 1140 rpm were almost similar, they had different adsorption capacities. The highest adsorption capacity was observed at 628 rpm rotor speed and 8.35 mg/g dye concentration to activated carbon loading ratio. The reason for the decrease in adsorption at 855 rpm could be attributed to the fact that the solid mass of activated carbon shifted towards the outer wall of the rotor with increasing rotor speed thereby decreasing the path length of the liquid flown within activated carbon. The liquid profile inside the rotor also took an ‘egg shell’ like shape due to the centrifugal force (Lubarda, 2013). This also contributed to the decrease in path length. With increasing rotational speed, the depth of the ‘egg shell’ increased and path length decreased further. In this case, the increase in mass transfer coefficient due to increasing centrifugal force (Panda, et al., 2011) could not compensate for the effect of decrease in liquid flow path length. However, when the rotor speed is further increased, the adsorption again increased. In this case, the increase in the mass transfer coefficient prevailed over the decrease in path length due to the displacement of the activated carbon and the water profile towards outer wall of the rotor (Das, et al., 2008).

4.3.1.4 Effect of feed rate on dye removal in RPB

Feed rate was one of the parameters that could affect the adsorption characteristics of DR23 in a rotating packed bed. Adsorption behaviour was observed for four different feed rates, namely 10 L/h, 20 L/h, 30 L/h and 40 L/h at the same rotor speed of 855 rpm and with 5 g of activated carbon loading. The liquid was recirculated from a reservoir containing 1 L of the dye solution. As can be seen in the Figure 4.30 (B), 82% and 80% of dye removal was obtained at the respective feed rate of 40 and 30 L/h, while 67% and 63% of dye removed at the respective feed rate of 20 and 10 L/h. Adsorption capacity of 9 mg/g did not vary for feed rates of 30 and 40 L/h. Adsorption at feed rate 10 and 20 L/h was almost constant in the first hour but feed rate of 10 L/h showed higher adsorption in the following hour. Higher feed rate increased the probability of contact between the activated carbon and liquid, which in turn increased the adsorption of the dye.

4.3.1.5 Effect of activated carbon loading on dye removal in RPB

In order to investigate the effect of activated carbon dose, experiments were carried out in 3 different loadings of 5 g, 10 g and 15 g, which corresponded to 255, 510, 765 kg/m, respectively, at the same rotor speed and feed rate. It can be observed from Figure 4.30C that the percent removal increased with higher activated carbon loading because of the availability of more adsorption sites. With increasing amount of activated carbon, the packing was more compact and there was less distortion of the pack due to high speed rotation. This ensured that the path length travelled by the liquid was long in comparison with low compaction when less quantity of activated carbon was used.

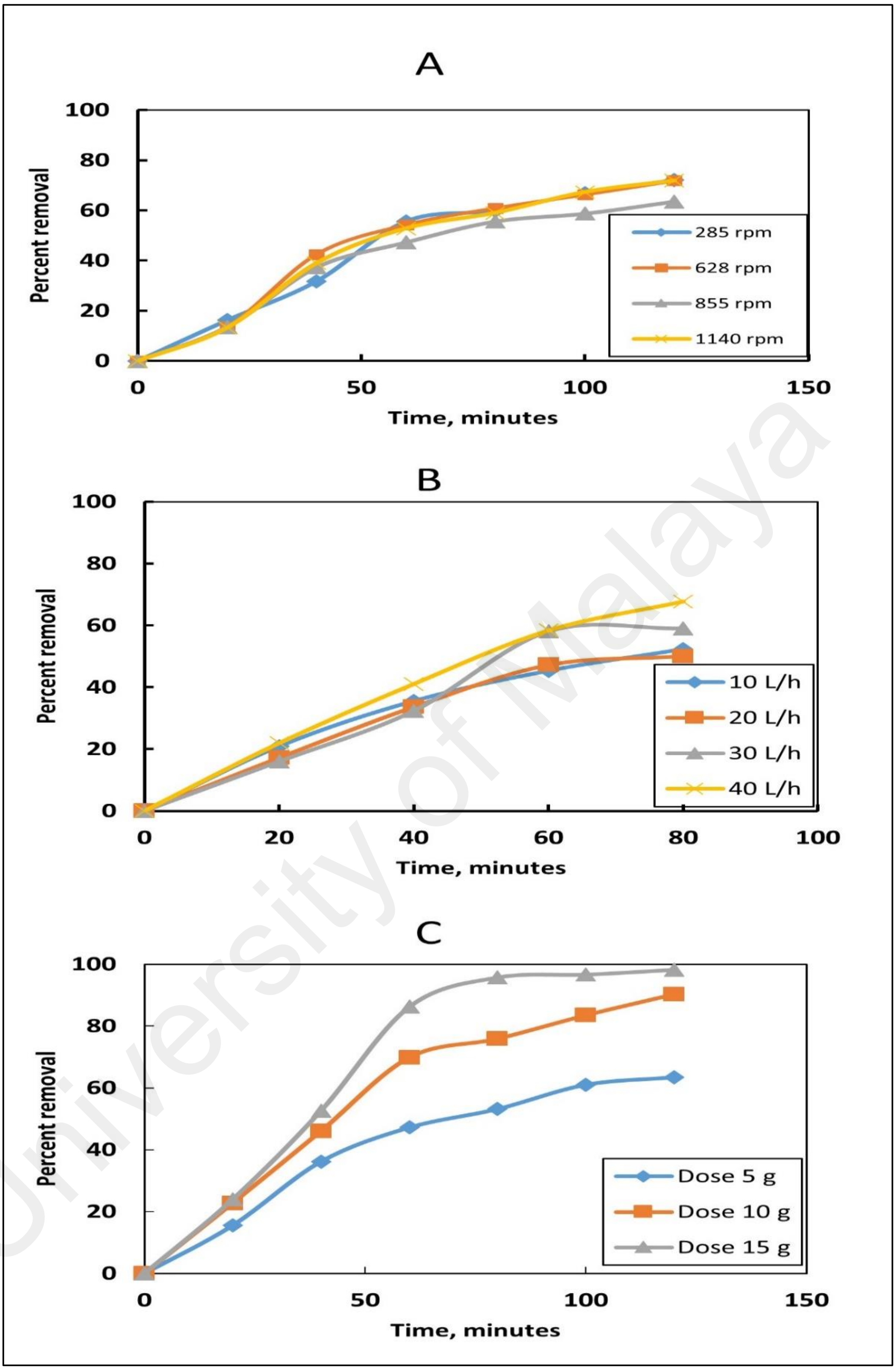

Figure 4.30 (A) Effect of rotor speed, (B) Effect of feed rate, (C) Effect of activated carbon loading on adsorption of DR23

4.3.2 Taguchi optimisation approach for chromium removal in a rotating packed bed contractor

The purpose of this study was to use activated carbon in RPB for the adsorption of chromium and to optimise the important process variables. Taguchi method was used to obtain a robust operating condition for RPB-HIGEE system. The operating parameters such as rotating speed of the rotor, liquid feed rate, activated carbon packing density and initial pH of the solution was chosen for the purpose. The kinetics and mechanism for the adsorption process was also examined.

4.3.2.1 Effects of the control factors and noise factor on the chromium adsorption in RPB

In accordance with the Taguchi design of L16 array, forty-eight experiments were performed, taking into account the three different levels of the noise factor. Table 4.22 shows the percent adsorption of chromium in RPB for the three levels of external noise factor.

Table 4.22 (A) Effect of rotor speed, (B) Effect of feed rate, (C) Effect of activated carbon loading on adsorption of DR23.

Rotating speed	**Feed rate**	**Packing density**	**Initial pH**	**Percent removal of Cr(VI)**		
				NF 1	**NF 2**	**NF 3**
400	20	153	2	60.18	59.57	58.1
400	30	255	3	64.5	63.46	63.45
400	40	357	4	55.3	55.09	55.02
400	50	510	5	50.47	59.78	59.65
800	20	255	5	63.1	62.43	61.1
800	30	153	4	60.93	68.44	62.25
800	40	510	3	81.77	84.87	84.43
800	50	357	2	85.69	84.23	84.19
1200	20	357	3	66.1	65.72	65.71
1200	30	510	2	77.03	75.67	75.43

Rotating speed	**Feed rate**	**Packing density**	**Initial pH**	**Percent removal of Cr(VI)**		
				NF 1	**NF 2**	**NF 3**
1200	40	153	5	92.46	87.79	92.13
1200	50	255	4	80.92	80.8	82.77
1600	20	510	4	67.88	68.04	68.85
1600	30	357	5	87.53	86.9	86.82
1600	40	255	2	67.48	65.49	63.23
1600	50	153	3	73.28	72.56	72.78

ANOVA was performed on the data obtained to determine those control factors, which have significant effect on the adsorption of dye. Table 4.23 represents the ANOVA of the experimental data. F-statistic describes the significance of a control factor on the quality characteristic, which in this case is adsorption. The F value for each control factor is the ratio of the mean of squared deviations to the mean of squared error. As mentioned earlier, usually if F > 4, it means that the change of the control factor has very significant effect on the quality characteristic (Barman, et al., 2011). From Table 4.23, it can be observed that the F-value for the rotating speed is the highest at 11.21 and it has high contribution (48.5%) towards influencing the result. Initial pH of the solution also plays a very important role in the removal of chromium with F-value 7.57 and the initial pH has 32.8% contribution towards removal of chromium. The F-value close to 2 suggests moderately significant effect (Kundu, et al., 2014b) and from Table 4.23, it can be observed that feed rate has moderately significant effect on chromium removal in RPB with F-value of 2.87, contributing 12.4% towards removal. Packing density is found to be statistically insignificant with F-value of 0.44, which made only about 2% contribution towards the removal of chromium in RPB.

Effects of control factors on the S/N ratio of the chromium adsorption by the prepared $MWAC_T$ can be observed in Figure 4.31. The maximum level average of S/N ratio in the four different levels are shown in in Table 4.24 and the values are marked in bold. The largest S/N performance corresponds to the best performance characteristic.

Table 4.23 Analysis of Variance for SN ratios for chromium removal in RPB

Source	DF	Seq SS	Adj SS	Adj MS	F	P	Percent contribution
Rotating speed (RPM)	3	14.25	14.25	4.75	11.21	0.039	48.55
Feed rate(L/h)	3	3.64	3.64	1.21	2.87	0.205	12.4
Packing density (kg/m^3)	3	0.5591	0.5591	0.19	0.44	0.741	1.91
Initial pH	3	9.63	9.63	3.21	7.57	0.065	32.82
Residual Error	3	1.27	1.27	0.4236			
Total	15	29.35					

Table 4.24 Response Table for S/N Ratios "Larger is better"

	Level average				Delta	Rank
	Level 1	Level 2	Level 3	Level 4		
Rotating speed (rpm)	35.34	37.24	**37.84**	37.26	2.5	1
Feed rate (L/h)	36.10	37.15	37.18	**37.25**	1.16	3
Packing density (kg/m^3)	36.98	36.62	**37.14**	36.93	0.51	4
Initial pH	**37.73**	37.62	36.39	35.93	1.8	2

The sequential (Seq SS) and adjusted (Adj SS) sums of squares in Table 4.23 are the same for all terms, which signifies that the design matrix is orthogonal. From Figure 4.31, it can be seen that the adsorption improves with the rotor speed. Effect of rotor speed on the adsorption of chromium could be one of the most important factors as the centrifugal force varies with the speed at which the rotor spins. Centrifugal force plays an important role in the mass transfer process in RPB.

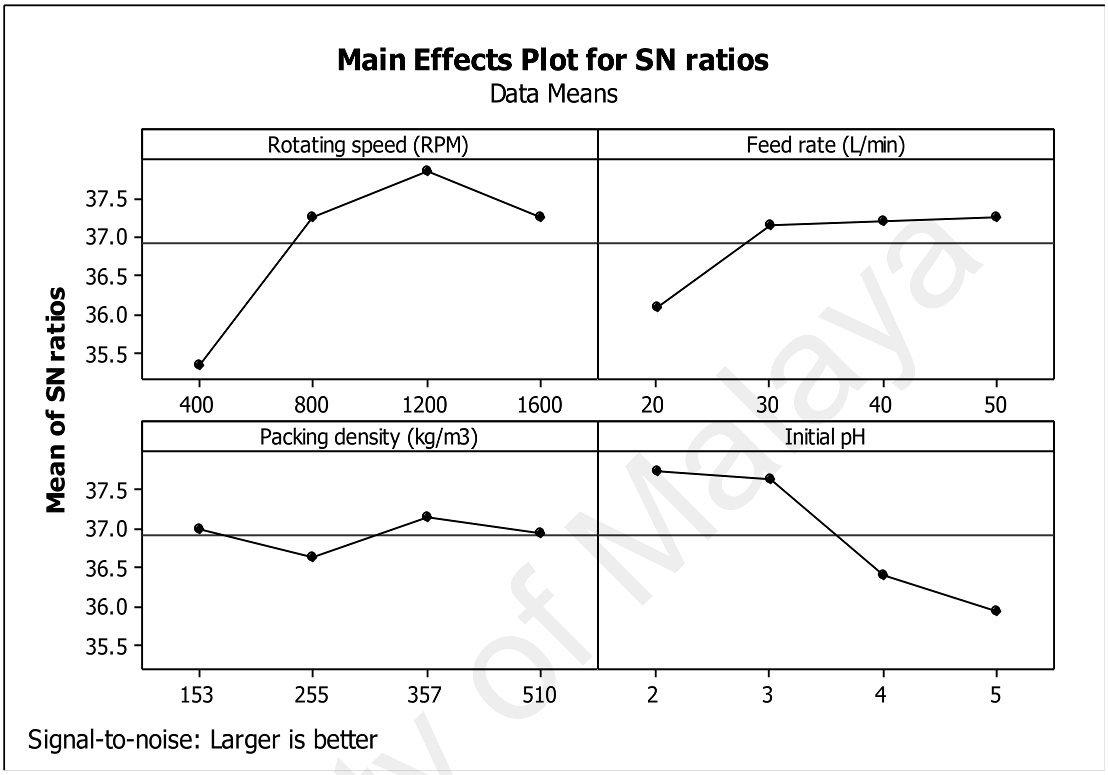

Figure 4.31 Main effect plot for S/N ratio for the adsorption of chromium

This centrifugal force can be several times higher than the gravitational force depending upon the rotating speed. This force facilitates mass transfer from liquid to solid activated carbon due to lower external mass transfer resistance (Das, et al., 2008). As the rotor speed increased from 400 rpm to 800 rpm, and finally to 1200 rpm, the higher centrifugal force aided the removal of chromium by increasing the mass transfer coefficient. With increasing speed of the rotor, the solid mass of activated carbon shifts towards the outer wall of the rotor and the path travelled by the solution within activated carbon decreases. However, the increase in the mass transfer coefficient due to increase in centrifugal force dominates over the effect of decreased path length due to displacement of activated carbon. Consequently, a better adsorption performance is obtained. In case of rotating speed of 1600 rpm, the adsorption performance deteriorated. The reason could be that the increase in mass transfer coefficient due to increasing centrifugal force could not compensate for the decrease in liquid flow path length. Initial pH of the solution also played an important role in the removal of the chromium. At very acidic pH, chromium exists as neutral species H_2CrO_4 or negatively charged species $HCrO_4^-$ and $Cr_2O_7^{2-}$ (Gherasim, et al., 2011). These species are better attracted by the protonated surface of the activated carbon when they come into contact with the acidic solution. At pH value 4 and 5, the performance deteriorated significantly due to electrostatic repulsion between the OH^- ions and the negatively charged $HCrO_4^-$ and $Cr_2O_7^{2-}$ ions present in the solution (Prasad and Abdullah, 2010). The S/N ratio for feed rate increased significantly from 20 L/h to 30 L/h. However, the increase is not very significant thereafter. At higher flow rate, the probability of contact between the $MWAC_T$ and liquid increased, which aided the adsorption of chromium onto $MWAC_T$. It was observed that the packing density has highest S/N ratio at its level three where the density was 357 kg/m^3.

The surface plots shown in Figure 4.32 (A), (B), (C) and (D) aids the understanding of the interactive effects of the operating parameters on the response, i.e. removal percentage. The interactive effects of rotating speed and the feed rate, as shown in Figure 4.32A, suggest that with increase in these two parameters, the removal percentage increased. However, beyond 1200 rpm, the removal percentage decreased, especially at higher value of the feed rate. The interactive surface plot of the initial pH and feed rate, as shown in Figure 4.32B, indicates that removal percentage is higher at lower levels of pH and higher levels of feed rate. When the interaction of initial pH and the rotating speed was considered, it was observed that the percent removal was higher at lower initial pH and higher rpm.

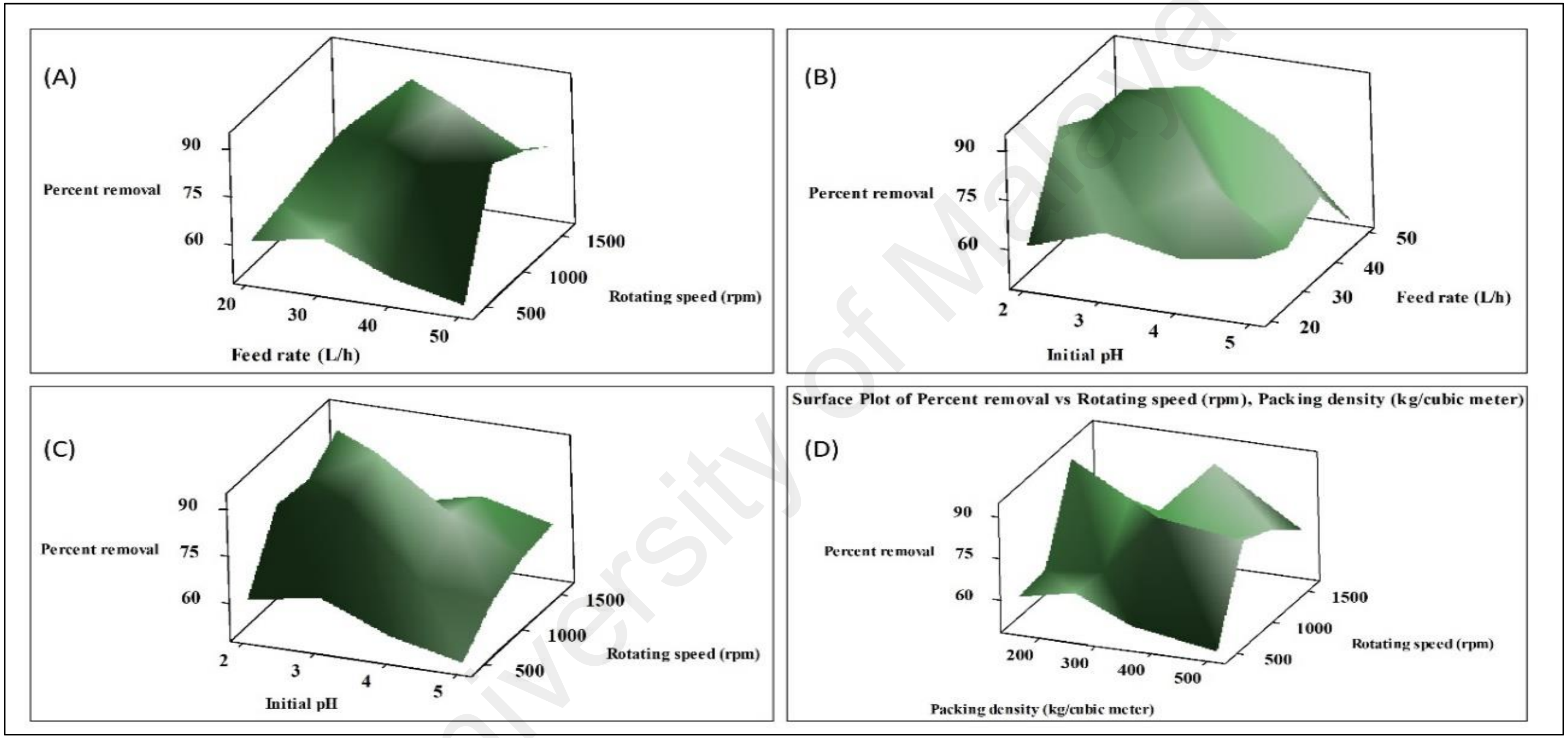

Figure 4.32 Three dimensional surface plot for the interactive effects (A) rotating speed and feed rate, (B) feed rate and initial pH, (C) rotating speed and initial pH, (D) rotating speed and packing density

However, after 1200 rpm, there was a decrease in percent removal, as evident from Figure 4.32 (C). The interaction of packing density and rotating speed suggests that the percent removal initially increased with increase in the level of packing density and rotating speed, as illustrated in Figure 4.32D; however, after a certain level, the percent removal decreased. These observations also suggest that there is an optimum point between the highest and lowest levels.

According to Taguchi method, the level with the highest S/N ratio should be the optimum level for that particular control factor (Kundu, et al., 2014b). Consequently, the optimum levels of the control factors for the removal of chromium in RPB contactor with MWAC$_T$ are tabulated in Table 4.25.

4.3.2.2 Confirmatory experiment

The combination of levels of the optimum condition as detailed in Table 4.25 is not present in the experimental matrix obtained according to Taguchi method. Hence, it is important to run the experiment at the optimum level to validate the prediction of the Taguchi method with the experimental result.

Table 4.25 Optimum condition and comparison of predicted and experimental results for chromium removal in RPB by MWACT

Investigating parameters	**Level**	**Value**	**Predicted**		**Experimental**	
Rotating speed (rpm)	3	1200	S/N ratio	Mean	S/N ratio	Mean
Feed rate (L/h)	4	50	39.20	90.34	39.26	91.83
Packing density (kg/m^3)	3	357				
Initial Solution pH	1	2				

It is evident from Table 4.25 that the predicted and experimental values are in very good agreement with each other. The mean value of the removal during the 16 experiments suggested by Taguchi method was 71.06, which was much lower than the mean obtained at the optimum value.

A comparative study between some recent works for chromium removal in a fixed bed column and this study is given in Table 4.26. It is evident from the Table 4.26 that the height of the RPB is much smaller than other fixed bed columns and the flow rate is much higher. This ensures high throughput and quick removal of chromium, thus leading to process intensification.

Table 4.26. Comparison of fixed bed study and present study for removal of chromium

Adsorbent used	**Initial concentration (mg/L)**	**Height of the column (cm)**	**Flow rate (L/h)**	**Removal %**	**Reference**
Multiwall carbon nanotubes/nano-iron oxide	20	-	0.06	90	(Gupta et al., 2011a)
Modified corn stalk	200	29	0.6	93	(Chen et al., 2012)
Waste pomace of olive oil factory	100	30	0.3	22	(Malkoc et al., 2006)
Aspergillus niger fungal biomass	10	79	0.144	>90	(Mungasavalli et al., 2007)
Mowital B30H resin immobilized	100	-	0.192	22.4	(Aksu et al., 2002)

Adsorbent used	Initial concentration (mg/L)	Height of the column (cm)	Flow rate (L/h)	Removal %	Reference
dried activated sludge					
Coconut coir pith	1532	60	1.8	97.3	(Suksabye et al., 2008)
Activated carbon from palm kernel shell	100	1	50	91.83	This study

4.3.2.3 Kinetic study

Kinetic study of the chromium adsorption in RPB on $MWAC_T$ was conducted and the resulting data were analysed separately by pseudo-first-order, pseudo-second-order and Elovich equations. The removal of chromium was found to be fast. It was observed that about 75% was removed within 20 min, as can be seen from Figure 4.33. The regression analysis was performed to measure the linear fitting of the data for these three kinetic models. The curves from the data fit are shown in Figure 4.34 (A), (B) and (C), respectively for pseudo-first-order, pseudo-second-order and Elovich kinetics.

The value of regression coefficient R^2 is used to select the rate equation describing the adsorption process. The value of regression coefficients for pseudo-first-order, pseudo-second-order and Elovich kinetic models were 0.9003, 0.9989 and 0.8140, respectively, demonstrating that the second order kinetic model could describe the adsorption kinetics of chromium on to $MWAC_T$ better than other models. This suggests that the chemisorption plays an important part in the rate limiting step involving valence forces developed due to the sharing or exchange of electrons between adsorbent and adsorbate (Kundu, et al., 2014b; Kushwaha, et al., 2008).

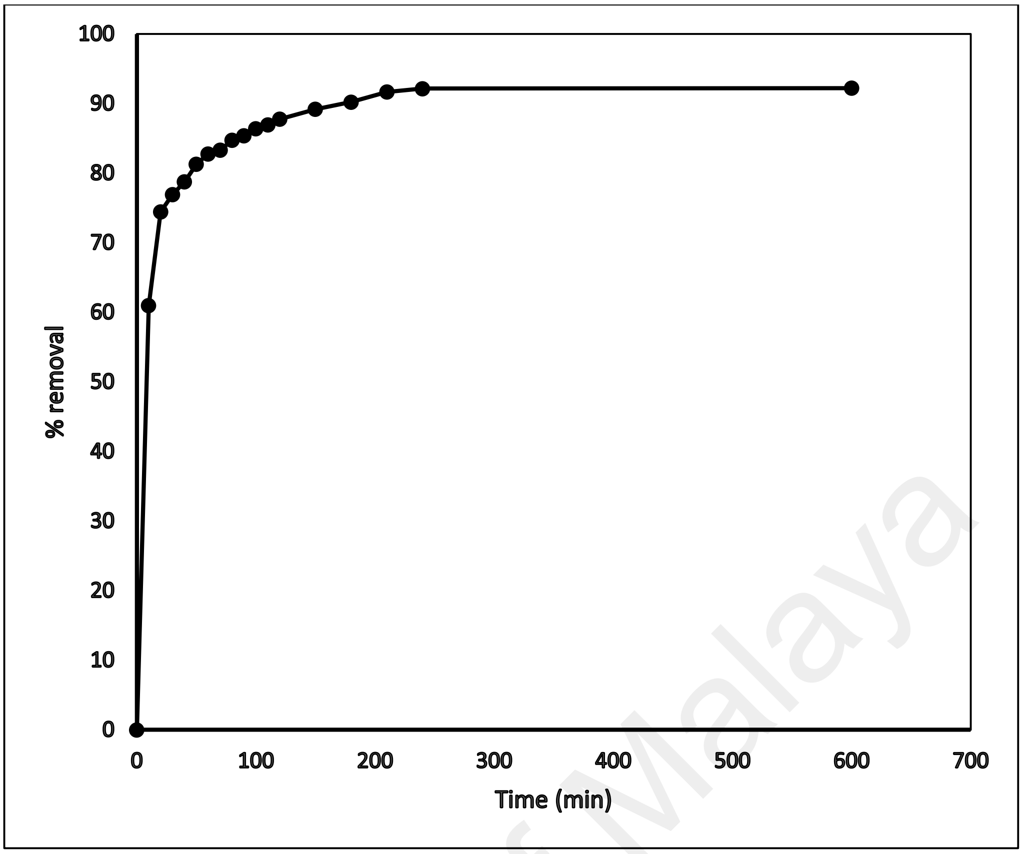

Figure 4.33 Removal of chromium with respect to time in RPB

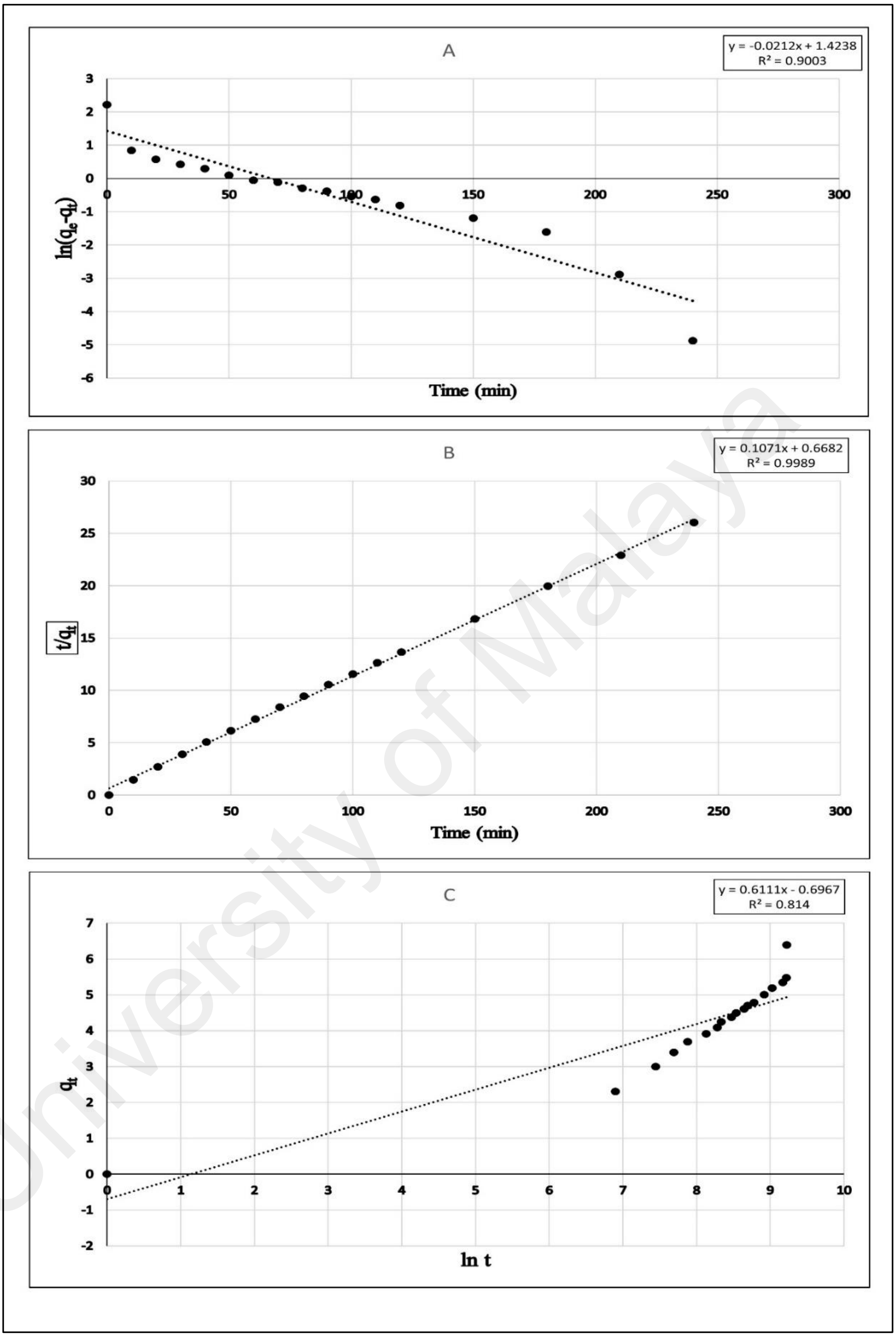

Figure 4.34 Regression analysis of the chromium adsorption data for A) Pseudo-first-order kinetics and B) pseudo-second-order kinetics, C) Elovich kinetic equation

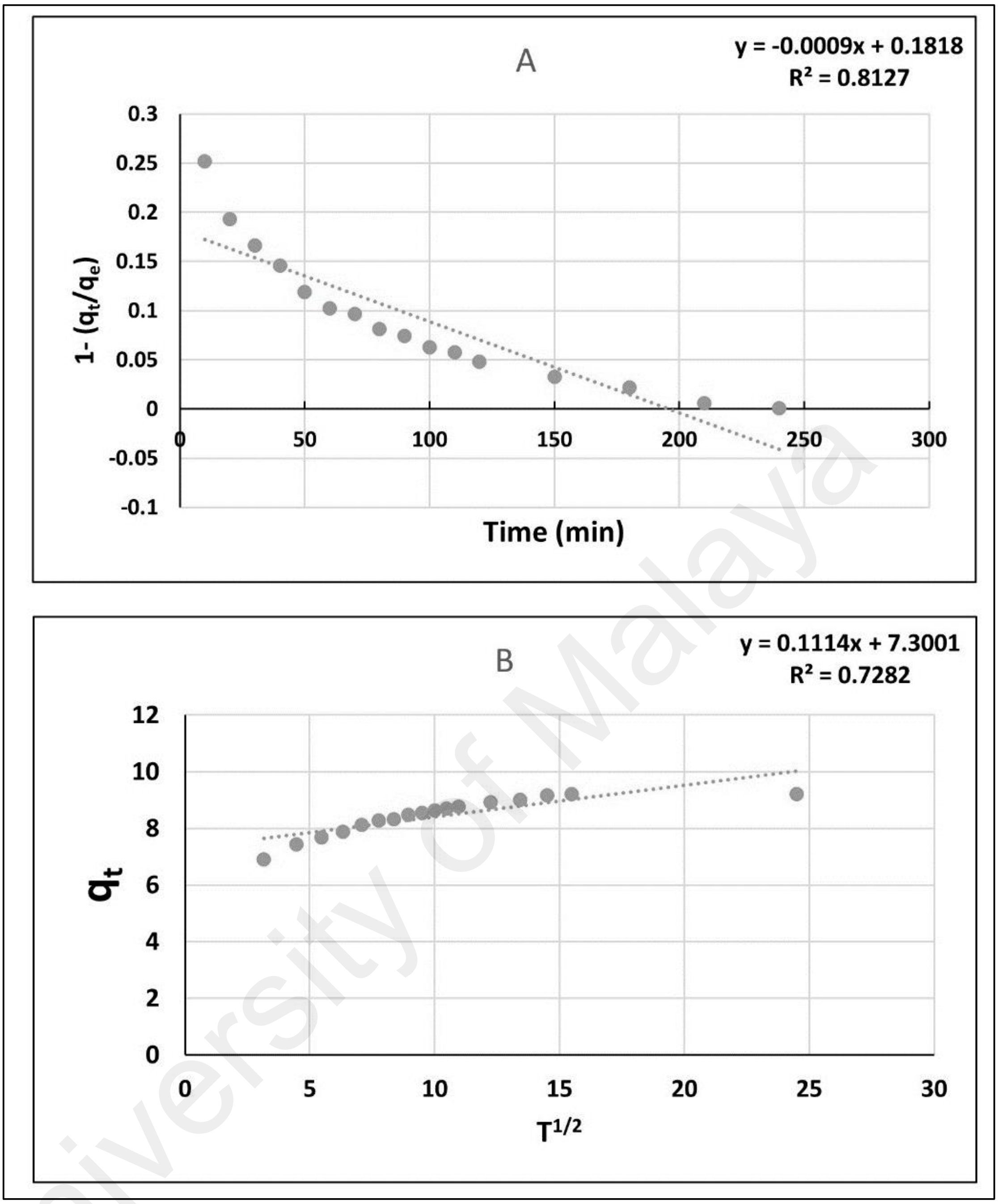

Figure 4.35 Regression analysis of the chromium adsorption data for A) film diffusion and B) intraparticle diffusion model.

The mechanism of the adsorption in RPB was investigated by the film diffusion model and intra-particle diffusion model. The data points obtained in the kinetic experiment were analysed by the models and the regression analyses were performed to assess the log-linear fitting of the data for these models. Figure 4.35 (A) and (B) represent the fitted curves for film diffusion and intra-particle diffusion models, respectively. The regression coefficient values for film diffusion and intra-particle diffusion models were 0.8127 and 0.7282, respectively. The value of the regression coefficients suggest that film diffusion was the predominating factor in the adsorption of chromium on $MWAC_T$.

CHAPTER 5: CONCLUSIONS AND RECOMMENDATIONS

5.1 Conclusion

In persuasion of developing an easy and affordable technique to treat industrial wastewater containing heavy metals and dyes, adsorption on activated carbon in a high gravimetric field was the principal approach adopted for the wastewater treatment in this study. Activated carbon was prepared using locally available raw material by microwave heating. The preparation conditions were optimised using Taguchi and RSM methods. The prepared activated carbon was used for removal of heavy metals such as chromium, zinc and dyes, namely, Direct Red 23 (DR23) and Methylene Blue (MB). The adsorption experiments were performed both in conventional shake flasks and in a rotating packed bed (RPB) contactor.

5.1.1 Preparation of activated carbon

Three different types of activated carbons were prepared from PKS by H_3PO_4 impregnation, followed by microwave activation. These were denoted as MWAC1, MWAC2 and MWAC3. Characterisation study showed that the activated carbon materials had high BET surface areas of 872 m^2/g, 1256 m^2/g, and 952 m^2/g, respectively. The pore size distribution and average pore size suggested that the activated carbon was mainly mesoporous. SEM micrographs clearly showed that the surface became highly porous after activation. Among the three types of activated carbon prepared in this study, MWAC2 was chosen, based on its high surface area and bulk density, for removal of Cr(VI) for this particular section of study.

Taguchi method was used to optimise the preparation condition of activated carbon from PKS by H_3PO_4 impregnation and microwave activation. The activated carbon was denoted as $MWAC_T$ and used for MB adsorption. The robust Taguchi method revealed the optimum condition for activated carbon preparation, which required microwave power of 800 W, irradiation time of 17 min, impregnation ratio of 2, and acid concentration of 85%. The heating time obtained was much shorter than conventional methods of activated carbon preparation thereby contributing to the savings of energy and cost. The noise factor (particle size of the raw material) had no effect on activated carbon quality. When optimum condition was employed, the activated carbon demonstrated high porosity with surface area of 1473.5 m^2/g. FTIR diagram confirms dehydration and removal of hydrogen from the raw material. Langmuir Isotherm and a pseudo-second-order kinetic model satisfactorily described equilibrium and kinetic data, respectively. $MWAC_T$ had a maximum MB adsorption capacity of 1000 mg/g. The preparation condition was further refined by fine-tuning the operating parameters. It was found that the required microwave power was 700W instead of 800W as suggested in the coarse optimisation. The activated carbon prepared in the refined experiment had much higher BET surface area of 1535 m^2/g.

In a second optimisation study, RSM was used to optimise the preparation condition of activated carbon. This activated carbon was used for Zn(II) removal. The heating time of activated carbon, which was prepared from PKS with H_2SO_4 impregnation, aided by microwave heating, was only 11.02 min. This is considerably shorter than conventional production method. A numerical model was successfully adopted with the use of Design Expert software that could predict the optimum condition satisfactorily. The suggested Zn(II) adsorption capacity and the yield of activated carbon were 13.73 mg/g and 77.73%, respectively, at optimum condition of 11.02 min of irradiation time, 676 W of microwave power, impregnation ratio of 0.68 and undiluted sulphuric acid. The Zn(II) adsorption capacity of the activated carbon was found to be 14.6 mg/g and the yield was 72% with prediction error of 6.41% and 7.1%, respectively. Characterisation study shows that the activated carbon developed high porosity while FTIR plot confirms dehydration as well as removal of hydrogen part from the raw material. BET surface area was found to be 1011 m^2/g, which is considerably high.

It is evident from the results that the preparation time of the activated carbon was significantly reduced while the quality of the activated carbon was not compromised. This reduces the overall cost and energy use for activated carbon preparation and thus contribute towards fulfilling the aim of the study.

5.1.2 Efficiency of the prepared activated carbon for removal of heavy metal and dye

The optimum process condition for the adsorption of Cr(VI) on MWAC 2 was obtained by the Box-Behnken experimental approach using RSM. This comprised an initial concentration of 60 mg/L, initial operating pH of 3, and operating temperature of 50 ^oC. The Freundlich Isotherm and a pseudo-second-order kinetic model, respectively can satisfactorily describe the adsorption process equilibrium and kinetic data. Thermodynamic study indicates a spontaneous adsorption process, while the process is endothermic in nature.

Taguchi method was used to find the optimum conditions for adsorption process of DR23 by activated carbon, $MWAC_T$. Robust Taguchi method indicated that the optimum condition would be initial concentration of 20 mg/L, solution pH of 2, $MWAC_T$ dose of 4 g/L and temperature of 30 ^oC. Almost complete removal of the dye was obtained at this optimum condition. Pseudo-second-order kinetics described the adsorption process satisfactorily, which suggests chemisorption as the probable mechanism for adsorption. The Langmuir isotherm model was most suitable for describing the process. The maximum adsorption capacity of $MWAC_T$ was found to be 24.75 mg/g from Langmuir isotherm model. The adsorption is thermodynamically more feasible at temperature 45 ^oC

for dye concentration of 100 mg/L. However, for lower concentration, the activated carbon is highly effective for removing DR23from water.

5.1.3 Evaluation of HIGEE technology in RPB for adsorption of heavy metal and dye

Adsorption of DR23 on commercially available activated carbon in a high gravimetric RPB contactor was tested successfully. The centrifugal force generated in the RPB, enhanced the removal of the dye due to reduced mass transfer resistance. The adsorption was fast and within 5 h; almost 93% dye was removed compared to 54% in the traditional shake flask experiment during the same period. Rotating speed of the rotor and liquid feed rate had significant effect on the removal of the dye.

Taguchi method was applied in this study to find out the optimum operating condition of RPB for the adsorption of chromium on $MWAC_{T.}$ An L16 array was used to obtain the experimental matrix. The optimum condition of adsorption could be described by rotating speed (RPM) of 1200 (level 3), feed rate (L/min) of 50 (level 4), packing density (Kg/m^3) of 179 (level 3) and initial solution pH of 2 (level 1). The experimental and predicted S/N ratios with values 39.26 and 39.20 were in very good agreement with each other at the optimum condition. A removal of 91% was obtained at the optimum condition. Pseudo-second-order kinetics described the adsorption satisfactorily while the film diffusion model could describe the mechanism.

Therefore, microwave heating largely reduced the production time of the activated carbon and the produced activated carbon found to be efficient in removing heavy metal and dye. Heavy metal and dye from wastewater were competently removed by adsorption on activated carbon in RPB. The RPB was much efficient in terms of adsorption capacity and time.

5.2 Recommendations

Although the production of activated carbon with the aid of microwave heating and adsorption of heavy metal and dye on to activated carbon in RPB were very effective and efficient, there remain scope of further research in this field. Hence, the following are recommendation that can be suggested to augment the research:

- The scaling up of the microwave system to produce substantial quantity of the activated carbon must be considered to match up with the requirement of the industry.
- Heavy metal other than chromium and zinc as well as mixture of heavy metals must also be tested for adsorption on to activated carbon in RPB.
- Different dyes are also required to be tested for adsorption on the prepared activated carbon in RPB.
- Desorption tests to regenerate the spent activated carbon are also required to be examined to make the system even more sustainable and environment friendly.
- Scale up of the RPB system is also to be considered for industrial use.

REFERENCES

Aber, S., Khataee, A., & Sheydaei, M. (2009). Optimization of activated carbon fiber preparation from kenaf using K_2HPO_4 as chemical activator for adsorption of phenolic compounds. *Bioresource Technology, 100*(24), 6586-6591.

Abnisa, F., Wan Daud, W. M. A., & Sahu, J. N. (2011). Optimization and characterization studies on bio-oil production from palm shell by pyrolysis using response surface methodology. *Biomass and Bioenergy, 35*(8), 3604-3616.

Acharya, J., Sahu, J. N., Sahoo, B. K., Mohanty, C. R., & Meikap, B. C. (2009). Removal of chromium(VI) from wastewater by activated carbon developed from tamarind wood activated with zinc chloride. *Chemical Engineering Journal, 150*(1), 25-39.

Adinarayana, K., & Ellaiah, P. (2002). Response surface optimization of the critical medium components for the production of alkaline protease by a newly isolated *Bacillus sp. Journal of Pharmacy and Pharmaceutical Sciences. , 5*(3), 272-278.

Aghamohammadi, N., Aziz, H. b. A., Isa, M. H., & Zinatizadeh, A. A. (2007). Powdered activated carbon augmented activated sludge process for treatment of semi-aerobic landfill leachate using response surface methodology. *Bioresource Technology, 98*(18), 3570-3578.

Ahmad, A., Mohd-Setapar, S. H., Chuong, C. S., Khatoon, A., Wani, W. A., Kumar, R., et al. (2015). Recent advances in new generation dye removal technologies: Novel search for approaches to reprocess wastewater. *RSC Advances, 5*(39), 30801-30818.

Ahmad, A., Rafatullah, M., Sulaiman, O., Ibrahim, M. H., Chii, Y. Y., & Siddique, B. M. (2009a). Removal of Cu(II) and Pb(II) ions from aqueous solutions by adsorption on sawdust of meranti wood. *Desalination, 247*(1–3), 636-646.

Ahmad, A., Rafatullah, M., Sulaiman, O., Ibrahim, M. H., & Hashim, R. (2009b). Scavenging behaviour of meranti sawdust in the removal of methylene blue from aqueous solution. *Journal of Hazardous Materials, 170*(1), 357-365.

Aksu, Z., Gönen, F., & Demircan, Z. (2002). Biosorption of chromium(VI) ions by mowital®B30H resin immobilized activated sludge in a packed bed: Comparison with granular activated carbon. *Process Biochemistry, 38*(2), 175-186.

Al-Rashdi, B. A. M., Johnson, D. J., & Hilal, N. (2013). Removal of heavy metal ions by nanofiltration. *Desalination, 315*(0), 2-17.

Al-Shannag, M., Al-Qodah, Z., Bani-Melhem, K., Qtaishat, M. R., & Alkasrawi, M. (2015). Heavy metal ions removal from metal plating wastewater using electrocoagulation: Kinetic study and process performance. *Chemical Engineering Journal, 260*(0), 749-756.

Al Aji, B., Yavuz, Y., & Koparal, A. S. (2012). Electrocoagulation of heavy metals containing model wastewater using monopolar iron electrodes. *Separation and Purification Technology, 86*(0), 248-254.

Ali, I., & Gupta, V. K. (2007). Advances in water treatment by adsorption technology. [10.1038/nprot.2006.370]. *Nature Protocols, 1*(6), 2661-2667.

Alvarez, M. T., Crespo, C., & Mattiasson, B. (2007). Precipitation of Zn(II), Cu(II) and Pb(II) at bench-scale using biogenic hydrogen sulfide from the utilization of volatile fatty acids. *Chemosphere, 66*(9), 1677-1683.

Alventosa-deLara, E., Barredo-Damas, S., Alcaina-Miranda, M. I., & Iborra-Clar, M. I. (2012). Ultrafiltration technology with a ceramic membrane for reactive dye removal: Optimization of membrane performance. *Journal of Hazardous Materials, 209–210*(0), 492-500.

Alyüz, B., & Veli, S. (2009). Kinetics and equilibrium studies for the removal of nickel and zinc from aqueous solutions by ion exchange resins. *Journal of Hazardous Materials, 167*(1–3), 482-488.

Amani-Ghadim, A. R., Aber, S., Olad, A., & Ashassi-Sorkhabi, H. (2013). Optimization of electrocoagulation process for removal of an azo dye using response surface methodology and investigation on the occurrence of destructive side reactions. *Chemical Engineering and Processing: Process Intensification, 64*(0), 68-78.

Amini, M., Arami, M., Mahmoodi, N. M., & Akbari, A. (2011). Dye removal from colored textile wastewater using acrylic grafted nanomembrane. *Desalination, 267*(1), 107-113.

Anandkumar, J., & Mandal, B. (2009). Removal of Cr(VI) from aqueous solution using bael fruit (Aegle Marmelos Correa) shell as an adsorbent. *Journal of Hazardous materials, 168*(2–3), 633-640.

Anees Ahmad, A. A., Rafatullah, M., & Danish, M. (2007). Sorption studies of Zn(II)- and Cd(II)ions from aqueous solution on treated sawdust of sissoo wood. *European Journal of Wood and Wood Products, 65*(6), 429-436.

Aouni, A., Fersi, C., Cuartas-Uribe, B., Bes-Pía, A., Alcaina-Miranda, M. I., & Dhahbi, M. (2012). Reactive dyes rejection and textile effluent treatment study using ultrafiltration and nanofiltration processes. *Desalination, 297*(0), 87-96.

Armenante, P. M. (1997). Precipitation of heavy metals from wastewaters Retrieved 16th January, 2015, from http://cpe.njit.edu/dlnotes/CHE685/Cls06-2.pdf

Arshad, M., Zafar, M. N., Younis, S., & Nadeem, R. (2008). The use of neem biomass for the biosorption of zinc from aqueous solutions. *Journal of Hazardous Materials, 157*(2–3), 534-540.

Arulkumar, M., Sathishkumar, P., & Palvannan, T. (2011). Optimization of Orange G dye adsorption by activated carbon of thespesia populnea pods using response surface methodology. *Journal of Hazardous Materials, 186*(1), 827-834.

Asterion. (2013). Metal hydroxide precipitation, 2015, from http://asterionstc.com/2013/10/metal-hydroxide-precipitation/

Atalay, S., & Ersöz, G. (2015). Advanced oxidation processes for removal of dyes from aqueous media *Green chemistry for dyes removal from wastewater* (pp. 83-117): John Wiley & Sons, Inc.

Athreya, S., & Venkatesh, Y. (2012). Application of Taguchi method for optimization of process parameters in improving the surface roughness of lathe facing operation. *International Refereed Journal of Engineering and Science (IRJES), 1*(3), 13-19.

Baccar, R., Bouzid, J., Feki, M., & Montiel, A. (2009). Preparation of activated carbon from tunisian olive-waste cakes and its application for adsorption of heavy metal ions. *Journal of Hazardous Materials, 162*(2–3), 1522-1529.

Baharuddin, N. H., Sulaiman, N. M. N., & Aroua, M. K. (2015). Removal of heavy metal ions from mixed solutions via polymer-enhanced ultrafiltration using starch as a water-soluble biopolymer. *Environmental Progress & Sustainable Energy, 34*(2), 359-367.

Barman, G., Kumar, A., & Khare, P. (2011). Removal of congo red by carbonized low-cost adsorbents: Process parameter optimization using a Taguchi experimental design. *Journal of Chemical & Engineering Data, 56*(11), 4102-4108.

Bayraktar, E. (2001). Response surface optimization of the separation of dl-tryptophan using an emulsion liquid membrane. *Process Biochemistry, 37*(2), 169-175.

Bhagawan, D., Poodari, S., Pothuraju, T., Srinivasulu, D., Shankaraiah, G., Yamuna Rani, M., et al. (2014). Effect of operational parameters on heavy metal removal by electrocoagulation. *Environmental Science and Pollution Research, 21*(24), 14166-14173.

BioScience, S. (2014). Rpm vs rcf, 2015, from http://www.sorbio.com/index.php/rpm-vs-rcf

BrbootI, M. M., AbiD, B. A., & Al-ShuwaikI, N. M. (2011). Removal of heavy metals using chemicals precipitation. *Engineering and Technology journal, 29*(3), 595-612.

Burns, J. R., & Ramshaw, C. (1996). Process intensification: Visual study of liquid maldistribution in rotating packed beds. *Chemical Engineering Science, 51*(8), 1347-1352.

Camarillo, R., Pérez, Á., Cañizares, P., & de Lucas, A. (2012). Removal of heavy metal ions by polymer enhanced ultrafiltration: Batch process modeling and thermodynamics of complexation reactions. *Desalination, 286*(0), 193-199.

Carmody, O., Frost, R., Xi, Y., & Kokot, S. (2007). Surface characterisation of selected sorbent materials for common hydrocarbon fuels. *Surface Science, 601*(9), 2066-2076.

Chang, C.-F., & Lee, S.-C. (2012). Adsorption behavior of pesticide Methomyl on activated carbon in a high gravity rotating packed bed reactor. *Water Research, 46*(9), 2869-2880.

Chang, Q., & Wang, G. (2007). Study on the macromolecular coagulant PeX which traps heavy metals. *Chemical Engineering Science, 62*(17), 4636-4643.

Chang, Y.-K., Chang, J.-E., Lin, T.-T., & Hsu, Y.-M. (2002). Integrated copper-containing wastewater treatment using xanthate process. *Journal of hazardous materials, 94*(1), 89-99.

Chang, Y.-Y., Yan, Y.-L., Tseng, C.-H., Syu, J.-Y., Lin, W.-Y., & Yuan, Y.-C. (2012). Development of an innovative circulating fluidized-bed with microwave system for controlling NOx. *Aerosol and Air Quality Research, 12*, 379-386.

Charerntanyarak, L. (1999). Heavy metals removal by chemical coagulation and precipitation. *Water Science and Technology, 39*(10–11), 135-138.

Chen, H. M., Guo, H. X., Ma, Y., Qin, Z. P., & Xie, G. L. (2014). Rejection of heavy metal ions with polyelectrolyte composite nanofiltration membrane. *Applied Mechanics and Materials, 529*, 87-91.

Chen, Q., Luo, Z., Hills, C., Xue, G., & Tyrer, M. (2009). Precipitation of heavy metals from wastewater using simulated flue gas: Sequent additions of fly ash, lime and carbon dioxide. *Water Research, 43*(10), 2605-2614.

Chen, S., Yue, Q., Gao, B., Li, Q., Xu, X., & Fu, K. (2012). Adsorption of hexavalent chromium from aqueous solution by modified corn stalk: A fixed-bed column study. *Bioresource Technology, 113*(0), 114-120.

Chen, Y.-H., Huang, Y.-H., Lin, R.-H., & Shang, N.-C. (2010). A continuous-flow biodiesel production process using a rotating packed bed. *Bioresource Technology, 101*(2), 668-673.

Chiang, C.-Y., Chen, Y.-S., Liang, M.-S., Lin, F.-Y., Tai, C. Y.-D., & Liu, H.-S. (2009). Absorption of ethanol into water and glycerol/water solution in a rotating packed bed. *Journal of the Taiwan Institute of Chemical Engineers, 40*(4), 418-423.

Cimino, G., Passerini, A., & Toscano, G. (2000). Removal of toxic cations and Cr(VI) from aqueous solution by hazelnut shell. *Water Research, 34*(11), 2955-2962.

Crini, G. (2006). Non-conventional low-cost adsorbents for dye removal: A review. *Bioresource Technology, 97*(9), 1061-1085.

Cronje, K. J., Chetty, K., Carsky, M., Sahu, J. N., & Meikap, B. C. (2011). Optimization of chromium(VI) sorption potential using developed activated carbon from sugarcane bagasse with chemical activation by zinc chloride. *Desalination, 275*(1–3), 276-284.

Cui, Y., Ge, Q., Liu, X.-Y., & Chung, T.-S. (2014). Novel forward osmosis process to effectively remove heavy metal ions. *Journal of Membrane Science, 467*(0), 188-194.

D. Panias, & Krestou, A. (2004). *Use of microwave energy in metallurgy*. Paper presented at the Advances in Mineral Resources Management and Environmental Geotechnology, Hania, Greece https://www.researchgate.net/publication/234107697_Use_of_Microwave_Energy_in_Metallurgy

Dąbrowski, A. (2001). Adsorption — from theory to practice. *Advances in Colloid and Interface Science, 93*(1–3), 135-224.

Dąbrowski, A., Hubicki, Z., Podkościelny, P., & Robens, E. (2004). Selective removal of the heavy metal ions from waters and industrial wastewaters by ion-exchange method. *Chemosphere, 56*(2), 91-106.

Dada, A., Olalekan, A., Olatunya, A., & DADA, O. (2012). Langmuir, Freundlich, Temkin and Dubinin–Radushkevich isotherms studies of equilibrium sorption of Zn^{2+} unto phosphoric acid modified rice husk. *IOSR Journal of Applied Chemistry, 3*(1), 38-45.

Dakiky, M., Khamis, M., Manassra, A., & Mer'eb, M. (2002). Selective adsorption of chromium(VI) in industrial wastewater using low-cost abundantly available adsorbents. *Advances in Environmental Research, 6*(4), 533-540.

Das, A., Bhowal, A., & Datta, S. (2008). Continuous biosorption in rotating packed-bed contactor. *Industrial & Engineering Chemistry Research, 47*(12), 4230-4235.

de Luna, M. D. G., Flores, E. D., Genuino, D. A. D., Futalan, C. M., & Wan, M.-W. (2013). Adsorption of Eriochrome Black T (EBT) dye using activated carbon prepared from waste rice hulls—optimization, isotherm and kinetic studies. *Journal of the Taiwan Institute of Chemical Engineers, 44*(4), 646-653.

Deng, H., Li, G., Yang, H., Tang, J., & Tang, J. (2010a). Preparation of activated carbons from cotton stalk by microwave assisted KOH and K_2CO_3 activation. *Chemical Engineering Journal, 163*(3), 373-381.

Deng, H., Yang, L., Tao, G., & Dai, J. (2009). Preparation and characterization of activated carbon from cotton stalk by microwave assisted chemical activation—application in methylene blue adsorption from aqueous solution. *Journal of Hazardous Materials, 166*(2–3), 1514-1521.

Deng, H., Zhang, G., Xu, X., Tao, G., & Dai, J. (2010b). Optimization of preparation of activated carbon from cotton stalk by microwave assisted phosphoric acid-chemical activation. *Journal of Hazardous Materials, 182*(1–3), 217-224.

Deng, W., Su, Y., Liu, S., & Shen, H. (2014). Microwave-assisted methane decomposition over pyrolysis residue of sewage sludge for hydrogen production. *International Journal of Hydrogen Energy, 39*(17), 9169-9179.

Dias, J. M., Alvim-Ferraz, M. C. M., Almeida, M. F., Rivera-Utrilla, J., & Sánchez-Polo, M. (2007). Waste materials for activated carbon preparation and its use in aqueous-phase treatment: A review. *Journal of Environmental Management, 85*(4), 833-846.

Dong, Y., Su, Y., Chen, W., Peng, J., Zhang, Y., & Jiang, Z. (2011). Ultrafiltration enhanced with activated carbon adsorption for efficient dye removal from aqueous solution. *Chinese Journal of Chemical Engineering, 19*(5), 863-869.

Doulati Ardejani, F., Badii, K., Limaee, N. Y., Shafaei, S. Z., & Mirhabibi, A. (2008). Adsorption of Direct Red 80 dye from aqueous solution onto almond shells: Effect of pH, initial concentration and shell type. *Journal of hazardous materials, 151*(2), 730-737.

Doulati Ardejani, F., Badii, K., Yousefi Limaee, N., Mahmoodi, N., Arami, M., Shafaei, S., et al. (2007). Numerical modelling and laboratory studies on the removal of Direct Red 23 and Direct Red 80 dyes from textile effluents using orange peel, a low-cost adsorbent. *Dyes and pigments, 73*(2), 178-185.

Dural, M. U., Cavas, L., Papageorgiou, S. K., & Katsaros, F. K. (2011). Methylene blue adsorption on activated carbon prepared from posidonia oceanica (l.) dead leaves: Kinetics and equilibrium studies. *Chemical Engineering Journal, 168*(1), 77-85.

El-Hendawy, A.-N. A., Alexander, A. J., Andrews, R. J., & Forrest, G. (2008). Effects of activation schemes on porous, surface and thermal properties of activated carbons prepared from cotton stalks. *Journal of Analytical and Applied Pyrolysis, 82*(2), 272-278.

El Samrani, A. G., Lartiges, B. S., & Villiéras, F. (2008). Chemical coagulation of combined sewer overflow: Heavy metal removal and treatment optimization. *Water Research, 42*(4–5), 951-960.

Emami, Z., & Azizian, S. (2014). Preparation of activated carbon from date sphate using microwave irradiation and investigation of its capability for removal of dye pollutant from aqueous media. *Journal of Analytical and Applied Pyrolysis, 108*(0), 176-184.

EPA, U. (2000). Wastewater technology fact sheet Retrieved 16th January 2015, from http://water.epa.gov/scitech/wastetech/upload/2002_06_28_mtb_chemical_precipitation.pdf

Fidalgo, B., Fernández, Y., Domínguez, A., Pis, J. J., & Menéndez, J. A. (2008). Microwave-assisted pyrolysis of CH_4/N_2 mixtures over activated carbon. *Journal of Analytical and Applied Pyrolysis, 82*(1), 158-162.

Fidalgo, B., & Menéndez, J. (2012). Study of energy consumption in a laboratory pilot plant for the microwave-assisted CO_2 reforming of CH_4. *Fuel processing technology, 95*, 55-61.

Foo, K. Y., & Hameed, B. H. (2011a). Microwave-assisted preparation of oil palm fiber activated carbon for methylene blue adsorption. *Chemical Engineering Journal, 166*(2), 792-795.

Foo, K. Y., & Hameed, B. H. (2011b). Microwave assisted preparation of activated carbon from pomelo skin for the removal of anionic and cationic dyes. *Chemical Engineering Journal, 173*(2), 385-390.

Foo, K. Y., & Hameed, B. H. (2011c). Preparation and characterization of activated carbon from pistachio nut shells via microwave-induced chemical activation. *Biomass and Bioenergy, 35*(7), 3257-3261.

Foo, K. Y., & Hameed, B. H. (2011d). Preparation and characterization of activated carbon from sunflower seed oil residue via microwave assisted K_2CO_3 activation. *Bioresour Technol, 102*(20), 9794-9799.

Foo, K. Y., & Hameed, B. H. (2011e). Preparation of oil palm (elaeis) empty fruit bunch activated carbon by microwave-assisted KOH activation for the adsorption of methylene blue. *Desalination, 275*(1–3), 302-305.

Foo, K. Y., & Hameed, B. H. (2011f). Utilization of rice husks as a feedstock for preparation of activated carbon by microwave induced KOH and K_2CO_3 activation. *Bioresource Technology, 102*(20), 9814-9817.

Foo, K. Y., & Hameed, B. H. (2012a). Microwave-assisted preparation and adsorption performance of activated carbon from biodiesel industry solid reside: Influence of operational parameters. *Bioresource Technology, 103*(1), 398-404.

Foo, K. Y., & Hameed, B. H. (2012b). Porous structure and adsorptive properties of pineapple peel based activated carbons prepared via microwave assisted KOH and K_2CO_3 activation. *Microporous and Mesoporous Materials, 148*(1), 191-195.

Foo, K. Y., & Hameed, B. H. (2012c). Preparation, characterization and evaluation of adsorptive properties of orange peel based activated carbon via microwave induced K_2CO_3 activation. *Bioresource Technology, 104*(0), 679-686.

Fu, F., & Wang, Q. (2011). Removal of heavy metal ions from wastewaters: A review. *Journal of Environmental Management, 92*(3), 407-418.

Gao, H., Liu, Y., Zeng, G., Xu, W., Li, T., & Xia, W. (2008). Characterization of Cr(VI) removal from aqueous solutions by a surplus agricultural waste—rice straw. *Journal of Hazardous materials, 150*(2), 446-452.

Gao, J., Sun, S.-P., Zhu, W.-P., & Chung, T.-S. (2014). Chelating polymer modified P84 nanofiltration (nf) hollow fiber membranes for high efficient heavy metal removal. *Water Research, 63*(0), 252-261.

Ghaedi, A. M., Ghaedi, M., Vafaei, A., Iravani, N., Keshavarz, M., Rad, M., et al. (2015). Adsorption of copper(II) using modified activated carbon prepared from pomegranate wood: Optimization by bee algorithm and response surface methodology. *Journal of Molecular Liquids, 206*, 195-206.

Gherasim, C.-V., Bourceanu, G., Olariu, R.-I., & Arsene, C. (2011). A novel polymer inclusion membrane applied in chromium(VI) separation from aqueous solutions. *Journal of Hazardous materials, 197*(0), 244-253.

Ghoreishi, S. M., & Haghighi, R. (2003). Chemical catalytic reaction and biological oxidation for treatment of non-biodegradable textile effluent. *Chemical Engineering Journal, 95*(1–3), 163-169.

Ghosh, P., Samanta, A. N., & Ray, S. (2011). Reduction of cod and removal of Zn^{2+} from rayon industry wastewater by combined electro-fenton treatment and chemical precipitation. *Desalination, 266*(1–3), 213-217.

Gode, F., & Pehlivan, E. (2006). Removal of chromium(III) from aqueous solutions using Lewatit S 100: The effect of pH, time, metal concentration and temperature. *Journal of Hazardous Materials*, *136*(2), 330-337.

Gottipati, R., & Mishra, S. (2010a). Process optimization of adsorption of Cr(VI) on activated carbons prepared from plant precursors by a two-level full factorial design. *Chemical Engineering Journal, 160*(1), 99-107.

Gottipati, R., & Mishra, S. (2010b). Process optimization of adsorption of Cr(VI) on activated carbons prepared from plant precursors by a two-level full factorial design. *Chemical Engineering Journal, 160*(1), 99-107.

Guo, Z.-R., Zhang, G., Fang, J., & Dou, X. (2006). Enhanced chromium recovery from tanning wastewater. *Journal of Cleaner Production, 14*(1), 75-79.

Gupta, V. K., Agarwal, S., & Saleh, T. A. (2011a). Chromium removal by combining the magnetic properties of iron oxide with adsorption properties of carbon nanotubes. *Water Research, 45*(6), 2207-2212.

Gupta, V. K., Ali, I., Saleh, T. A., Nayak, A., & Agarwal, S. (2012a). Chemical treatment technologies for waste-water recycling-an overview. *RSC Advances, 2*(16), 6380-6388.

Gupta, V. K., Jain, R., Agarwal, S., Nayak, A., & Shrivastava, M. (2012b). Photodegradation of hazardous dye quinoline yellow catalyzed by TiO_2. *Journal of Colloid and Interface Science, 366*(1), 135-140.

Gupta, V. K., Jain, R., Agarwal, S., & Shrivastava, M. (2011b). Kinetics of photo-catalytic degradation of hazardous dye tropaeoline 000 using UV/TiO_2 in a UV reactor. *Colloids and Surfaces A: Physicochemical and Engineering Aspects, 378*(1–3), 22-26.

Gupta, V. K., Jain, R., Nayak, A., Agarwal, S., & Shrivastava, M. (2011c). Removal of the hazardous dye—tartrazine by photodegradation on titanium dioxide surface. *Materials Science and Engineering: C, 31*(5), 1062-1067.

Gupta, V. K., & Rastogi, A. (2008). Sorption and desorption studies of chromium(vi) from nonviable cyanobacterium nostoc muscorum biomass. *Journal of Hazardous Materials, 154*(1–3), 347-354.

Hameed, B., Din, A. M., & Ahmad, A. (2007). Adsorption of methylene blue onto bamboo-based activated carbon: Kinetics and equilibrium studies. *Journal of Hazardous materials, 141*(3), 819-825.

Hankins, N. P., Lu, N., & Hilal, N. (2006). Enhanced removal of heavy metal ions bound to humic acid by polyelectrolyte flocculation. *Separation and Purification Technology, 51*(1), 48-56.

Hasan, S., Hashim, M. A., & Gupta, B. S. (2000). Adsorption of Ni(SO_4) on Malaysian rubber-wood ash. *Bioresource Technology, 72*(2), 153-158.

Hashemian, S., & Foroghimoqhadam, A. (2014). Effect of copper doping on $CoTiO_3$ ilmenite type nanoparticles for removal of congo red from aqueous solution. [Article]. *Chemical Engineering Journal, 235*, 299-306.

Haswell, S. J., & Howarth, N. (1999). Perturbation of a solid phase separation process by a non-thermal microwave effect. *Analytica Chimica Acta, 387*(2), 113-120.

Hesas, R. H., Arami-Niya, A., Daud, W. M. A. W., & Sahu, J. (2013). Preparation and characterization of activated carbon from apple waste by microwave-assisted phosphoric acid activation: Application in methylene blue adsorption. *BioResources, 8*(2), 2950-2966.

Hoseinzadeh Hesas, R., Arami-Niya, A., Wan Daud, W. M. A., & Sahu, J. N. Preparation of granular activated carbon from oil palm shell by microwave-induced chemical activation: Optimisation using surface response methodology. *Chemical Engineering Research and Design*(in press).

Hoseinzadeh Hesas, R., Arami-Niya, A., Wan Daud, W. M. A., & Sahu, J. N. (2013a). Comparison of oil palm shell-based activated carbons produced by microwave and conventional heating methods using zinc chloride activation. *Journal of Analytical and Applied Pyrolysis, 104*(0), 176-184.

Hoseinzadeh Hesas, R., Arami-Niya, A., Wan Daud, W. M. A., & Sahu, J. N. (2013b). Preparation of granular activated carbon from oil palm shell by microwave-induced chemical activation: Optimisation using surface response methodology. *Chemical Engineering Research and Design, 91*(12), 2447-2456.

Hoseinzadeh Hesas, R., Wan Daud, W. M. A., Sahu, J. N., & Arami-Niya, A. (2013c). The effects of a microwave heating method on the production of activated carbon from agricultural waste: A review. *Journal of Analytical and Applied Pyrolysis, 100*(0), 1-11.

Hsu, L.-J., & Lin, C.-C. (2012). Binary VOCs absorption in a rotating packed bed with blade packings. *Journal of Environmental Management, 98*(0), 175-182.

Huang, L., Sun, Y., Wang, W., Yue, Q., & Yang, T. (2011). Comparative study on characterization of activated carbons prepared by microwave and conventional heating methods and application in removal of oxytetracycline (OTC). *Chemical Engineering Journal, 171*(3), 1446-1453.

Jassim, M. S., Rochelle, G., Eimer, D., & Ramshaw, C. (2007). Carbon dioxide absorption and desorption in aqueous monoethanolamine solutions in a rotating packed bed. *Industrial & Engineering Chemistry Research, 46*(9), 2823-2833.

Jiang, X., Liu, Y., & Gu, M. (2011). Absorption of sulphur dioxide with sodium citrate buffer solution in a rotating packed bed. *Chinese Journal of Chemical Engineering, 19*(4), 687-692.

Jones, D. A., Lelyveld, T. P., Mavrofidis, S. D., Kingman, S. W., & Miles, N. J. (2002). Microwave heating applications in environmental engineering—a review. *Resources, Conservation and Recycling, 34*(2), 75-90.

Kanagaraj, J., & Mandal, A. (2012). Combined biodegradation and ozonation for removal of tannins and dyes for the reduction of pollution loads. *Environmental Science and Pollution Research, 19*(1), 42-52.

Kanagaraj, P., Nagendran, A., Rana, D., Matsuura, T., Neelakandan, S., Karthikkumar, T., et al. (2015). Influence of n-phthaloyl chitosan on poly (ether imide) ultrafiltration membranes and its application in biomolecules and toxic heavy metal ion separation and their antifouling properties. *Applied Surface Science, 329*(0), 165-173.

Kang, S.-Y., Lee, J.-U., Moon, S.-H., & Kim, K.-W. (2004). Competitive adsorption characteristics of Co^{2+}, Ni^{2+}, and Cr^{3+} by IRN-77 cation exchange resin in synthesized wastewater. *Chemosphere, 56*(2), 141-147.

Kappe, C. O., Stadler, A., & Dallinger, D. (2012). *Microwaves in organic and medicinal chemistry*: John Wiley & Sons.

Karacan, F., Ozden, U., & Karacan, S. (2007). Optimization of manufacturing conditions for activated carbon from turkish lignite by chemical activation using response surface methodology. *Applied Thermal Engineering, 27*(7), 1212-1218.

Karimi, L., Zohoori, S., & Yazdanshenas, M. E. (2014). Photocatalytic degradation of azo dyes in aqueous solutions under uv irradiation using nano-strontium titanate as the nanophotocatalyst. *Journal of Saudi Chemical Society, 18*(5), 581-588.

Kavand, M., Kaghazchi, T., & Soleimani, M. (2014). Optimization of parameters for competitive adsorption of heavy metal ions (Pb^{+2}, Ni^{+2}, Cd^{+2}) onto activated carbon. [journal article]. *Korean Journal of Chemical Engineering, 31*(4), 692-700.

Kelleher, T., & Fair, J. R. (1996). Distillation studies in a high-gravity contactor. [doi: 10.1021/ie950662a]. *Industrial & Engineering Chemistry Research, 35*(12), 4646-4655.

Khan, M. A., Ngabura, M., Choong, T. S. Y., Masood, H., & Chuah, L. A. (2012). Biosorption and desorption of nickel on oil cake: Batch and column studies. *Bioresource Technology, 103*(1), 35-42.

Kiil, S., Michelsen, M. L., & Dam-Johansen, K. (1998). Experimental investigation and modeling of a wet flue gas desulfurization pilot plant. *Industrial & Engineering Chemistry Research, 37*(7), 2792-2806.

Kiran, B., Kaushik, A., & Kaushik, C. P. (2007). Response surface methodological approach for optimizing removal of Cr (VI) from aqueous solution using immobilized cyanobacterium. *Chemical Engineering Journal, 126*(2–3), 147-153.

Kirby, E. D. (2006). A parameter design study in a turning operation using the taguchi method. 1-14.

Kong, Y., & Cha, C. Y. (1995). NOx abatement with carbon adsorbents and microwave energy. *Energy & fuels, 9*(6), 971-975.

Kongsricharoern, N., & Polprasert, C. (1995). Electrochemical precipitation of chromium (Cr^{6+}) from an electroplating wastewater. *Water Science and Technology, 31*(9), 109-117.

Körbahti, B. K., Artut, K., Geçgel, C., & Özer, A. (2011). Electrochemical decolorization of textile dyes and removal of metal ions from textile dye and metal ion binary mixtures. *Chemical Engineering Journal, 173*(3), 677-688.

Kosińska, K., & Miśkiewicz, T. (2012). Precipitation of heavy metals from industrial wastewater by desulfovibrio desulfuricans. *Environment Protection Engineering, 38*(2).

Ku, Y., & Jung, I.-L. (2001). Photocatalytic reduction of Cr (VI) in aqueous solutions by UV irradiation with the presence of titanium dioxide. *Water Research, 35*(1), 135-142.

Kubota, M., Hata, A., & Matsuda, H. (2009). Preparation of activated carbon from phenolic resin by koh chemical activation under microwave heating. *Carbon, 47*(12), 2805-2811.

Kumar, M. P. S., & Phanikumar, B. R. (2012). Response surface modelling of Cr^{6+} adsorption from aqueous solution by neem bark powder: Box–behnken experimental approach. *Environmental Science and Pollution Research*, 1-17.

Kundu, A., Redzwan, G., Sahu, J. N., Mukherjee, S., Gupta, B. S., & Hashim, M. A. (2014a). Hexavalent chromium adsorption by a novel activated carbon prepared by microwave activation. *BioResources, 9*(1), 1498-1518.

Kundu, A., Sen Gupta, B., Hashim, M. A., & Redzwan, G. (2014b). Taguchi optimization approach for production of activated carbon from phosphoric acid impregnated palm kernel shell by microwave heating. *Journal of Cleaner Production*.

Kushwaha, S., Sodaye, S., & Padmaja, P. (2008). *Equilibrium, kinetics and thermodynamic studies for adsorption of Hg (II) on palm shell powder.* Paper presented at the Proceedings of World Academy of Science, Engineering and Technology.

Landaburu-Aguirre, J., Pongrácz, E., Sarpola, A., & Keiski, R. L. (2012). Simultaneous removal of heavy metals from phosphorous rich real wastewaters by micellar-enhanced ultrafiltration. *Separation and Purification Technology, 88*(0), 130-137.

Li, H., Deng, Z., Wu, T., Liu, R., Loewen, S., & Tsao, R. (2012). Microwave-assisted extraction of phenolics with maximal antioxidant activities in tomatoes. *Food Chemistry, 130*(4), 928-936.

Li, K., Zheng, Z., & Li, Y. (2010a). Characterization and lead adsorption properties of activated carbons prepared from cotton stalk by one-step H_3PO_4 activation. *Journal of Hazardous Materials, 181*(1–3), 440-447.

Li, W., Zhang, L.-b., Peng, J.-h., Li, N., & Zhu, X.-y. (2008). Preparation of high surface area activated carbons from tobacco stems with K_2CO_3 activation using microwave radiation. *Industrial Crops and Products*, *27*(3), 341-347.

Li, Y., Fabiano-Tixier, A. S., Vian, M. A., & Chemat, F. (2013). Solvent-free microwave extraction of bioactive compounds provides a tool for green analytical chemistry. *TrAC Trends in Analytical Chemistry, 47*, 1-11.

Li, Y., Liu, Y., Zhang, L., Su, Q., & Jin, G. (2010b). Absorption of nox into nitric acid solution in rotating packed bed. *Chinese Journal of Chemical Engineering, 18*(2), 244-248.

Lidström, P., Tierney, J., Wathey, B., & Westman, J. (2001). Microwave assisted organic synthesis—a review. *Tetrahedron, 57*(45), 9225-9283.

Lin, C.-C., & Chen, B.-C. (2011). Carbon dioxide absorption in a cross-flow rotating packed bed. *Chemical Engineering Research and Design, 89*(9), 1722-1729.

Lin, C.-C., Ho, J.-M., & Hsieh, H.-L. (2012). Feasibility of using a rotating packed bed in preparing Fe_3O_4 nanoparticles. *Chemical Engineering Journal, 203*(0), 88-94.

Lin, C.-C., Lin, Y.-H., & Tan, C.-S. (2010a). Evaluation of alkanolamine solutions for carbon dioxide removal in cross-flow rotating packed beds. *Journal of Hazardous Materials, 175*(1–3), 344-351.

Lin, C.-C., & Liu, H.-S. (1999). Adsorption in a centrifugal field: Basic dye adsorption by activated carbon. *Industrial & Engineering Chemistry Research, 39*(1), 161-167.

Lin, L., Yuan, S., Chen, J., Wang, L., Wan, J., & Lu, X. (2010b). Treatment of chloramphenicol-contaminated soil by microwave radiation. *Chemosphere, 78*(1), 66-71.

Liu, Q.-S., Zheng, T., Wang, P., & Guo, L. (2010). Preparation and characterization of activated carbon from bamboo by microwave-induced phosphoric acid activation. *Industrial Crops and Products, 31*(2), 233-238.

Liu, Y., Yan, J., Yuan, D., Li, Q., & Wu, X. (2013). The study of lead removal from aqueous solution using an electrochemical method with a stainless steel net electrode coated with single wall carbon nanotubes. *Chemical Engineering Journal, 218*(0), 81-88.

Lubarda, V. (2013). The shape of a liquid surface in a uniformly rotating cylinder in the presence of surface tension. *Acta Mechanica, 224*(7), 1365-1382.

Luo, Y., Chu, G.-W., Zou, H.-K., Wang, F., Xiang, Y., Shao, L., et al. (2012). Mass transfer studies in a rotating packed bed with novel rotors: Chemisorption of CO_2. *Industrial & Engineering Chemistry Research, 51*(26), 9164-9172.

Machida, M., Kikuchi, Y., Aikawa, M., & Tatsumoto, H. (2004). Kinetics of adsorption and desorption of pb(ii) in aqueous solution on activated carbon by two-site adsorption model. *Colloids and Surfaces A: Physicochemical and Engineering Aspects, 240*(1–3), 179-186.

Maher, A., Sadeghi, M., & Moheb, A. (2014). Heavy metal elimination from drinking water using nanofiltration membrane technology and process optimization using response surface methodology. *Desalination, 352*(0), 166-173.

Mahmoodi, N. M. (2011). Photocatalytic ozonation of dyes using copper ferrite nanoparticle prepared by co-precipitation method. *Desalination, 279*(1–3), 332-337.

Mahmoodi, N. M. (2013). Photocatalytic ozonation of dyes using multiwalled carbon nanotube. *Journal of Molecular Catalysis A: Chemical, 366*(0), 254-260.

Mahmoud, A., & Hoadley, A. F. A. (2012). An evaluation of a hybrid ion exchange electrodialysis process in the recovery of heavy metals from simulated dilute industrial wastewater. *Water Research, 46*(10), 3364-3376.

Malkoc, E., Nuhoglu, Y., & Dundar, M. (2006). Adsorption of chromium(VI) on pomace—an olive oil industry waste: Batch and column studies. *Journal of Hazardous Materials, 138*(1), 142-151.

Manivannan, N., Balachandran, W., Beleca, R., & Abbod, M. (2015). Microwave plasma system design and modelling for marine diesel exhaust gas abatement of NOx and SOx.

Marsh, H., & Reinoso, F. R. (2006). *Activated carbon*: Elsevier.

Mata, Y. N., Blázquez, M. L., Ballester, A., González, F., & Muñoz, J. A. (2010). Studies on sorption, desorption, regeneration and reuse of sugar-beet pectin gels for heavy metal removal. *Journal of Hazardous Materials, 178*(1–3), 243-248.

Matlock, M. M., Howerton, B. S., Van Aelstyn, M. A., Nordstrom, F. L., & Atwood, D. A. (2002). Advanced mercury removal from gold leachate solutions prior to gold and silver extraction: A field study from an active gold mine in peru. *Environmental Science & Technology, 36*(7), 1636-1639.

Maurya, S. K., Parashuram, K., Singh, P. S., Ray, P., & Reddy, A. V. R. (2012). Preparation of polysulfone–polyamide thin film composite hollow fiber nanofiltration membranes and their performance in the treatment of aqueous dye solutions. *Desalination, 304*(0), 11-19.

Mehrasbi, M. R., Farahmandkia, Z., Taghibeigloo, B., & Taromi, A. (2009). Adsorption of lead and cadmium from aqueous solution by using almond shells. *Water, Air, and Soil Pollution, 199*(1-4), 343-351.

Menéndez, J. A., Arenillas, A., Fidalgo, B., Fernández, Y., Zubizarreta, L., Calvo, E. G., et al. (2010). Microwave heating processes involving carbon materials. *Fuel Processing Technology, 91*(1), 1-8.

Mezzanotte, V., Fornaroli, R., Canobbio, S., Zoia, L., & Orlandi, M. (2013). Colour removal and carbonyl by-production in high dose ozonation for effluent polishing. *Chemosphere, 91*(5), 629-634.

Mohanty, K., Jha, M., Meikap, B. C., & Biswas, M. N. (2005). Removal of chromium (VI) from dilute aqueous solutions by activated carbon developed from terminalia arjuna nuts activated with zinc chloride. *Chemical Engineering Science, 60*(11), 3049-3059.

Mondal, A., Pramanik, A., Bhowal, A., & Datta, S. (2012). Distillation studies in rotating packed bed with split packing. *Chemical Engineering Research and Design, 90*(4), 453-457.

Montgomery, D. C., Montgomery, D. C., & Montgomery, D. C. (1984). *Design and analysis of experiments* (Vol. 7): Wiley New York.

Motasemi, F., & Afzal, M. T. (2013). A review on the microwave-assisted pyrolysis technique. *Renewable and Sustainable Energy Reviews, 28*(0), 317-330.

Mukherjee, S., Pariatamby, A., Sahu, J. N., & Gupta, B. S. (2013). Clarification of rubber mill wastewater by a plant based biopolymer- comparison with common inorganic coagulants. *Journal of Chemical Technology & Biotechnology*, n/a-n/a.

Mun, S., Cho, S.-H., Kim, T.-S., Oh, B.-T., & Yoon, J. (2009). Inactivation of ascaris eggs in soil by microwave treatment compared to uv and ozone treatment. *Chemosphere, 77*(2), 285-290.

Mungasavalli, D. P., Viraraghavan, T., & Jin, Y.-C. (2007). Biosorption of chromium from aqueous solutions by pretreated aspergillus niger: Batch and column studies. *Colloids and Surfaces A: Physicochemical and Engineering Aspects, 301*(1–3), 214-223.

Nabais, J. M. V., Laginhas, C. E. C., Carrott, P. J. M., & Ribeiro Carrott, M. M. L. (2011). Production of activated carbons from almond shell. *Fuel Processing Technology, 92*(2), 234-240.

Naiya, T. K., Chowdhury, P., Bhattacharya, A. K., & Das, S. K. (2009). Saw dust and neem bark as low-cost natural biosorbent for adsorptive removal of Zn (II) and Cd (II) ions from aqueous solutions. *Chemical Engineering Journal, 148*(1), 68-79.

Ng, C. M., Chen, P. C., & Manickam, S. (2012). Green high-gravitational synthesis of silver nanoparticles using a rotating packed bed reactor (RPBR). *Industrial & Engineering Chemistry Research, 51*(15), 5375-5381.

Njikam, E., & Schiewer, S. (2012). Optimization and kinetic modeling of cadmium desorption from citrus peels: A process for biosorbent regeneration. *Journal of Hazardous Materials, 213–214*(0), 242-248.

Njoku, V. O., Foo, K. Y., Asif, M., & Hameed, B. H. (2014). Preparation of activated carbons from rambutan (*Nephelium lappaceum*) peel by microwave-induced KOH activation for acid yellow 17 dye adsorption. *Chemical Engineering Journal, 250*(0), 198-204.

Norit-AC. Retrieved 15/07/2012, from http://www.norit-ac.com/english/activatedcarbon.asp?submenuCat=introduction

O'Neill, C., Hawkes, F. R., Hawkes, D. L., Lourenço, N. D., Pinheiro, H. M., & Delée, W. (1999). Colour in textile effluents – sources, measurement, discharge consents and simulation: A review. *Journal of Chemical Technology & Biotechnology, 74*(11), 1009-1018.

Owlad, M., Aroua, M. K., & Wan Daud, W. M. A. (2010). Hexavalent chromium adsorption on impregnated palm shell activated carbon with polyethyleneimine. *Bioresource Technology, 101*(14), 5098-5103.

Özverdi, A., & Erdem, M. (2006). Cu^{2+}, Cd^{2+} and Pb^{2+} adsorption from aqueous solutions by pyrite and synthetic iron sulphide. *Journal of Hazardous Materials, 137*(1), 626-632.

Panda, M., Bhowal, A., & Datta, S. (2011). Removal of hexavalent chromium by biosorption process in rotating packed bed. *Environmental Science & Technology, 45*(19), 8460-8466.

Pang, F. M., Kumar, P., Teng, T. T., Mohd Omar, A. K., & Wasewar, K. L. (2011). Removal of lead, zinc and iron by coagulation–flocculation. *Journal of the Taiwan Institute of Chemical Engineers, 42*(5), 809-815.

Pasquet, V., Chérouvrier, J.-R., Farhat, F., Thiéry, V., Piot, J.-M., Bérard, J.-B., et al. (2011). Study on the microalgal pigments extraction process: Performance of microwave assisted extraction. *Process Biochemistry, 46*(1), 59-67.

Pehlivan, E., & Cetin, S. (2009). Sorption of Cr(VI) ions on two lewatit-anion exchange resins and their quantitative determination using uv–visible spectrophotometer. *Journal of Hazardous Materials, 163*(1), 448-453.

Phadke, M. S. (2009). *Quality engineering using robust design* (2nd ed.): Pearson.

Pham, D. T., & Castellani, M. (2009). The bees algorithm: Modelling foraging behaviour to solve continuous optimization problems. *Proceedings of the Institution of Mechanical Engineers, Part C: Journal of Mechanical Engineering Science, 223*(12), 2919-2938.

Pinilla, J., Torres, D., Lázaro, M., Suelves, I., Moliner, R., Canadas, I., et al. (2012). Metallic and carbonaceous–based catalysts performance in the solar catalytic decomposition of methane for hydrogen and carbon production. *international journal of hydrogen energy, 37*(12), 9645-9655.

Prakash, S., Rajesh, A. M., & Shahi, V. K. (2011). Chlorine-tolerant poly electrolyte membrane for electrochemical dye degradation. *Chemical Engineering Journal, 168*(1), 108-114.

Prasad, A. G. D., & Abdullah, M. A. (2010). Biosorption of Cr (VI) from synthetic wastewater using the fruit shell of gulmohar (*Delonix regia*): Application to electroplating wastewater. *BioResources, 5*(2), 838-853.

Qiu, Y.-R., & Mao, L.-J. (2013). Removal of heavy metal ions from aqueous solution by ultrafiltration assisted with copolymer of maleic acid and acrylic acid. *Desalination, 329*(0), 78-85.

Rafatullah, M., Sulaiman, O., Hashim, R., & Ahmad, A. (2010a). Adsorption of copper (II) onto different adsorbents. [doi: 10.1080/01932690903224003]. *Journal of Dispersion Science and Technology, 31*(7), 918-930.

Rafatullah, M., Sulaiman, O., Hashim, R., & Ahmad, A. (2010b). Adsorption of methylene blue on low-cost adsorbents: A review. *Journal of Hazardous Materials, 177*(1–3), 70-80.

Ramshaw, C., & Mallinson, R. H. (1981). USA Patent No.: U. S. Patent.

Rao, D. P., Bhowal, A., & Goswami, P. S. (2004). Process intensification in rotating packed beds (HIGEE): An appraisal. *Industrial & Engineering Chemistry Research, 43*(4), 1150-1162.

Ravikumar, K., & Sheeja, A. (2013). Heavy metal removal from water using moringa oleifera seed coagulant and double filtration. *International Journal of Scientific & Engineering Research,, 4*(5), 10-13.

Robinson, J. P., Kingman, S. W., Snape, C. E., Shang, H., Barranco, R., & Saeid, A. (2009). Separation of polyaromatic hydrocarbons from contaminated soils using microwave heating. *Separation and Purification Technology, 69*(3), 249-254.

Robinson, T., McMullan, G., Marchant, R., & Nigam, P. (2001). Remediation of dyes in textile effluent: A critical review on current treatment technologies with a proposed alternative. *Bioresource Technology, 77*(3), 247-255.

Rosales, E., Pazos, M., & Sanromán, M. A. (2011). Comparative efficiencies of the decolourisation of leather dyes by enzymatic and electrochemical treatments. *Desalination, 278*(1–3), 312-317.

Rosales, E., Pazos, M., Sanromán, M. A., & Tavares, T. (2012). Application of zeolite-arthrobacter viscosus system for the removal of heavy metal and dye: Chromium and Azure b. *Desalination, 284*(0), 150-156.

Rouquerol, J., Avnir, D., Fairbridge, C., Everett, D., Haynes, J., Pernicone, N., et al. (1994). Recommendations for the characterization of porous solids (technical report). *Pure and Applied Chemistry, 66*(8), 1739.

Routray, W., & Orsat, V. (2012). Microwave-assisted extraction of flavonoids: A review. *Food and Bioprocess Technology, 5*(2), 409-424.

Rozada, F., Otero, M., Morán, A., & García, A. I. (2005). Activated carbons from sewage sludge and discarded tyres: Production and optimization. *Journal of Hazardous Materials, 124*(1–3), 181-191.

Rubio, J., Souza, M. L., & Smith, R. W. (2002). Overview of flotation as a wastewater treatment technique. *Minerals Engineering, 15*(3), 139-155.

Sahu, J. N., Acharya, J., Sahoo, B. K., & Meikap, B. C. (2016). Optimization of lead (II) sorption potential using developed activated carbon from tamarind wood with chemical activation by zinc chloride. *Desalination and Water Treatment, 57*(5), 2006-2017.

San Miguel, G., Fowler, G. D., & Sollars, C. J. (2003). A study of the characteristics of activated carbons produced by steam and carbon dioxide activation of waste tyre rubber. *Carbon, 41*(5), 1009-1016.

Sarin, V., & Pant, K. (2006). Removal of chromium from industrial waste by using eucalyptus bark. *Bioresource Technology, 97*(1), 15-20.

Scala, F., D'Ascenzo, M., & Lancia, A. (2004). Modeling flue gas desulfurization by spray-dry absorption. *Separation and Purification Technology, 34*(1–3), 143-153.

Selvi, K., Pattabhi, S., & Kadirvelu, K. (2001). Removal of Cr(VI) from aqueous solution by adsorption onto activated carbon. *Bioresource Technology, 80*(1), 87-89.

Sen Gupta, B., & Ako, J. (2005). Application of guar gum as a flocculant aid in food processing and potable water treatment. *European Food Research and Technology, 221*(6), 746-751.

Sen, R., & Swaminathan, T. (2004). Response surface modeling and optimization to elucidate and analyze the effects of inoculum age and size on surfactin production. [doi: 10.1016/j.bej.2004.06.006]. *Biochemical Engineering Journal, 21*(2), 141-148.

Senthilkumar, S., Basha, C. A., Perumalsamy, M., & Prabhu, H. J. (2012). Electrochemical oxidation and aerobic biodegradation with isolated bacterial strains for dye wastewater: Combined and integrated approach. *Electrochimica Acta, 77*(0), 171-178.

Siboni, M. S., Azizian, S., & Lee, S. (2011). The removal of hexavalent chromium from aqueous solutions using modified holly sawdust: Equilibrium and kinetics studies. *Environmental Engineering Research, 16*(2), 55-60.

Singh, K., & Arora, S. (2011). Removal of synthetic textile dyes from wastewaters: A critical review on present treatment technologies. *Critical Reviews in Environmental Science and Technology, 41*(9), 807-878.

Sittig, M. (1991). *Handbook of toxic and hazardous chemicals.* (3rd ed.). Park Ridge, NJ: Noyes Publications.

Srivastava, R., & Rupainwar, D. (2011). A comparative evaluation for adsorption of dye on neem bark and mango bark powder. *Indian Journal of Chemical Technology, 18*, 67-75.

Stankiewicz, A. I., & Moulijn, J. A. (2000). Process intensification: Transforming chemical engineering. *Chemical Engineering Progress, 96*(1), 22-34.

Suksabye, P., Thiravetyan, P., & Nakbanpote, W. (2008). Column study of chromium(VI) adsorption from electroplating industry by coconut coir pith. *J Hazard Mater, 160*(1), 56-62.

Sun, B.-C., Wang, X.-M., Chen, J.-M., Chu, G.-W., Chen, J.-F., & Shao, L. (2011). Synthesis of nano-$CaCO_3$ by simultaneous absorption of CO_2 and NH_3 into $CaCl_2$

solution in a rotating packed bed. *Chemical Engineering Journal, 168*(2), 731-736.

Sun, C., & Liu, H. (2008). Application of non-ionic surfactant in the microwave-assisted extraction of alkaloids from *Rhizoma coptidis*. *Analytica chimica acta, 612*(2), 160-164.

Sun, Q., & Yang, L. (2003). The adsorption of basic dyes from aqueous solution on modified peat–resin particle. *Water Research, 37*(7), 1535-1544.

Sun, W., Wu, Z., Li, Y., & Tan, T. (2002). Sodium-enhanced limestone wet fgd in rotating-stream tray scrubber. *Huan Jing Ke Xue, 23*(5), 105-108.

Tan, K. F., Chu, K. H., Sen Gupta, B., & Hashim, M. A. (2002). Studies on fixed-bed biosorption and elution of copper using polyvinyl alcohol-immobilized seaweed biomass. *Journal of Environmental Science and Health, Part A, 37*(9), 1621-1632.

Tay, T., Ucar, S., & Karagöz, S. (2009). Preparation and characterization of activated carbon from waste biomass. *Journal of Hazardous Materials, 165*(1–3), 481-485.

Tchobanoglous, G., & Burton, F. L. (1991). Wastewater engineering. *MANAGEMENT, 7*, 1-4.

Teo, C. C., Chong, W. P. K., & Ho, Y. S. (2013). Development and application of microwave-assisted extraction technique in biological sample preparation for small molecule analysis. *Metabolomics, 9*(5), 1109-1128.

Thong, Z., Han, G., Cui, Y., Gao, J., Chung, T.-S., Chan, S. Y., et al. (2014). Novel nanofiltration membranes consisting of a sulfonated pentablock copolymer rejection layer for heavy metal removal. *Environmental Science & Technology, 48*(23), 13880-13887.

Thostenson, E. T., & Chou, T. W. (1999). Microwave processing: Fundamentals and applications. *Composites Part A: Applied Science and Manufacturing, 30*(9), 1055-1071.

Tung, H.-H., & Mah, R. S. H. (1985). Modeling liquid mass transfer in higee separation process. *Chemical Engineering Communications, 39*(1-6), 147-153.

Turhan, K., Durukan, I., Ozturkcan, S. A., & Turgut, Z. (2012). Decolorization of textile basic dye in aqueous solution by ozone. *Dyes and Pigments, 92*(3), 897-901.

Vahid, B., & Khataee, A. (2013). Photoassisted electrochemical recirculation system with boron-doped diamond anode and carbon nanotubes containing cathode for degradation of a model azo dye. *Electrochimica Acta, 88*(0), 614-620.

Van Loock, W. (2006). European regulations, safety issues in rf and microwave power. In M. Willert-Porada (Ed.), *Advances in microwave and radio frequency processing* (pp. 85-91): Springer Berlin Heidelberg.

Vedrenne, M., Vasquez-Medrano, R., Prato-Garcia, D., Frontana-Uribe, B. A., & Ibanez, J. G. (2012). Characterization and detoxification of a mature landfill leachate using a combined coagulation–flocculation/photo fenton treatment. *Journal of Hazardous Materials, 205–206*(0), 208-215.

Vinodh, R., Padmavathi, R., & Sangeetha, D. (2011). Separation of heavy metals from water samples using anion exchange polymers by adsorption process. *Desalination, 267*(2–3), 267-276.

Walker, G. M., & Weatherley, L. R. (1997). Adsorption of acid dyes on to granular activated carbon in fixed beds. *Water Research, 31*(8), 2093-2101.

Wang, G. Q., Xu, Z. C., Yu, Y. L., & Ji, J. B. (2008). Performance of a rotating zigzag bed—a new HIGEE. *Chemical Engineering and Processing: Process Intensification, 47*(12), 2131-2139.

Wang, T., Tan, S., & Liang, C. (2009). Preparation and characterization of activated carbon from wood via microwave-induced $ZnCl_2$ activation. *Carbon, 47*(7), 1880-1883.

Weber, W. J. (1972). *Physicochemical processes for water quality control*: Wiley Interscience.

Wei, Z., Zeng, G., Xie, Z., Ma, C., Liu, X., Sun, J., et al. (2011). Microwave catalytic NOx and SO_2 removal using FeCu/zeolite as catalyst. *Fuel, 90*(4), 1599-1603.

Wiesmann, U., Choi, I. S., & Dombrowski, E.-M. (2007). *Fundamentals of biological wastewater treatment*: John Wiley & Sons.

Witek-Krowiak, A., Podstawczyk, D., Chojnacka, K., Dawiec, A., & Marycz, K. (2013). Modelling and optimization of chromium(III) biosorption on soybean meal. [Article]. *Central European Journal of Chemistry, 11*(9), 1505-1517.

Wu, T.-N. (2008). Environmental perspectives of microwave applications as remedial alternatives: Review. *Practice Periodical of Hazardous, Toxic, and Radioactive Waste Management, 12*(2), 102-115.

XIA, H.-y., PENG, J.-h., ZHANG, L.-b., MA, X.-y., TU, J.-h., & Zhang, S.-m. (2007). Study on the preparation of granular activated carbon from tobacco stems by microwave radiation and water vapor. *Chemical Engineering (China), 1*, 012.

Xiao, X., Liu, D., Yan, Y., Wu, Z., Wu, Z., & Cravotto, G. (2015). Preparation of activated carbon from Xinjiang region coal by microwave activation and its application in naphthalene, phenanthrene, and pyrene adsorption. *Journal of the Taiwan Institute of Chemical Engineers, in press*(0).

Xin-hui, D., Srinivasakannan, C., Jin-hui, P., Li-bo, Z., & Zheng-yong, Z. (2011). Preparation of activated carbon from jatropha hull with microwave heating: Optimization using response surface methodology. *Fuel Processing Technology, 92*(3), 394-400.

Xing, W., Ngo, H. H., Kim, S. H., Guo, W. S., & Hagare, P. (2008). Adsorption and bioadsorption of granular activated carbon (GAC) for dissolved organic carbon (DOC) removal in wastewater. *Bioresource Technology, 99*(18), 8674-8678.

Xu, M., Yin, P., Liu, X., Tang, Q., Qu, R., & Xu, Q. (2013). Utilization of rice husks modified by organomultiphosphonic acids as low-cost biosorbents for enhanced adsorption of heavy metal ions. *Bioresource Technology, 149*, 420-424.

Xu, T. (2005). Ion exchange membranes: State of their development and perspective. *Journal of Membrane Science, 263*(1–2), 1-29.

Yao, M., Zhang, Q., Hand, D. W., Perram, D., & Taylor, R. (2009). Adsorption and regeneration on activated carbon fiber cloth for volatile organic compounds at indoor concentration levels. *Journal of the Air & Waste Management Association, 59*(1), 31-36.

Yin, P., Xu, M., Qu, R., Chen, H., Liu, X., Zhang, J., et al. (2013). Uptake of gold (III) from waste gold solution onto biomass-based adsorbents organophosphonic acid functionalized spent buckwheat hulls. *Bioresource Technology, 128*, 36-43.

Ying, X., & Fang, Z. (2006). Experimental research on heavy metal wastewater treatment with dipropyl dithiophosphate. *Journal of Hazardous Materials, 137*(3), 1636-1642.

Yu, C.-H., Cheng, H.-H., & Tan, C.-S. (2012a). CO_2 capture by alkanolamine solutions containing diethylenetriamine and piperazine in a rotating packed bed. *International Journal of Greenhouse Gas Control, 9*(0), 136-147.

Yu, S., Chen, Z., Cheng, Q., Lü, Z., Liu, M., & Gao, C. (2012b). Application of thin-film composite hollow fiber membrane to submerged nanofiltration of anionic dye aqueous solutions. *Separation and Purification Technology, 88*(0), 121-129.

Yuen, F. K., & Hameed, B. H. (2009). Recent developments in the preparation and regeneration of activated carbons by microwaves. *Advances in Colloid and Interface Science, 149*(1–2), 19-27.

Zhang, L.-L., Wang, J.-X., Sun, Q., Zeng, X.-F., & Chen, J.-F. (2012). Removal of nitric oxide in rotating packed bed by ferrous chelate solution. *Chemical Engineering Journal, 181–182*(0), 624-629.

Zhang, L.-L., Wang, J.-X., Xiang, Y., Zeng, X.-F., & Chen, J.-F. (2011). Absorption of carbon dioxide with ionic liquid in a rotating packed bed contactor: Mass transfer study. *Industrial & Engineering Chemistry Research, 50*(11), 6957-6964.

Zhao, H., Shao, L., & Chen, J.-F. (2010). High-gravity process intensification technology and application. *Chemical Engineering Journal, 156*(3), 588-593.

Zlotorzynski, A. (1995). The application of microwave radiation to analytical and environmental chemistry. *Critical Reviews in Analytical Chemistry, 25*(1), 43-76.

Zolfaghari, G., Esmaili-Sari, A., Anbia, M., Younesi, H., Amirmahmoodi, S., & Ghafari-Nazari, A. (2011). Taguchi optimization approach for Pb(II) and Hg(II) removal from aqueous solutions using modified mesoporous carbon. *Journal of Hazardous Materials, 192*(3), 1046-1055.

Zolgharnein, J., Shahmoradi, A., & Ghasemi, J. B. (2013). Comparative study of Box–Behnken, central composite, and doehlert matrix for multivariate optimization of Pb (II) adsorption onto robinia tree leaves. *Journal of Chemometrics, 27*(1-2), 12-20.

LIST OF PUBLICATIONS

PUBLICATION

1. Kundu, A., Redzwan, G., Sahu, J. N., Mukherjee, S., Gupta, B. S., & Hashim, M. A. (2014). Hexavalent Chromium Adsorption by a Novel Activated Carbon Prepared by Microwave Activation. *BioResources,* 9(1), 1498-1518. (ISI Q1 IF: 1.309)
2. Kundu, A., SenGupta, B., Hashim, M. A., & Redzwan, G. Taguchi optimization approach for production of activated carbon from phosphoric acid impregnated palm kernel shell by microwave heating. *Journal of Cleaner Production*. 105, 420-427. (ISI Q1, IF: 3.398)
3. Kundu, A., Hashim, M. A., SenGupta, B., Sahu, J. N., Mubarak, N. M., & Redzwan, G. (2015). Optimization of the process variables in production of activated carbon by microwave heating. *RSC Advances,* 5, 35899-35908. (ISI Q1, IF: 3.708)
4. Kundu, A., SenGupta, B., Hashim, M. A., & Redzwan, G. (2015) Taguchi optimisation approach for chromium removal in a rotating packed bed contractor. *Journal of the Taiwan Institute of Chemical Engineers* (Accepted) (ISI Q1, IF: 2.637)
5. Kundu, A., Hassan L. S., Redzwan, G., Robinson, D., Hashim, M. A., & SenGupta, B. (2015). Application of a rotating packed bed contactor for removal of Direct Red 23 by adsorption. *Desalination and Water Treatment* (Accepted) (ISI Q3, IF: 1.173)

CONFERENCE ARTICLES

1. Kundu, A., Sahu, JN., & Redzwan, G. (2013). Lead Adsorption by Microwave Assisted H3PO4 Activated Carbon prepared from Palm Shell: Kinetics and Isotherm Studies and Optimization of operating condition with RSM. The eighth mathematical and physical science graduate congress. Bangkok, Thailand, 8-10 December, 2012.
2. Kundu, A., Sahu, JN., Gupta, B. S., Hashim, M. A., & Redzwan, G. (2013). Preparation of Granulated Activated Carbon for Heavy Metal Adsorption by Microwave Technology. University of Malaya Researchers' Conference. Kuala Lumpur, Malaysia, 19 – 20 November 2013.

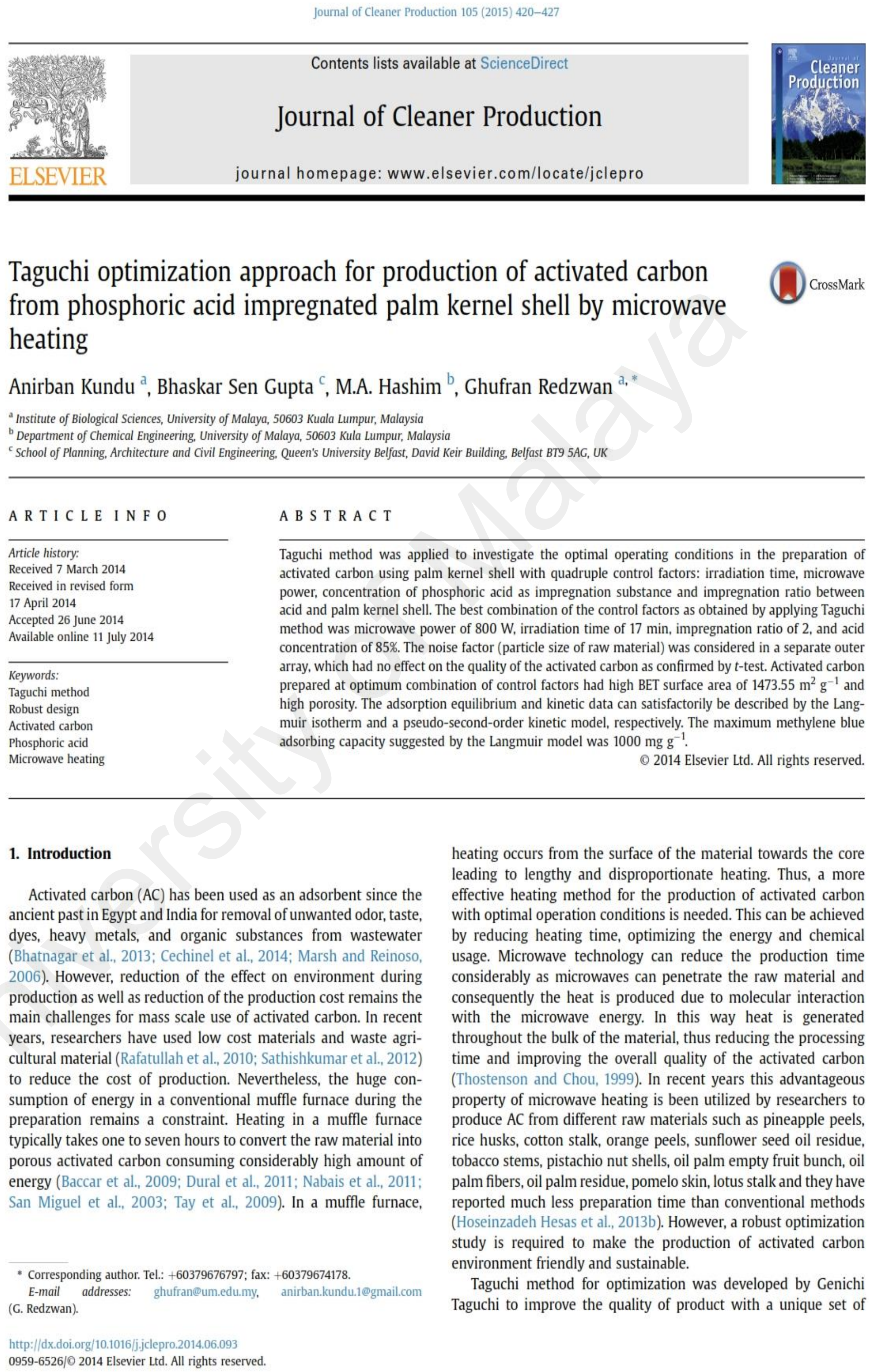

Journal of Cleaner Production 105 (2015) 420–427

Contents lists available at ScienceDirect

Journal of Cleaner Production

journal homepage: www.elsevier.com/locate/jclepro

Taguchi optimization approach for production of activated carbon from phosphoric acid impregnated palm kernel shell by microwave heating

Anirban Kundu [a], Bhaskar Sen Gupta [c], M.A. Hashim [b], Ghufran Redzwan [a, *]

[a] *Institute of Biological Sciences, University of Malaya, 50603 Kuala Lumpur, Malaysia*
[b] *Department of Chemical Engineering, University of Malaya, 50603 Kula Lumpur, Malaysia*
[c] *School of Planning, Architecture and Civil Engineering, Queen's University Belfast, David Keir Building, Belfast BT9 5AG, UK*

ARTICLE INFO

Article history:
Received 7 March 2014
Received in revised form
17 April 2014
Accepted 26 June 2014
Available online 11 July 2014

Keywords:
Taguchi method
Robust design
Activated carbon
Phosphoric acid
Microwave heating

ABSTRACT

Taguchi method was applied to investigate the optimal operating conditions in the preparation of activated carbon using palm kernel shell with quadruple control factors: irradiation time, microwave power, concentration of phosphoric acid as impregnation substance and impregnation ratio between acid and palm kernel shell. The best combination of the control factors as obtained by applying Taguchi method was microwave power of 800 W, irradiation time of 17 min, impregnation ratio of 2, and acid concentration of 85%. The noise factor (particle size of raw material) was considered in a separate outer array, which had no effect on the quality of the activated carbon as confirmed by *t*-test. Activated carbon prepared at optimum combination of control factors had high BET surface area of 1473.55 $m^2 g^{-1}$ and high porosity. The adsorption equilibrium and kinetic data can satisfactorily be described by the Langmuir isotherm and a pseudo-second-order kinetic model, respectively. The maximum methylene blue adsorbing capacity suggested by the Langmuir model was 1000 mg g^{-1}.

1. Introduction

Activated carbon (AC) has been used as an adsorbent since the ancient past in Egypt and India for removal of unwanted odor, taste, dyes, heavy metals, and organic substances from wastewater (Bhatnagar et al., 2013; Cechinel et al., 2014; Marsh and Reinoso, 2006). However, reduction of the effect on environment during production as well as reduction of the production cost remains the main challenges for mass scale use of activated carbon. In recent years, researchers have used low cost materials and waste agricultural material (Rafatullah et al., 2010; Sathishkumar et al., 2012) to reduce the cost of production. Nevertheless, the huge consumption of energy in a conventional muffle furnace during the preparation remains a constraint. Heating in a muffle furnace typically takes one to seven hours to convert the raw material into porous activated carbon consuming considerably high amount of energy (Baccar et al., 2009; Dural et al., 2011; Nabais et al., 2011; San Miguel et al., 2003; Tay et al., 2009). In a muffle furnace, heating occurs from the surface of the material towards the core leading to lengthy and disproportionate heating. Thus, a more effective heating method for the production of activated carbon with optimal operation conditions is needed. This can be achieved by reducing heating time, optimizing the energy and chemical usage. Microwave technology can reduce the production time considerably as microwaves can penetrate the raw material and consequently the heat is produced due to molecular interaction with the microwave energy. In this way heat is generated throughout the bulk of the material, thus reducing the processing time and improving the overall quality of the activated carbon (Thostenson and Chou, 1999). In recent years this advantageous property of microwave heating is been utilized by researchers to produce AC from different raw materials such as pineapple peels, rice husks, cotton stalk, orange peels, sunflower seed oil residue, tobacco stems, pistachio nut shells, oil palm empty fruit bunch, oil palm fibers, oil palm residue, pomelo skin, lotus stalk and they have reported much less preparation time than conventional methods (Hoseinzadeh Hesas et al., 2013b). However, a robust optimization study is required to make the production of activated carbon environment friendly and sustainable.

Taguchi method for optimization was developed by Genichi Taguchi to improve the quality of product with a unique set of

---

* Corresponding author. Tel.: +60379676797; fax: +60379674178.
E-mail addresses: ghufran@um.edu.my, anirban.kundu.1@gmail.com (G. Redzwan).

http://dx.doi.org/10.1016/j.jclepro.2014.06.093
0959-6526/© 2014 Elsevier Ltd. All rights reserved.

RSC Advances

PAPER

View Article Online
View Journal | View Issue

Cite this: *RSC Adv.*, 2015, **5**, 35899

Optimisation of the process variables in production of activated carbon by microwave heating

Anirban Kundu,[a] Bhaskar Sen Gupta,[b] M. A. Hashim,[c] J. N. Sahu,[d] Mubarak Mujawar[ce] and Ghufran Redzwan*[a]

This study aims to investigate the optimal operating conditions in order to obtain cost effective production of activated carbon (AC) from palm kernel shell (PKS) by microwave heating. Interactions among the independent variables, namely irradiation time (*T*), microwave power (*W*), impregnation ratio between impregnating substances and PKS, and the concentration of impregnating substance (sulphuric acid) were considered for optimising the process parameters during the production of AC, aided by Central Composite Design. The optimum conditions for the independent process variables were 11.02 minutes of irradiation time, microwave power of 676 W and impregnation ratio of 0.68. The AC produced in this work had a surface area of 1011 m^2 g^{-1} with high porosity as shown by scanning electron microscopy (SEM). Zinc was used to verify the potential of AC as an adsorbent. Zinc removal at the optimum conditions was found to be 13.72 mg g^{-1}. Such a Zn removal value is comparable with the earlier work of other researchers who used a conventional way of producing the AC. It is believed that microwave technology can be used for the production of AC in a short time with high energy efficiency, *e.g.*, 11 minutes against 2–5 hours of reactivation for conventional methods.

Received 23rd December 2014
Accepted 10th April 2015

DOI: 10.1039/c4ra16900j

www.rsc.org/advances

1. Introduction

Activated carbon (AC) is a unique and versatile adsorbent that has been used since the ancient times by Egyptians and Indians for removal of unwanted odour, taste, dyes, heavy metals and organic substances. In modern times, it has been widely used by the chemical industry for removal, separation and pre-concentration of both metallic and organic species from water and waste water.[1–3] There have been persistent efforts to prepare AC from low cost materials[4] to reduce the production cost. However, the cost of energy for the production of AC remains a concern. A typical production process of the AC requires heating the carbonaceous materials for one to seven hours to convert them into porous AC.[5–9] The requirement for this long heating time may be due to the fact that, heating occurs through convection, conduction, and radiation of thermal energy from the surface of the material towards the core. This creates a bottleneck in the manufacturing process.

Thus, the objective of this study was to investigate the optimal operating conditions for cost effective production of AC. The important factors that contribute to production cost are heating time as well energy and chemical use. The use of microwave technology could facilitate cost effective production,[10,11] as in the case of microwave heating, the thermal energy is produced due to molecular interaction with the microwave energy. The microwave penetrates the material and the microwave energy is converted to thermal energy. Thus, heat is generated throughout the bulk of the material and distribute more efficiently within the material. This can reduce the processing time and improve the overall product quality.[12]

Response surface methodology (RSM) is a collection of mathematical and statistical techniques which aid the analysis of experimental data and the optimisation of the result within a given range of operating parameters.[13] A Box-Wilson Central Composite Design, more familiar by the name of central composite design (CCD), is one of the most popular response surface methodology (RSM) designs due to the advantages that, CCDs are very efficient in providing important information on effects of the experimental variables and experimental error in a minimum number of experimental runs. The flexibility of CCDs allows studying different experimental regions of interest and operability conditions with the help of several varieties of CCD.[14–16]

In the conventional one-factor-at a time experiments, number of experiments are very large as well as, no interaction effects are studied. However, in RSM, reaction parameters can be varied simultaneously as required to generate data and that data can be

---

[a] *Institute of Biological Sciences, University of Malaya, 50603, Kuala Lumpur, Malaysia. E-mail: ghufran@um.edu.my; Fax: +6 0379674178; Tel: +6 0379676797*

[b] *Water Academy, School of the Built Environment, Heriot-Watt University, Edinburgh Campus, EH14 4AS, Scotland*

[c] *Department of Chemical Engineering, University of Malaya, 50603, Kula Lumpur, Malaysia*

[d] *Department of Petroleum and Chemical Engineering, Faculty of Engineering, Institut Teknologi Brunei, P.O. Box 2909, Tungku Gadong, Brunei Darussalam*

[e] *Department of Chemical and Petroleum Engineering, Faculty of Engineering, UCSI University, Kuala Lumpur 56000, Malaysia*

Hexavalent Chromium Adsorption by a Novel Activated Carbon Prepared by Microwave Activation

Anirban Kundu,[a] Ghufran Redzwan,[a] Jaya Narayan Sahu,[d] Sumona Mukherjee,[a] Bhaskar Sen Gupta,[c] and Mohd Ali Hashim [b],*

Microwave heating reduces the preparation time and improves the adsorption quality of activated carbon. In this study, activated carbon was prepared by impregnation of palm kernel fiber with phosphoric acid followed by microwave activation. Three different types of activated carbon were prepared, having high surface areas of 872 m^2 g^{-1}, 1256 m^2 g^{-1}, and 952 m^2 g^{-1} and pore volumes of 0.598 cc g^{-1}, 1.010 cc g^{-1}, and 0.778 cc g^{-1}, respectively. The combined effects of the different process parameters, such as the initial adsorbate concentration, pH, and temperature, on adsorption efficiency were explored with the help of Box-Behnken design for response surface methodology (RSM). The adsorption rate could be expressed by a polynomial equation as the function of the independent variables. The hexavalent chromium adsorption rate was found to be 19.1 mg g^{-1} at the optimized conditions of the process parameters, *i.e.*, initial concentration of 60 mg L^{-1}, pH of 3, and operating temperature of 50 °C. Adsorption of Cr(VI) by the prepared activated carbon was spontaneous and followed second-order kinetics. The adsorption mechanism can be described by the Freundlich Isotherm model. The prepared activated carbon has demonstrated comparable performance to other available activated carbons for the adsorption of Cr(VI).

Keywords: Activated carbon; Palm kernel fiber; RSM; Box-Behnken; Chromium

Contact information: a: Institute of Biological Sciences, University of Malaya, 50603, Kuala Lumpur, Malaysia; b: Department of Chemical Engineering, University of Malaya, 50603, Kuala Lumpur, Malaysia; c: School of Planning, Architecture and Civil Engineering, Queen's University Belfast, David Keir Building, Belfast, BT9 5AG, UK; d: Department of Petroleum and Chemical Engineering, Faculty of Engineering, Institut Teknologi Brunei, Tungku Gadong, P.O. Box 2909, Brunei Darussalam;
** Corresponding author: alihashim@um.edu.my*

INTRODUCTION

Heavy metals, because of their significant potential toxicity and bio-magnification capability, have become one of the most hazardous groups of pollutants in the last century. Efforts to reduce the concentration of heavy metals in liquid effluent have been increasingly stressed for compliance with permissible discharge levels and for fulfilling ethical obligations (Machida *et al.* 2004). Chromium, like other heavy metals such as lead, zinc, cadmium, and copper, is a toxic metal that is released into the environment through anthropogenic activities. Chromium compounds are used in different industrial processes, such as tanning, electroplating, pigmentation, catalyst for corrosion inhibitors, textile dyeing, steel fabrication, inorganic chemicals, paper and pulp, and wood preservatives (Nguyen *et al.* 2013). In water, chromium is mainly available in trivalent and hexavalent forms. The hexavalent form of chromium causes cancer and is considered to be more hazardous than its trivalent species (Bello *et al.* 1999). Prolonged exposure to

Kundu *et al.* (2014). "Cr(VI) adsorption by carbon," *BioResources* 9(1), 1498-1518. 1498

Journal of the Taiwan Institute of Chemical Engineers 000 (2015) 1–7

Contents lists available at ScienceDirect

Journal of the Taiwan Institute of Chemical Engineers

journal homepage: www.elsevier.com/locate/jtice

Taguchi optimisation approach for chromium removal in a rotating packed bed contractor

Anirban Kundu[a], Bhaskar SenGupta[b], M.A. Hashim[c], Ghufran Redzwan[a,*]

[a] Institute of Biological Sciences, University of Malaya, 50603, Kuala Lumpur, Malaysia
[b] Water Academy, School of the Built Environment, Heriot-Watt University, Edinburgh Campus, EH14 4AS, Scotland
[c] Department of Chemical Engineering, University of Malaya, 50603, Kuala Lumpur, Malaysia

ARTICLE INFO

Article history:
Received 10 March 2015
Revised 28 April 2015
Accepted 9 May 2015
Available online xxx

Keywords:
Rotating packed bed
Taguchi method
Optimisation
Chromium
Signal to noise ratio
Adsorption

ABSTRACT

Rotating packed bed (RPB) is a doughnut shaped bed, which is spun at high speed to generate centrifugal force to pass fluid through an adsorbent bed at a high velocity. The centrifugal force, which is much larger than the gravitational force reduces mass transfer resistance for transporting adsorbate molecules to the adsorbent. In this study, the optimum condition of the working parameters of a RPB contactor for removal of chromium by activated carbon was investigated with the aid of Taguchi method. Four parameters, namely, rotating speed (rpm), feed rate (L/h), packing density (kg/m^3) and initial solution pH were chosen as the control factors while initial concentration of chromium was chosen as the external noise factor. The optimum condition for the adsorption was found to be rotating speed (rpm) of 1200 (level 3), feed rate (L/h) of 50 (level 4), packing density (kg/m^3) of 179 (level 3), and initial solution pH of 2 (level 1). The experimental and predicted S/N ratios with values 39.26 and 39.20 were in very good agreement with each other at the optimum condition. A removal of 91% was obtained at the optimum condition. Pseudo second order kinetics described the adsorption rate satisfactorily while the mechanism could be described by the film diffusion model.

1. Introduction

Concept of a rotating packed bed (RPB) as a mass transfer equipment was developed by Ramshaw and Mallinson in 1979 [1]. A RPB works on the principle that the gravitation flow of fluid through a packed bed is replaced by a centrifugal field, which could be even 1000 times stronger than the gravitational field [2]. This technology is named as HIGEE, an acronym for high gravity. A doughnut shaped bed is spun at high speed to achieve this centrifugal force in a RPB. Initially the RPB-HIGEE systems were used in separation processes such as distillation and absorption, however, it can also be applied in mass transfer limited reacting systems. Traditionally the fixed bed systems are used to treat wastewater by adsorption. The bed height and the flow rate ranges from 10 to 40 cm and 0.22 to 1.8 L/h, respectively [3–6]. In this case, the gravitational force is responsible for the flow of liquid through the bed, which often suffers from clogging and decline in throughput. Additionally, the problem of channel formation inside the column and fouling hinder the proper utilisation of the total adsorption bed. The poor mass transfer efficiency and large size of the columns make these conventional processes expensive and difficult to handle [7]. Advantages of using high gravimetric systems are higher throughput, formation of thinner liquid film over the packing resulting in decreased external mass transfer resistance, use of higher surface packing per unit volume of packed bed, better distribution of liquid over the packing and lower static holdup. This would aid in reducing the size of the processing equipment significantly in comparison to a conventional packed bed and is therefore, likely to reduce the overall cost of wastewater treatment [8,9].

Adsorption onto activated carbon is one of the best methods for heavy metal removal. However, the size of the facility to use activated carbon is generally large in industry to facilitate the high volume of effluent. Due to the high throughput, the RPB-HIGEE can be useful in treating high volume of wastewater. Lin and Liu [8] studied the adsorption of basic dye Basic Yellow 2 on activated carbon in a centrifugal adsorption bed and found that the adsorption of the dye was influenced by centrifugal acceleration. Das et al., [6] explored the mass transfer characteristics of continuous biosorption of Cu(II) ions on *Catla catla* fish scale under centrifugal acceleration in a rotating packed-bed (RPB) contactor. They reported enhancement in volumetric mass transfer coefficient with increasing rotor speed. Panda et al., [10] used crude tamarind (*Tamarindus indica*) fruit shell (TFS) to remove hexavalent chromium ions from an aqueous solution in a RPB

---

[*] Corresponding author. Tel.: +60379676797; fax: +60379674178.
E-mail addresses: anirban.kundu.1@gmail.com (A. Kundu), ghufran@um.edu.my (G. Redzwan).

http://dx.doi.org/10.1016/j.jtice.2015.05.022
1876-1070/© 2015 Taiwan Institute of Chemical Engineers. Published by Elsevier B.V. All rights reserved.

Please cite this article as: A. Kundu et al., Taguchi optimisation approach for chromium removal in a rotating packed bed contactor, Journal of the Taiwan Institute of Chemical Engineers (2015), http://dx.doi.org/10.1016/j.jtice.2015.05.022

Desalination and Water Treatment (2015) 1–9
www.deswater.com
doi: 10.1080/19443994.2015.1060165

Application of a rotating packed bed contactor for removal of Direct Red 23 by adsorption

Anirban Kundu[a], Lili Shakira Hassan[b], Ghufran Redzwan[a], Desmond Robinson[b], Mohd. Ali Hashim[c], Bhaskar SenGupta[d,*]

[a]*Institute of Biological Sciences, University of Malaya, Kuala Lumpur 50603, Malaysia, Tel. +60379676797; emails: kundu.anirban@yahoo.com (A. Kundu), ghufran@um.edu.my (G. Redzwan)*
[b]*School of Planning, Architecture and Civil Engineering, Queen's University Belfast, David Keir Building, Belfast, BT9 5AG, UK, Tel. +44 0 28 9097 4025; emails: leelyhassan@gmail.com (L. Shakira Hassan), des.robinson@qub.ac.uk (D. Robinson)*
[c]*Department of Chemical Engineering, University of Malaya, Kula Lumpur 50603, Malaysia, Tel. +60379675296; email: alihashim@um.edu.my*
[d]*Water Academy, School of the Built Environment, Heriot-Watt University, Edinburgh Campus, EH14 4AS Scotland, Tel. +44 0 131 451 8171; email: b.sengupta@hw.ac.uk*

Received 7 November 2014; Accepted 3 June 2015

ABSTRACT

In this work, a rotating packed bed (RPB) contactor was applied to adsorb Direct Red 23 dye onto commercially available activated carbon. A RPB is a doughnut shaped contactor, which rotates on a vertical axis and centrifugal force acts as the driving force for fluid-particle contact in the contactor. This centrifugal force, which is several times higher than the gravitational force, aids the adsorption process with enhanced mass transfer coefficient. The commercially available activated carbon used in this work had moderate BET surface area of 583 $m^2 g^{-1}$ and was mainly meso-porous with an average pore size of 22 Å. The adsorption characteristics of the activated carbon were studied in a shake flask and a RPB. The dye removal in RPB was 93% compared to 55% in a shake flask in 5 h for the same amount of activated carbon and dye solution. Rotor speed and feed rate were important parameters for the removal of the dye in a RPB. It was found that rotor speed of 628 rpm and feed rate of 40 L h^{-1} yielded the best adsorption efficiency.

Keywords: Rotating packed bed; Process intensification; Adsorption; Activated carbon; Direct Red 23

1. Introduction

Industries such as textile, cosmetics and paper and pulp are known for producing large volumes of coloured effluent, which are difficult to treat due to the high chemical stability of dyes. Conventional physicochemical and biological treatment processes often prove inadequate to meet the discharge standards of different countries. Some of the treatment processes like membrane filtration, electrochemical, photo oxidation and chemicals such as Fenton reagent or hypochlorite have been used to treat wastewater containing dye. However, all the processes have their own demerits associated with cost and sludge disposal [1–7].

---

*Corresponding author.